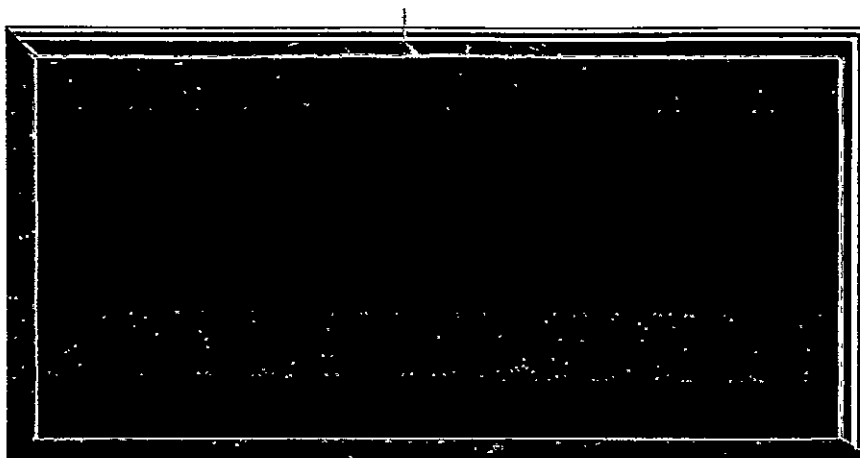


2
m 1A



| | | | |
|-------------------|-------------------|-------------------------------|------------|
| FACILITY FORM 602 | N 71-16803 | (ACCESSION NUMBER) | (THRU) |
| | 113 | (PAGES) | G3 |
| | CR-103010 | (NASA CR OR TMX OR AD NUMBER) | 31 |
| | | | (CATEGORY) |



Reproduced by
NATIONAL TECHNICAL
INFORMATION SERVICE
Springfield, Va. 22151

GENERAL  ELECTRIC

CR-103010
DOCUMENT NO. 70 HVO 39

DETERMINATION OF THE
WIND RESPONSE OF SATURN V
BY STATISTICAL METHODS
VOLUME I

DECEMBER 24, 1970
CONTRACT NO. NAS8-25477

GENERAL ELECTRIC
APOLLO SYSTEMS
HUNTSVILLE OPERATIONS
HUNTSVILLE, ALABAMA

DETERMINATION OF THE
WIND RESPONSE OF SATURN V
BY STATISTICAL METHODS
VOLUME I


DECEMBER 24, 1970

This work was performed under the direction
of MSFC, AERO-Astroynamics Laboratory, Dynamics
and Flight Mechanics Division

Work Performed By:

D. W. Rowe
B. Gaggini
H. Graf
D. Hurd

Report Prepared By:


Dale W. Rowe
Project Engineer

Approval

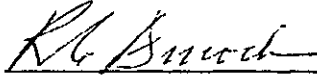

R. C. Smock, Manager
Analytical Engineering

TABLE OF CONTENTS

| <u>SECTION</u> | <u>PAGE</u> | |
|----------------|--|------|
| 1.0 | INTRODUCTION | 1-1 |
| 1.1 | The Problem | 1-2 |
| 1.2 | Summary of Results | 1-3 |
| 1.3 | Recommendations | 1-4 |
| 2.0 | THE ADJOINT METHOD | 2-1 |
| 2.1 | Reviewing the Method | 2-2 |
| 2.2 | Application to Saturn V Response Statistics | 2-5 |
| 3.0 | WIND MODEL DEVELOPMENT | 3-1 |
| 3.1 | Data Requirements for "Ideal" Wind Model | 3-2 |
| 3.2 | Available Wind Statistics - Limitations and Assumptions | 3-4 |
| 3.3 | Final Wind Model Specifications | 3-7 |
| 3.4 | Filter Synthesis | 3-10 |
| | 3.4.1 The Synthesis Problem | 3-10 |
| | 3.4.2 Linear Regression Method | 3-11 |
| | 3.4.3 Parameter Optimization Method | 3-15 |
| | 3.4.4 Constrained Response Optimization Method | 3-17 |
| | 3.4.5 Impulse Response Generation/Curve Fit Method | 3-22 |
| | 3.4.6 Transformation from Altitude to Time Domain | 3-24 |
| | 3.4.7 Wind Model Output | 3-24 |
| 4.0 | SATURN V VEHICLE MODEL | 4-1 |
| 4.1 | Forward Vehicle Model | 4-1 |
| | 4.1.1 Vehicle Dynamics and Control Equations | 4-3 |
| | 4.1.2 Bending Dynamics Equations | 4-7 |
| | 4.1.3 Sloshing Dynamics Equations | 4-9 |
| | 4.1.4 Bending Loads Equations | 4-12 |
| | 4.1.5 Stochastic Thrust Model | 4-13 |
| | 4.1.6 Stochastic Center-of-Pressure Model | 4-13 |
| 4.2 | Adjoint Vehicle Model | 4-21 |
| | 4.2.1 Forming the Adjoint | 4-21 |
| | 4.2.2 Program Initial Value Calculation | 4-22 |
| | 4.2.3 Operating the Model | 4-22 |

TABLE OF CONTENTS (Continued)

| <u>SECTION</u> | | <u>PAGE</u> |
|----------------|--|-------------|
| 5.0 | RESULTS | 5-1 |
| 5.1 | Bending Response Statistics | 5-1 |
| 5.2 | Angle of Attack Statistics | 5-1 |
| 5.3 | Engine Deflection Angle Statistics | 5-2 |
| 5.4 | Run Time Reduction Efforts | 5-2 |
| 6.0 | REFERENCES | 6-1 |
| 7.0 | APPENDICIES | |
| | Appendix A - Calculating Covariance Derivatives | |
| | Appendix B - Calculating Numerator Coefficients- Linear Regression Method | |
| | Appendix C - Optimization Algorithm | |
| | Appendix D - Calculating Filter Coefficients From Constrained Response Coefficients | |
| | Appendix E - Converting Altitude Domain Coefficients to Flight-Time Domain | |
| | Appendix F - Vehicle Nomenclature | |

SECTION 1.0

INTRODUCTION

Determination of Wind Response of Saturn V by Statistical Methods

1.0 INTRODUCTION

1.1 The Problem

This report describes the development and application of a non-stationary statistical method of estimating the response statistics of a vertically rising vehicle. The method used is based on the solution of the adjoint differential equations of the vehicle. The technique is referred to as "The Method of Adjoint Systems", (Ref. 1).

The method of adjoint systems has received increased attention in recent years. This increased popularity is due to more widespread recognition of the power of the method. Application of the method to the problem described in this report illustrates this power.

The problem attacked in this study was

given;

- ° Wind field statistics - (non-stationary),
- ° Thrust variation statistics (non-stationary),
- ° Center of Pressure variation statistics (non-stationary),
- ° Vehicle model parameters (time-varying).

Determine the resulting Saturn V

- ° Mean-plus-three-sigma bending moment at a selected station,
- ° Mean-plus-three-sigma angle of attack,
- ° Mean-plus-three-sigma engine angle,

response in the region of peak dynamic pressure/angle of attack.

Through application of the adjoint method, the vehicle response statistics itemized above are obtained in a very efficient manner.

In the sections which follow the method of adjoint systems is explained; the variational models of wind, thrust and center-of-pressure are described; the vehicle model is described; and results are analyzed.

The most difficult and time consuming part of the effort was synthesis of the wind filter. A considerable portion of this report is devoted to this most difficult and important problem. The wind filter model work described has important applications outside its use with the adjoint method. It's application to load relief controller design is an example of one such application, (Ref. 2).

1.2 Summary of Results

All major objectives of the effort were met, with one significant exception. This exception being the omission of the small scale wind effects, or turbulence, model. This omission resulted from the unavailability of covariance data defining the turbulence model.

The most significant result was the demonstrated ability of the method of adjoint systems to accurately predict vehicle response statistics efficiently. The key words here are accurately and efficiently.

The method proved to be accurate in that response statistics obtained using this method compared favorably with response statistics estimated by the more conventional ensemble averaging techniques.

The method proved efficient in that, with one computer run, the bending moment, angle of attack, or engine deflection angle statistics resulting from combined stochastic variations in wind, thrust and center of pressure can be calculated. The ensemble averaging technique requires from 100 to 500 runs to obtain this information for a selected flight time. In contrast to the previous adjoint effort (Ref. 3) average computer run time on the IBM 7094 averaged 12 minutes per run as compared with 40 minutes in the previous effort.

This reduction in run time was achieved through loosening the overly restrictive tolerance constraints on the predictor-corrector integration algorithm.

Other significant results of this effort were:

- ° A method for synthesizing a filter capable of matching non-stationary wind statistics was developed. The filter resulting was verified and actually used to obtain vehicle response statistics. The filter generated statistics within the 90% confidence interval of the wind data.
- ° Stochastic models representing statistical thrust and center of pressure variations were developed and used with the wind model to obtain response

statistics from the combined effects of stochastically varying winds, thrust magnitude and center of pressure location.

Numerical results from application of the adjoint technique are presented in Section 5.0. Filter output statistics are presented in Section 3.0.

1.3 Recommendations

The following changes to the implementation are recommended:

- Program the adjoint model on a hybrid computer. Cost savings associated with operation on a hybrid would be significant.
- Incorporate other (and better) stochastic variational models of vehicle parameters. The models used were limited to white noise models of XCP location and thrust magnitude.
- Develop and incorporate a wind turbulence model.

To fully capitalize on developments of this effort, the following extensions to other applications are recommended:

- Apply the developed method to Space Shuttle Analysis. The efficiency of the method lends itself to any statistical response study. The similarity of the Space Shuttle statistical response analysis requirements makes it a natural application.
- Apply the wind model to other problems, notably load-relief controller design, wind predictor models and other simulation applications.
- Apply the Wind Filter Synthesis methodology to other stochastic model synthesis requirements.

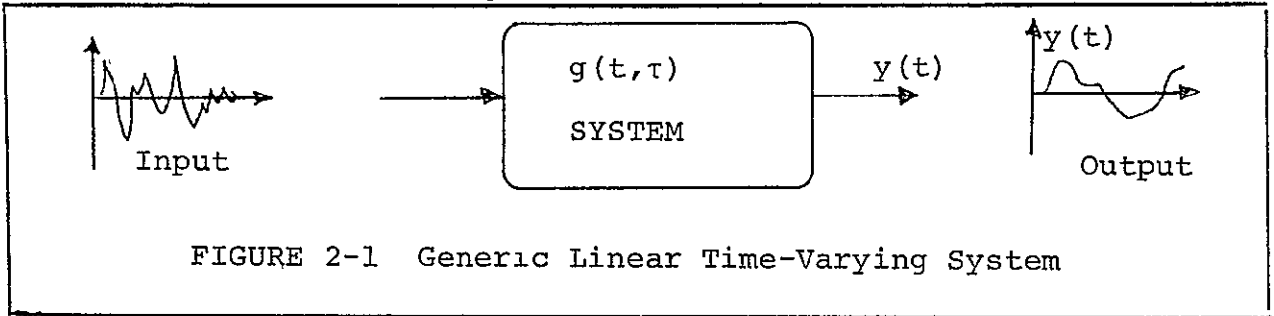
SECTION 2.0

THE ADJOINT METHOD

2.0 THE ADJOINT METHOD

2.1 Reviewing the Method

The adjoint method is applicable to linear time varying systems. To illustrate it's application, consider the time varying system of Figure 2-1.



In this figure, $g(t, \tau)$ is the system weighting function. The mean square response, or autocorrelation of the system output is given by:

$$\phi_{YY}(t_2) = \overline{y(t_2)^2} = \int_{-\infty}^{t_2} g(t_2, \tau_1) d\tau_1 \int_{-\infty}^{t_2} g(t_1, \tau_2) \phi_{XX}(\tau_1, \tau_2) d\tau_2, \quad (2-1)^*$$

where:

ϕ_{YY} = autocorrelation of the output,

$g(t, \tau)$ = system weighting function, and

ϕ_{XX} = autocorrelation of the input.

If the system input is gaussian white noise, equation (2-1) simplifies to:

$$\phi_{YY}(t_2) = \overline{y(t_2)^2} = \int_{-\infty}^{t_2} g(t_2, \tau)^2 d\tau \quad (2-2)$$

* See Ref. 3, p 2-9.

The method of adjoint systems is applied at this point to generate $g(t_2, \tau)$ as a function of " τ " for a selected value of t_2 .

The procedures that are developed for this purpose are quite simple. The logical derivation of these procedures is covered in Lanning and Battin, (ref. 4) Appendix F, page 398, and will not be covered in this report.

One method of forming the adjoint of a system is to start with an analog representation of the system and convert this representation to an adjoint model. The step by step conversion procedure is described in Rogers and Connolly, (ref. 5) page 236 as follows:

- (1) Turn each element in the loop around and reverse the direction of signal flow.
- (2) Let the time-varying elements start from time t_2 and run backward relative to their action in the regular system.
- (3) Interchange inputs and outputs of the system. The new input will be $\delta(\tau)$. The output will be $g(t_2, \tau)$.

To illustrate these rules, consider the system of Figure 2-2 and its adjoint transformation, Figure 2-3. If the time varying coefficient, $f(t)$, in the original system is equal to t , then in the adjoint model it becomes $(t_2 - \tau)$.

To simplify the transformation of a system to its adjoint, the following rules should be adhered to in drawing the original computer-circuit diagrams.

- (1) No potentiometer should have more than one output. Use multiple isolated potentiometers instead.
- (2) Consider amplifier and summers to have only gains of unity. Gain reapportionment between potentiometers and amplifiers may be performed in the adjoint system.

This procedure was utilized, even though the equations were solved on a digital computer. The DYNASAR algorithm was used in implementing the solution. DYNASAR permits the engineer to think in terms of analog computer diagrams and solutions while actually solving the equations numerically on a digital computer. General Electric report "Development of Adaptive Modular Analysis Techniques, (ref. 6) written

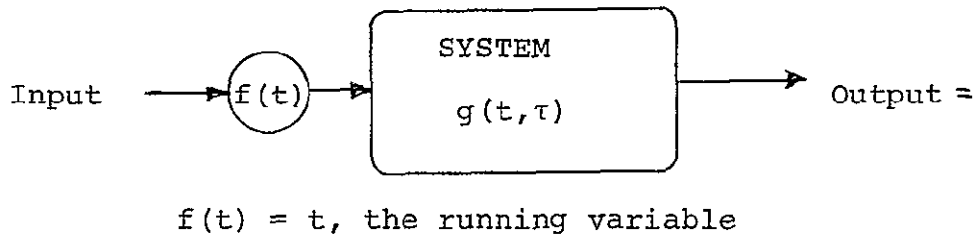


FIGURE 2-2 Forward System Model With Time-Varying Coefficient.

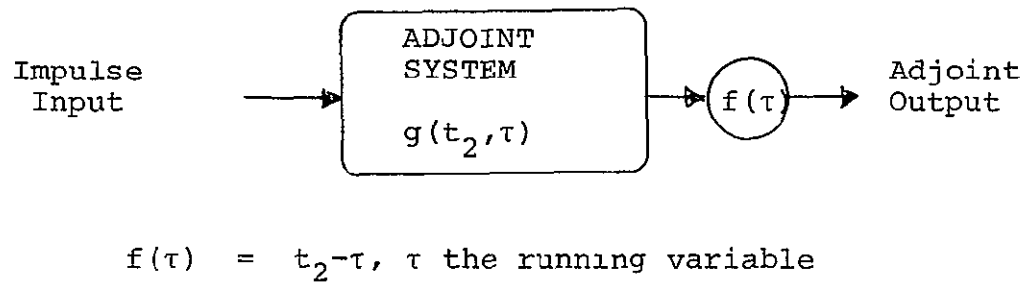


FIGURE 2-3 Adjoint of System of Figure 2-2.

under NASA Contract NAS8-18005 describes the DYNASAR algorithm and its use in detail.

An alternate approach to defining the system adjoint using a state variable development is described in DeRusso, Close, and Roy, State Variables for Engineers, (ref. 7) pp 376-394.

Once the adjoint model is generated, the mean square response is obtained by applying equation (2-2). The solution of equation (2-2) is mechanized by utilizing the adjoint model as shown in Figure 2-3. Figure 2-2 shows the forward model of a system for which a mean square response due to noise is desired. By applying the rules described above, the adjoint of this system can be drawn as shown in Figure 2-3. The impulse response of the adjoint model yields the desired mean square response of the system for any defined time, t_2 . The impulse input function is introduced by loading the integrators in the adjoint system with the appropriate initial conditions. A novel way of accomplishing this loading of initial conditions is described in section 4 of this report.

2.2 Application to Saturn V Response Statistics

By assuming that $g(t, \tau)$, in Figure 2-2, represents the weighting function of the Saturn V vehicle (relating wind to vehicle bending moment). The method of adjoint systems can be applied to determine the mean square value (i.e. variance) of the bending moment. An immediate observation is that, as formulated, the applicability of the method of adjoint systems to the solution of this problem is predicated on the assumption that the input be white noise. Obviously, the wind cannot be considered white noise. The solution to this problem is very simple, conceptually.

If a filter is synthesized such that when forced with white noise, the output signal has the covariance equal of that of the wind, the combined system (vehicle plus filter) represents the desired problem formulation. Figure 2-4 shows the combined vehicle - wind filter model. Figure 2-5 shows the adjoint model of this combined system.

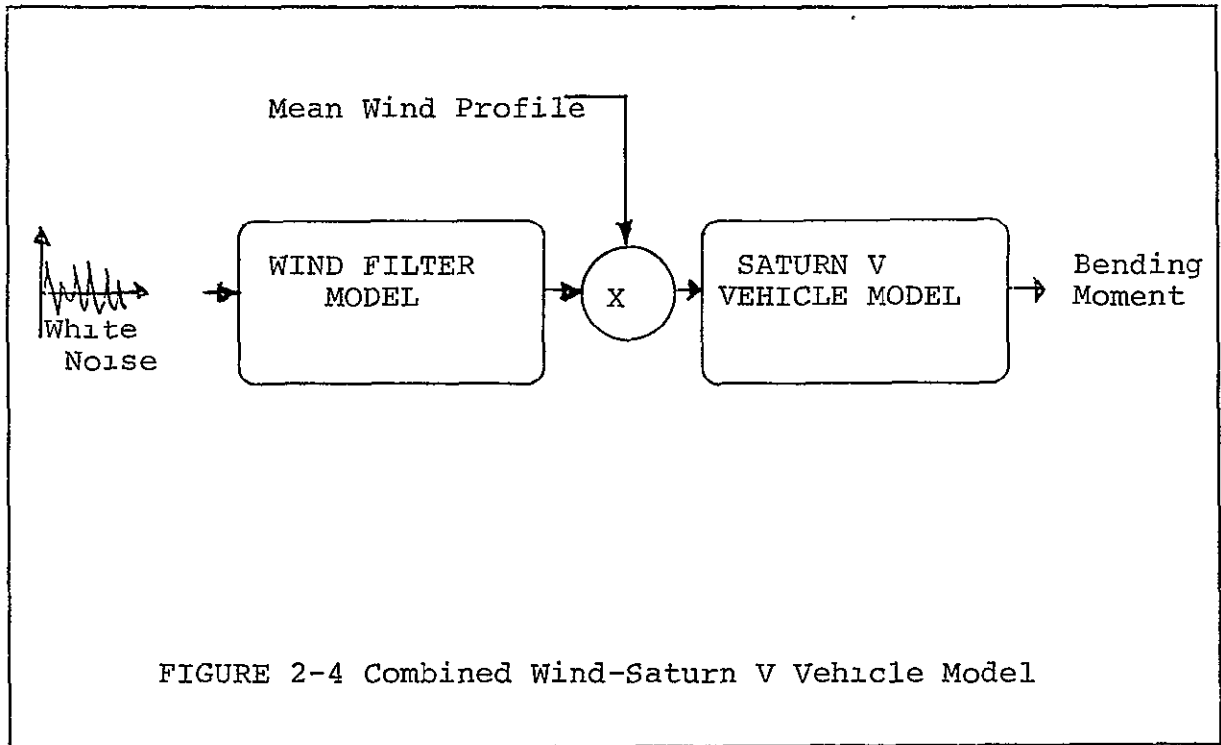


FIGURE 2-4 Combined Wind-Saturn V Vehicle Model

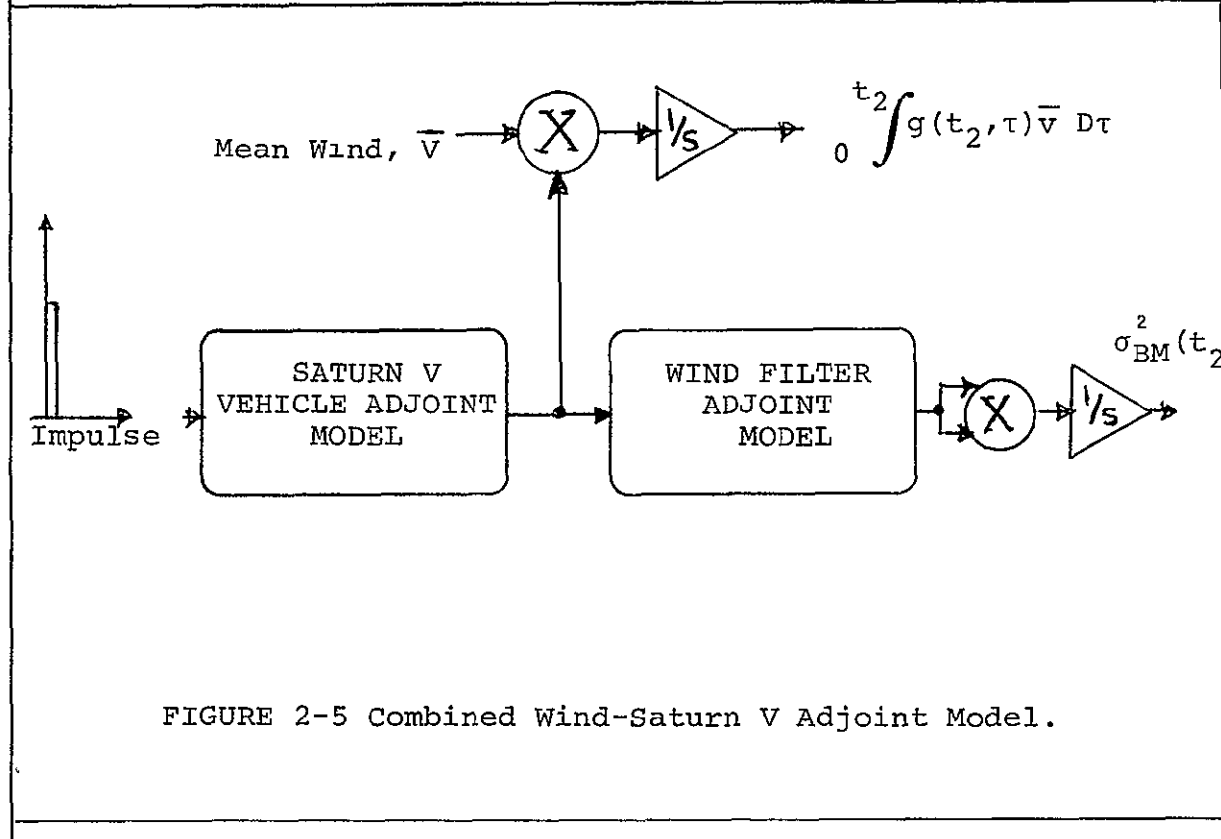
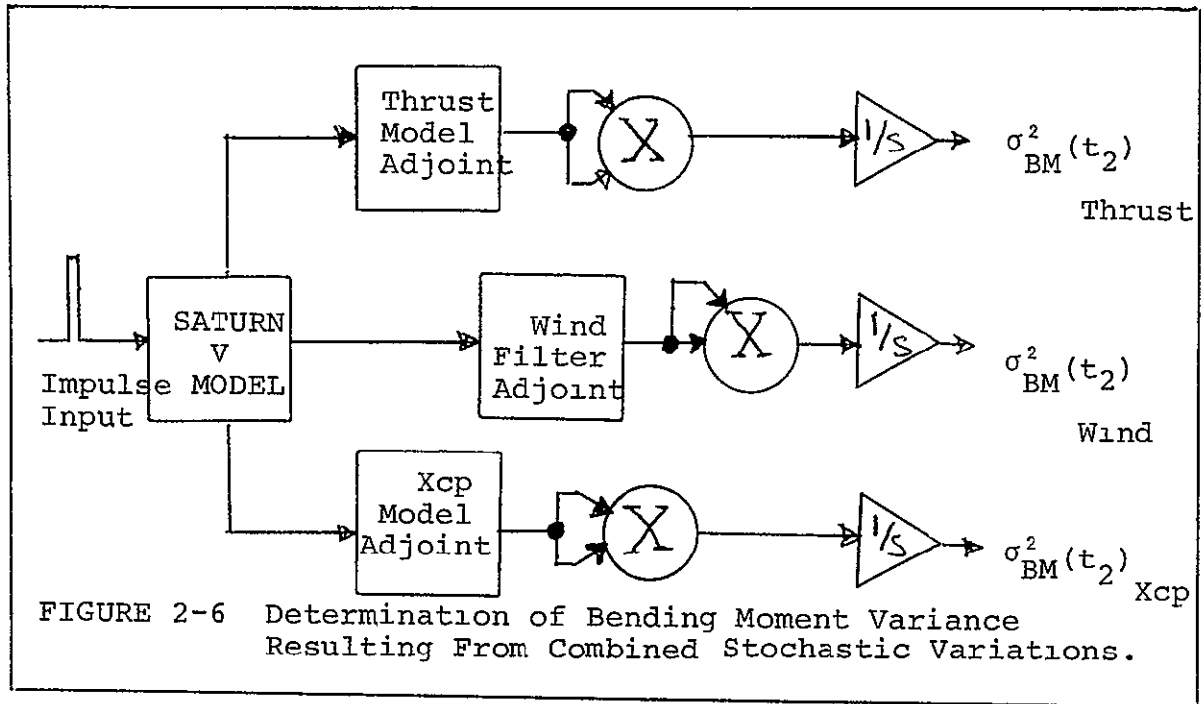


FIGURE 2-5 Combined Wind-Saturn V Adjoint Model.

Figure 2-5 illustrates application of the adjoint model to obtain the mean and variance of the vehicle bending moment at a given flight time, t_2 .

Using the same approach, the variance of the bending moment due to stochastic variations in center of pressure and thrust is determined. These statistics can be calculated at the same time, on the same simulation model. Figure 2-6 illustrates how this is done.



Extending the adjoint method to calculating response statistics other than bending moment response is straight forward. For each response statistic desired, a new $g(t_2, t)$ is generated. This was done in this study to obtain angle of attack and engine deflection statistics. The results, Section 5, summarizes these response statistics.

SECTION 3.0

WIND MODEL DEVELOPMENT

3.0 WIND MODEL DEVELOPMENT

3.1 Data Requirements for "Ideal" Wind Model

Granularity of Covariance Data

In order to obtain first and second vehicle response moments (mean and covariances), means and covariances of the incident wind, $V_W(t)$, must be known. Ideally, the wind model should contain covariance data at altitude intervals fine enough to define forcing frequencies in the range of the first several vehicle bending modal frequencies. In the case of the Saturn V Vehicle the rigid body mode is in the neighborhood of 1 radian per second and the first three elastic modes are approximately 6, 13 and 18 radians per second. This means that the wind statistics must be calculated in fine enough increments to include frequencies up to approximately 20 radians per second. To convert this requirement to a specific sampling interval, knowledge of the vehicle velocity in the area of interest and application of the sampling theorem is required. At peak dynamic pressure the vehicle velocity is approximately 500 meters/second. The 3rd bending modal frequency is 20 radians per second or 3.18 cycles per second.

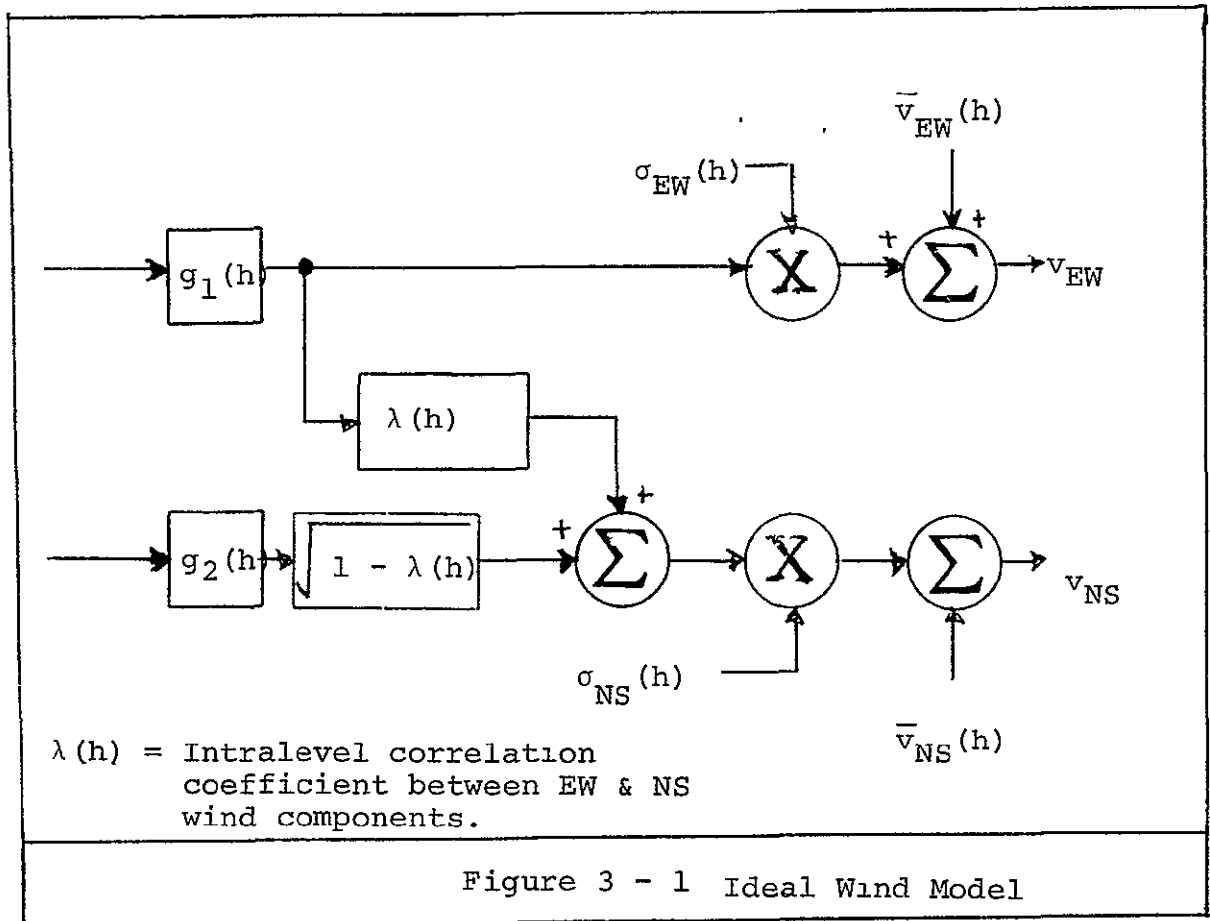
Then;

$$\begin{aligned} \text{(Wind Wave Length)} &= \frac{V \text{ (Velocity of Vehicle)}}{f \text{ (3rd modal frequency)}} \\ &= \frac{500 \text{ m/sec}}{3.18 \text{ c/s}} = 157 \text{ meters.} \end{aligned}$$

Using the sampling theorem, it is required that a signal be sampled at least every half cycle to determine its presence. This means that covariance data must be available in intervals of less than approximately 75 meters in altitude. The ideal filter should match the covariance at these 75 meter increments.

Directional Components

The complete wind model includes statistics of the east-west components (zonal) and north-south (meridional) components as well as correlations between the components. The general form of this wind model is shown in Figure 3-1.



Sample Size and Statistical Grouping by Month,

Season of Year

Of course the ideal sample size of wind soundings is infinity. The real question though, is how should the available data be grouped. For example, the data could be grouped by day and the windiest day statistics selected as the statistics to design to. This would insure that on any given day (even the windiest), the probability of structural failure would not exceed a specified value. The problem here is lack of sufficient data for a given calendar day to place any confidence on the statistics for that day.

If the windiest week were selected, the probability of exceeding the structural limit of the vehicle launched in the windiest week could be established. However, if the windiest day of the windiest week were selected as the launch date, the probability of structural failure would be greater than the specified amount. In addition, it is possible that the windiest day may not even occur in the windiest week.

Another consideration is that over a given period of time, for example a week or month, the statistics are relatively stationary with time. Therefore, there is some logic in taking a larger grouping, such as a week or month for establishing the design wind statistics.

To summarize, there are conflicting considerations in establishing the "best" grouping of data for defining the wind statistics to be matched by the "ideal" wind model. Balancing these considerations resulted in selecting the windiest month statistics, (March) as the best grouping for design purposes.

3.2 Available Wind Statistics - Limitations and Assumptions

Source of Statistical Data on Wind

Two sources of wind data were available for use:

- (1) Computer printout of Mean and Covariance of winds over Cape Kennedy as measured by the Jimsphere Wind Sounding Program. This printout was an output of NASA-MSFC Contract NAS8-21444 (Ref. 8)
- (2) NASA T ND 3815, "Scalar and Component Wind Correlations between Altitude Levels for Cape Kennedy, Florida and Santa Monica, California". (Ref. 9)

Both sources utilize tracking of an ascending balloon, as the method for obtaining wind velocity data. Data at 50 meter increments was obtained from the Jimsphere measured data. The rawinsonde data yielded statistics in 1000 meter increments.

Use of data obtained in this manner requires assumptions of statistical regularity and time constancy. The statistical regularity assumption means that if the measurements were taken sometime in the future, the same statistics would result. The time constancy assumption is that, over a time interval corresponding to the ascent of the balloon, the wind at a specific altitude is constant. This assumption has been experimentally verified by comparing the winds calculated from balloons released at one-hour intervals. The correctness of this assumption regarding turbulence remains questionable, however, (see reference 10.)

Recognizing the assumptions inherent in the raw wind measurements (and accepting them as valid, as most do), it remains to identify the shortcomings of the statistical data derived from these measurements. The constraints these limitations placed on the wind filter synthesis effort can then be itemized.

Limitations of Available Wind Statistics

- (1) Jimsphere Mean and Covariance Data from Contract NAS 8-21444, (Ref. 8)

The original intention was to use this data as a model for developing the wind filter. This data was selected because it was available in 50 meter increments. (The other source of data gave covariance data only in 1000 meter increments.) The shortcomings of this data however, included;

- The data was based on annual wind measurements.

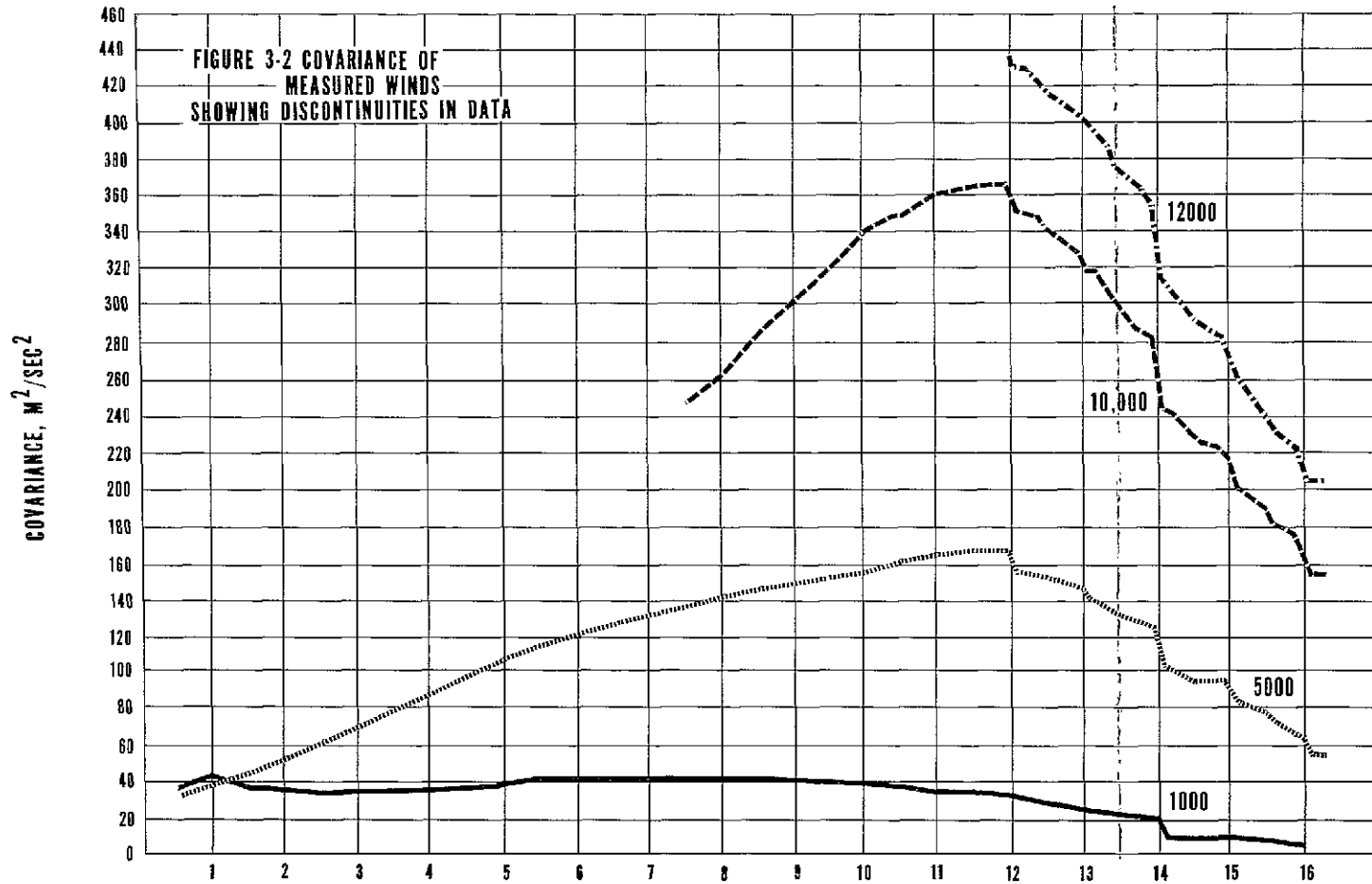
Thus, design of a vehicle based on these statistics would be adequate for a launch date picked at random, but would be underdesigned for a vehicle launched on a typical windy March day.

- The data contained only the Zonal wind component statistics.
- The data contained discontinuities in the covariance curves.

These discontinuities consisted of step decreases at 1000 meter increments above an altitude of 12 Kilometers, see Figure 3-2. These step decreases appeared to result from loss in Jimsphere data at these 1 Km intervals. Examination of a sample of Jimsphere profiles, (from Ref. 11,) revealed that some of the Jimsphere information was lost at higher altitudes. It was always the profiles showing the largest wind magnitudes that were lost at the high altitudes. Thus, the missing data represented only the higher magnitude winds. The omission of these high values in the calculation of wind covariances resulted in step decreases in the covariance curves at the altitudes where the Jimsphere profiles were terminated. These discontinuities not only represent biased covariance data, but greatly affect filter synthesis. Filter synthesis requires calculating derivatives of the covariance curves.

- The data contained small irregularities.

In addition to the discontinuities, small irregularities occurred randomly in the covariance data. It was difficult to establish if these irregularities contained covariance information or if they were primarily due to lack of an infinite sample size. It was concluded that the later was true. This meant that the covariance data must be smoothed to eliminate these irregularities.



FOLDOUT FRAME

1

FOLDOUT FRAME

3-5

2

(2) Rawinsonde Mean and Covariance Data from NASA TN D 3815, (Ref. 9).

This data was available from 8 years of twice daily measurements over Cape Kennedy. From this large sample of data, it was possible to consider the March wind statistics, which was one objective from an "ideal" wind model standpoint. The 8 years of twice daily wind measurements resulted in $30 \times 8 \times 2 = 480$ samples for the month of March. However, since the wind remains correlated for approximately 3 days, there were only $480/6=80$ independent samples. This is a sufficient sample size, but the problem associated with this data was;

- The data was available in only 1000 meter increments.

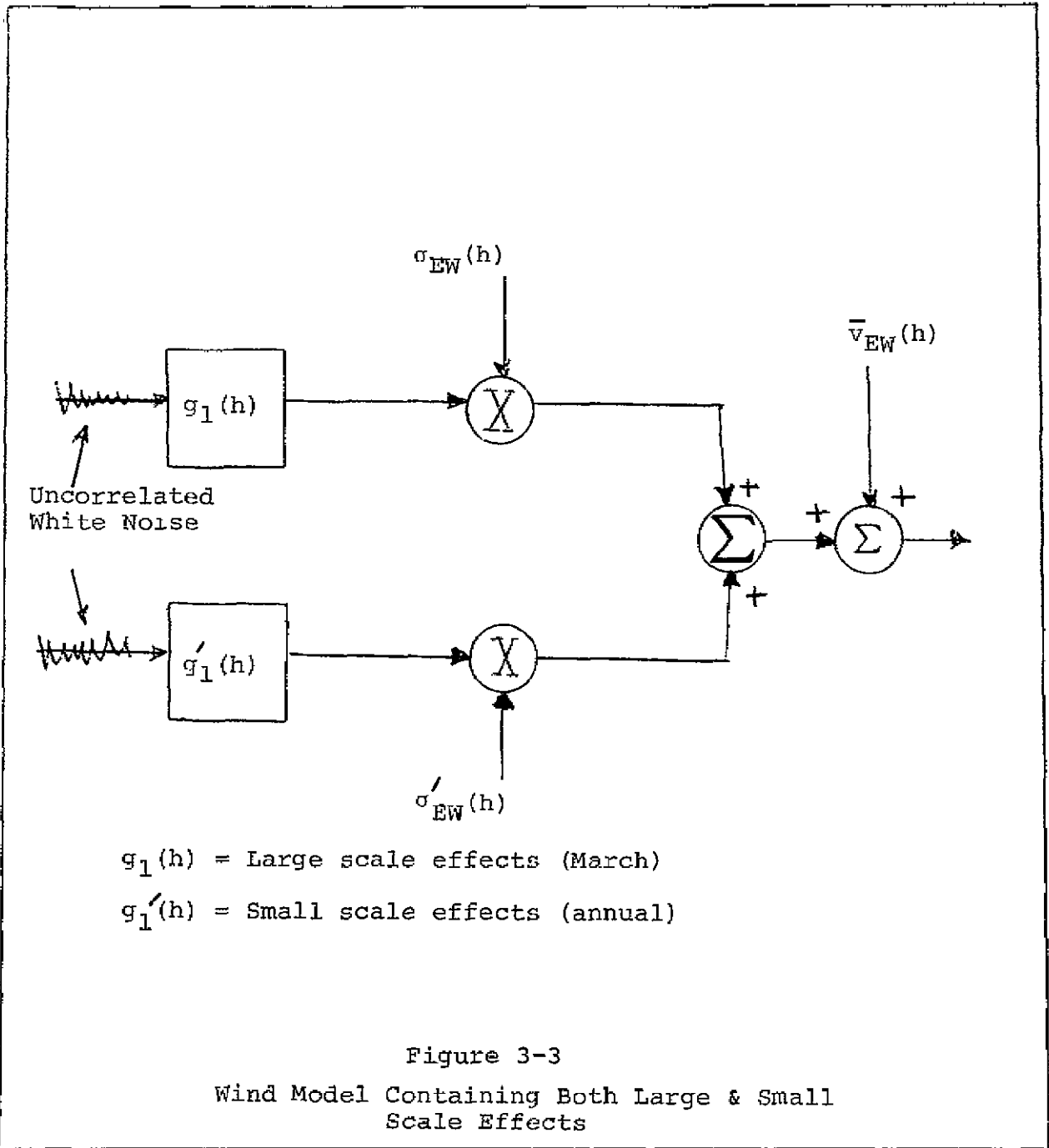
This is insufficient to include the "small scale" or turbulence information.

3.3 Final Wind Model Specification

As a result of data limitations the following approach to wind model design was taken:

- Use two sets of data; the rawinsonde data for large scale effects and the Jimsphere for small scale or turbulence effects.
- Model the large scale effects by synthesizing a filter capable of converting white noise to an output having the covariance of the rawinsonde measured winds.
- Model small scale effects by passing each of 1200 Jimsphere profiles through a high pass filter, filtering out all the large scale, low frequency, (rawinsonde-measured) effects and leaving only turbulence. The ensemble of turbulence profiles then is processed to obtain the covariance information.
- Model small scale effects by synthesizing a filter capable of converting white noise to a signal having the covariance of the wind turbulence.
- The total wind model then consists of two wind filters for each directional component (N-S, E-W). The output of the two filters, one representing large scale effects, the other representing turbulence, are then summed, producing a synthetic

wind field having both large and small scale effects. Figure 3-3 illustrates the form of the resulting wind model of the zonal (E-W) winds.



The model depicted in Figure 3-3 implies the assumption of statistical independence of turbulence and large scale effects. That is, the magnitude of the turbulence is independent of the magnitude of the large scale effects. This assumption is only approximately true, and its acceptability was to be checked when the turbulence component was extracted from the Jimsphere data. If it turned out not to be true, a correlation coefficient would be introduced between the signal from the large scale effects filter and that from the turbulence filter. This would be accomplished in a manner similar to that shown in Figure 3-1 for incorporating a correlation coefficient between E-W and N-S winds.

Because of time constraints only the zonal wind model was considered. The task of separating the turbulence from the Jimsphere data and obtaining its covariance was assumed by S&E-AERO-YE. Because of problems in processing this data the results were not available at the time of publication of this report. Thus, only the large-scale model was synthesized.

Working within the constraints described above;

- (1) The model shall consist of a zonal wind model made up of two elements
 - ° a large scale effects model
 - ° a turbulence model
- (2) The model shall be valid from 0 to 16 Kilometers
- (3) The large scale effects model shall consist of a linear, time varying filter capable of converting white noise to an output having the same covariance as the winds over Cape Kennedy during the month of March. The output statistics shall be within the 90% confidence limits of the rawinsonde data from NASA-TND-3815).
- (4) The turbulence model shall consist of a linear, time varying filter capable of converting white noise to an output having the covariance of the turbulence portion of the winds over Cape Kennedy. Covariance of the turbulence shall be determined in the manner described above. It shall be based on the most complete set of Jimsphere data available and thus be based on ensemble averaging over a complete year (as opposed to the month of March). The output covariances shall be within the 90%

confidence limits of the covariance data obtained in this manner.

- (5) If turbulence is found to be correlated with large scale effects, a correlation coefficient as a function of altitude shall be calculated and incorporated in the model.
- (6) Time permitting, a meridional wind model having the same specifications as those listed in items 1 - 5 above shall be synthesized. The two models shall be related by the intralevel correlation coefficient between the zonal and meridional wind components, as shown in Figure 3-1.

It is unfortunate that turbulence data never became available. The influence of turbulence statistics on overall vehicle response, would be an interesting statistical relationship. It is highly recommended that this effort be reinitiated when this data becomes available.

3.4 Filter Synthesis

3.4.1 The Synthesis Problem

The problem of constructing a filter meeting the specifications itemized in the preceding paragraph is a particularly difficult one. The difficulty stems from the non-stationarity of the statistics being matched. In order to match the non-stationary statistics, synthesis of a time varying filter is required. No general solution to this problem is known. Several approaches to synthesis were tried. These included;

- ° Linear Regression
- ° Parameter Optimization
- ° Constrained Response Optimization
- ° Impulse Response Generation/Curve Fit.

The method ultimately used was the Constrained Response Optimization method.

Since the names assigned to the methods are not completely descriptive, a brief description of each is given here, together with an evaluation.

3.4.2 Linear Regression Method

Background

This method of filter synthesis was used by Bailey, Palmer & Wheeler in NASA CR-846 (Ref. 12), and subsequently by Palmer as described in the final report on contract NAS 8-21444 (Ref. 8). In both efforts, annual zonal wind statistics were used as a basis for the wind model. In the first effort the covariance data was derived at 1000 meter increments from 600 Jimsphere wind soundings. In the NAS 8-21444 effort, covariance data was derived at 50 meter increments from 1200 Jimsphere soundings. Results from these efforts were not used here for these reasons;

- The models derived from these statistics were annual wind models instead of the desired March wind model.
- In the 1000 meter model, output statistics could not be verified (see Ref. 3, p 2-18).
- Examination of the 50 meter covariance data, (Ref. 8), showed discontinuities in the covariance curves, (see Figure 3-2). Since the linear regression method uses derivatives of the covariance curves in determining the filter coefficients, the discontinuities resulted in wildly varying coefficients. There is no physical reason for the discontinuities and hence coefficients derived from this data are significantly in error.

Since the filters developed in the above efforts were not directly usable, synthesis was required. One approach was to take advantage of the linear regression work from the above mentioned efforts and apply the same methods to the March wind covariance data with minor modifications.

Description of Method

The linear regression method is a two step method. The first step yields the time varying coefficients on the left hand side of the filter equation; and the second step yields the right hand side coefficients. To illustrate, the filter equation for an nth order filter in the altitude domain is;

$$a_n(h) \frac{d^n X(h)}{dh^n} + \dots + a_0(h) X(h) = b_m(h) \frac{d^m \eta(h)}{d(h)^m} + \dots + b_0(h) \eta(h)$$

where;

$a_i(h), b_j(h)$ = Altitude varying coefficients

$X(h)$ = filter output

$\eta(h)$ = white noise input to filter.

The $a_i(h)$ coefficients are determined first, then the $b_j(h)$ coefficients are determined.

As derived in Ref. (8), the covariance of the filter output, satisfies its differential equation;

$$a_n(h_2) \frac{d^n C(h_2, h)}{dh_2^n} + \dots + a_0(h_2) C(h_2, h) = b_m(h_2) \frac{d^m g(h_2, h)}{dh_2^m} + \dots + b_0(h_2) g(h_2, h), \quad (3-2)$$

where:

$C(h_2, h)$ = Covariance between the filter output at altitudes h_2 and h

$g(h_2, h)$ = Response of the filter at altitude " h_2 " due to an impulse input at altitude " h ".

It is easily seen that for $h > h_2$, (ie, an impulse input after the response to it is measured) $g(h_2, h) \equiv 0$. Equation 3-2 then can be written as;

$$a_n(h_2) \frac{d^n C(h_2, h)}{dh_2^n} + \dots + a_0(h_2) C(h_2, h) = 0; \quad h > h_2 \quad (3-3)$$

For a third order filter, equation (3-3) becomes;

$$\frac{d^3 C(h_2, h)}{d^3 h_2} + a_2(h_2) \frac{d^2 C(h_2, h)}{d^2 h_2} + a_1(h_2) \frac{dC(h_2, h)}{d h_2} + a_0(h_2) C(h_2, h) = 0; \quad h_2 > h$$

(3-4)

It is seen that if the derivatives of the covariance between altitudes h_2 , and h (h and h_2 are known), the $a_i(h_2)$, $i=0, 1, 2$ can be determined uniquely if there are exactly 3 equations of the form of Eq. (3-4), (i.e., 3 values of h used). If more equations of this form are available, a linear regression procedure is used. This procedure is formulated as follows:

For a fixed h_2 , find the set of $a_0(h_2)$, $a_1(h_2)$ and $a_2(h_2)$ which, when substituted into;

$$C'''(h_2, h_i) + a_2(h_2)C''(h_2, h_i) + a_1(h_2)C'(h_2, h_i) + a_0(h_2)C(h_2, h_i) = 0,$$

for $i = 1, 2, \dots, r$

minimizes;

$$\sum_{i=1}^n \left[C'''(h_2, h_i) + a_2(h_2)C''(h_2, h_i) + a_1(h_2)C'(h_2, h_i) + a_0(h_2)C(h_2, h_i) \right]^2$$

(3-5)

$$\text{where } C' = \frac{d \text{Cov}(h_2, h_i)}{dh_2}$$

For example the "a" coefficients for an altitude of 8 kilometers are obtained from the least squares fit to;

$$\frac{d^3 C(8, 7)}{d h_2^3} + a_2(8) \frac{d^2 C(8, 7)}{d h_2^2} + a_1(8) \frac{d C(8, 7)}{d h_2} + a_0(8) C(8, 7) = 0$$

$$\frac{d^3 C(8, 6)}{d h_2^3} + a_2(8) \frac{d^2 C(8, 6)}{d h_2^2} + a_1(8) \frac{d C(8, 6)}{d h_2} + a_0(8) C(8, 6) = 0$$

$$\vdots$$

$$\frac{d^3 C(8, 1)}{d h_2^3} + a_2(8) \frac{d^2 C(8, 1)}{d h_2^2} + a_1(8) \frac{d C(8, 1)}{d h_2} + a_0(8) C(8, 1) = 0$$

This was the procedure used to obtain the filter coefficients. The method used to obtain the derivatives of the covariance data required in equation 3-4 is described in Appendix A.

The second step in the linear regression method is determination of the right hand side coefficients. The method used was a direct extension of the method used in Ref. (8) for a second order filter. The same logic was used for the third order filter. The equations describing the procedure used to get both second and third order filter numerator coefficients are given in Appendix B.

Evaluation of the Method

Two sets of filter coefficients were obtained using the linear regression method,

- (1) 2nd order filter coefficients, and
- (2) 3rd order filter coefficients.

In neither case did the filters defined by these coefficients yield covariances within the 90% confidence intervals of the given covariance curves. In fact, the results were not even of the same order of magnitude.

The problem source is in evaluation of the right hand side coefficients. This problem can be illustrated by considering the equations for obtaining the right side coefficients of the second order filter. From equation B-7 in Appendix B the coefficient $b_1(h_2)$ is given by:

$$b_1(h_2) = \sqrt{\frac{dC(h_2, h)}{dh} \Big|_{h=h_2^-} - \frac{dC(h_2, h)}{dh} \Big|_{h=h_2^+}} \quad (3-6)$$

Only near the point $h \approx h_2^- \approx h_2^+$ is this equation valid. The data from which the covariance derivatives are taken are 1000 meters apart. Thus, there is no adequate way to evaluate the $b_1(h_2)$ coefficient.

Physically, there is no reason why the derivatives at h_2^+ , and h_2^- should be different from each other. If this is assumed, the $b_1(h_2)$ coefficient would always be = zero. This was tried but did not yield any better results.

The method was dropped after all attempts to verify the results from it failed.

3.4.3 Parameter Optimization Method

Background

When the filter derived from the linear regression method failed to yield covariances within the specified limits of the given covariances, an effort was made to improve the estimates of the coefficients. This improvement effort was applied to the second order filter only. The method employed consisted of changing the four altitude varying coefficients in the direction which tended to minimize the error squared between the covariances of the wind and the covariances of the filter output.

Description of Method

The parameter optimization method was applied in several ways. The objective function in all cases was minimization of the sum-of-the-errors squared between actual and calculated covariances;

$$\text{Obj. Function} = J = \sum_{i=1}^{16 \text{ Km}} \sum_{j=i}^{16 \text{ Km}} [\text{Cov}_A(i,j) - \text{Cov}_C(i,j)]^2, \quad (3-7)$$

where:

$\text{Cov}_A(i,j)$ = Actual covariance of wind at altitudes i & j
for the month of March

$\text{Cov}_C(i,j)$ = Calculated covariance of the filter adjoint.

In one case the filter coefficients were allowed to change by a constant multiple factor;

$$b_0(i) \text{ NEW} = K_0 b_0(i) \text{ OLD}$$

$$b_1(i) \text{ NEW} = K_1 b_1(i) \text{ OLD}$$

$$a_0(i) \text{ NEW} = K_2 a_0(i) \text{ OLD}$$

$$a_1(i) \text{ NEW} = K_3 a_1(i) \text{ OLD}$$

The four "K's" which yielded the smallest objective function were then determined using the "hillclimbing" optimization procedure. This procedure yielded K_i 's of;

$$K_0 = -.00558$$

$$K_1 = .42605$$

$$K_2 = .05575$$

$$K_3 = 1.095$$

These K's were based on minimizing the error squared of the covariances over the first 8 kilometers. The procedure resulted in reducing the sum-of-the errors squared of the 36 covariances from 9.7×10^5 to 8.13×10^4 . In terms of average error in the covariances this is a reduction from $164M^2/Sec^2$ to an average error of $47.5M^2/Sec^2$. Although this is considerably lower in terms of average error, it is still unacceptable. It appeared that the coefficients must be allowed to vary independently at all altitudes. When this was tried using the coefficients obtained from the above procedure as a starting point, the average error in covariance was reduced from $47.5M^2/Sec^2$ to $46.1M^2/Sec^2$. This was not a significant improvement.

A second application of the optimization procedure to obtain better estimates of the filter coefficients was tried. This application was based on the idea that no physical reason exists for a discontinuity in the derivatives of the covariance curves $C(h_2, h)$ at $h = h_2$. From equation (3-6) we saw that the " b_1 " filter coefficient is determined from the difference in derivatives at $h = h_2$;

$$b_1(h_2) = \sqrt{\left. \frac{dC(h_2, h)}{dh} \right|_{h=h_2^-} - \left. \frac{dC(h_2, h)}{dh} \right|_{h=h_2^+}} \quad (3-6)$$

Assuming the value under the square root sign is = 0;

$$b_1(h_2) = 0, h_2 = 0, \dots, 16 \text{ Km.}$$

The optimization scheme was applied to the $a_1(h_2)$, $a_0(h_2)$, and $b_0(h_2)$ coefficients. The originally calculated " $a_i(h)$ " coefficients were used as a starting point for the optimization procedure. The starting values for the $b_0(h_2)$ coefficient were selected by forcing the $b_0(h_2)$ coefficients to yield the correct variances. The $a_0(h_2)$ & $b_0(h_2)$ were then varied to minimize the sum of the errors in the covariances over the first ten kilometers. This procedure yielded an average error in the covariances of 20 M^2/Sec^2 over the first 10 Kilometers. At this point, the optimization routine became "caged", and slight improvement become costly.

The computer program used to optimize the second order filter coefficients in this manner is listed in Volume 2 of this report.

Evaluation of Method

The parameter optimization method is a brute force attempt at finding filter coefficients. It is extremely costly computationally. For this reason the method is not desirable. Another problem with the technique is it's susceptibility to local minimums. When the average error in the covariances reached 20 meters²/ Sec², a local minimum was reached and improvement became impossible.

The method was applied to determining coefficients only up to 10 kilometers. The reason for this was to limit the number of variables allowed to vary in the optimization routine. If the technique would have converged more rapidly, the procedure would have been extended to the full 16,000 meter range of interest. Also, improvement of the third order coefficients would have been attempted. Computation expense prevented extension of the technique.

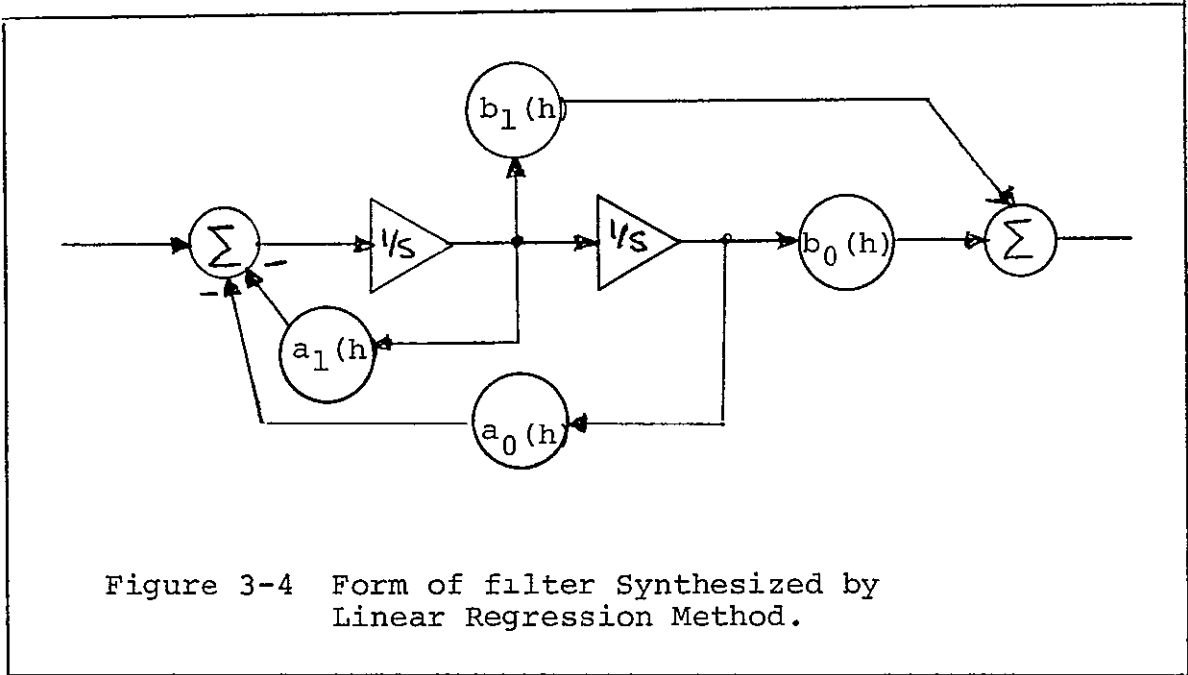
3.4.4 Constrained Response Optimization Method

Background

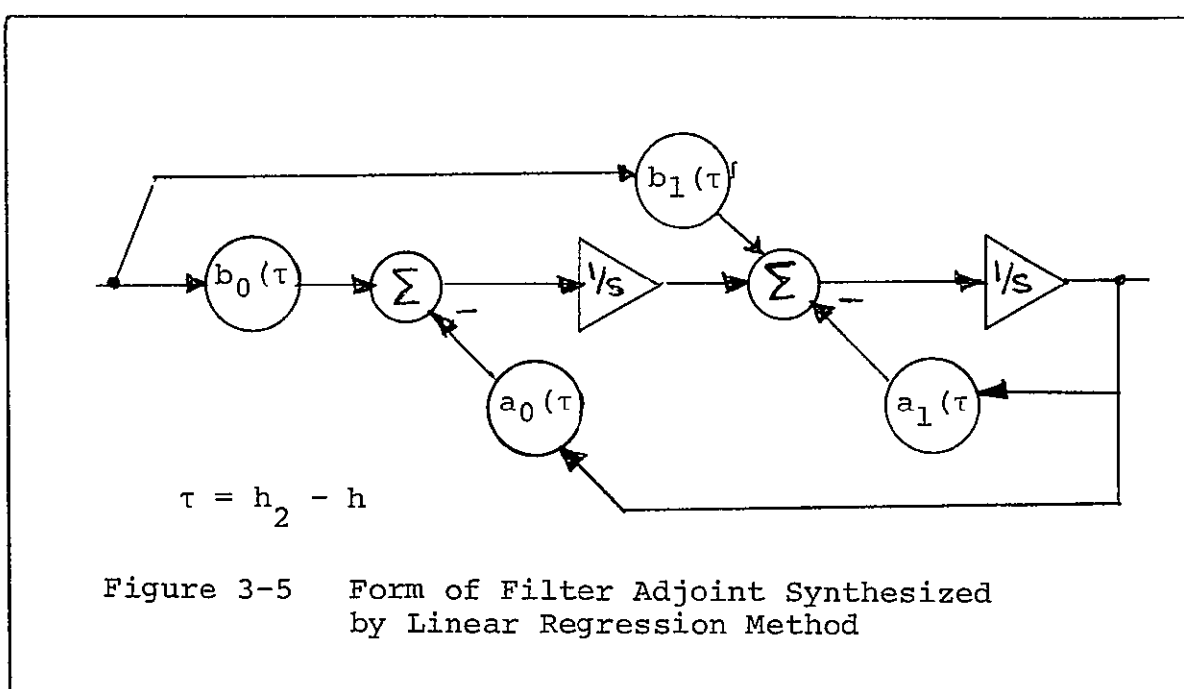
Because of the excessive computer run times and local minimum problems associated with the parameter optimization method of paragraph 3.4.3, an alternate approach was initiated. This alternate method used the same optimization scheme and same objective function, but utilized a different set of adjustable parameters for matching the covariance of the wind. To illustrate the method, it is desirable to compare it with the previously described parameter optimization method.

In the parameter optimization method we started with an estimate of the filter coefficients as determined from the linear regression procedure. These estimates defined

a second order filter of the form shown in Figure 3-4.
 The filter defined in this manner is verified by



first forming its adjoint. This is done by the rules
 of paragraph 2.1. The resulting adjoint model is shown
 in Figure 3-5.



When forced with a unit impulse at an altitude h_2 , (i.e. set all coefficients equal to their value at h_2)², the output of the filter is the weighting function $g(h_2, h)$, generated as a function of h . As developed in paragraph 2.1, this $g(h_2, h)$ can be squared and integrated for $h = 0$ to h_2 , yielding the variance of the output of the filter at altitude h_2 ;

$$\sigma^2(h_2) = \text{COV}(h_2, h_2) = \int_0^{h_2} g^2(h_2, h) dh. \quad (3-8)$$

Or, two separate simulation models of the filter can be used to obtain the covariance between the outputs at two different altitudes. This is accomplished by forcing the adjoints of the two models at different altitudes, h_2 and h_1 , multiplying the responses and integrating the product to obtain the covariance between the filter outputs at h_2 , and $h_1, \leq h_2$;

$$\text{COV}(h_2, h_1) = \int_0^{h_1} g(h_2, h) g(h_1, h) dh. \quad (3-9)$$

By repeating this process for all combinations of h_2 and $h_1, h_2 = 0, 16; h_1 = 0, h_2$, the covariance curves defining the filter output statistics are obtained, thus forming a basis for comparison with the actual measured wind statistics.

It is seen that this filter verification procedure is quite lengthy computationally. In order to accurately generate the impulse response functions, $g(h_2, h)$ from the digital simulation models of the filters, it is necessary to use a small integration interval. Because of this requirement for a small integration interval, run times to obtain the complete covariance matrix are quite lengthy. Using the GE 635 time share system, it takes approximately 15 minutes of terminal time (approximately \$.00 computer cost) just to generate the covariance matrix at 1000 meter increments, (ie 136 values of covariance).

In order to apply the parameter optimization procedure described in the paragraph 3.4.3 it is required to calculate this covariance matrix many, many times in order to determine which coefficients should be changed, how much they should be changed, and at what altitudes they should be changed in order to minimize the sum of the errors squared over the entire covariance matrix.

Description of Method

The "Constrained response optimization method" described here significantly reduces the time required to determine the covariance matrix. The source of this time savings is a result of an allowable lengthening of the integration interval by a factor of 100. This 2 orders of magnitude increase in integration interval not only makes the optimization procedure feasible, but permits consideration of higher order filters.

The significant difference in this method and the straight parameter optimization method of paragraph 3.4.3 is in the manner in which the impulse response curves, $g(h_2, h)$ are generated. In the parameter optimization method, these curves were generated from the output of the filter adjoint digital simulation models.

In the constrained response optimization procedure, these response curves are generated from an assumed analytical expression;

$$g(h_2, h) = A(h_2) e^{\alpha_1(h) * h} + B(h_2) e^{\alpha_2(h) * h} \cos(\omega(h)h + \psi(h_2)). \quad (3-10)$$

The optimization problem here, is to find the set of coefficients, $A(h_2)$, $B(h_2)$, $\alpha_1(h)$, $\alpha_2(h)$, $\omega(h)$ and $\psi(h_2)$ which minimize the objective function, equation 3-7. In this procedure, the only required integration is that of the product of the $g(h_2, h) * g(h_1, h)$ for all pairs of h_2, h_1 .

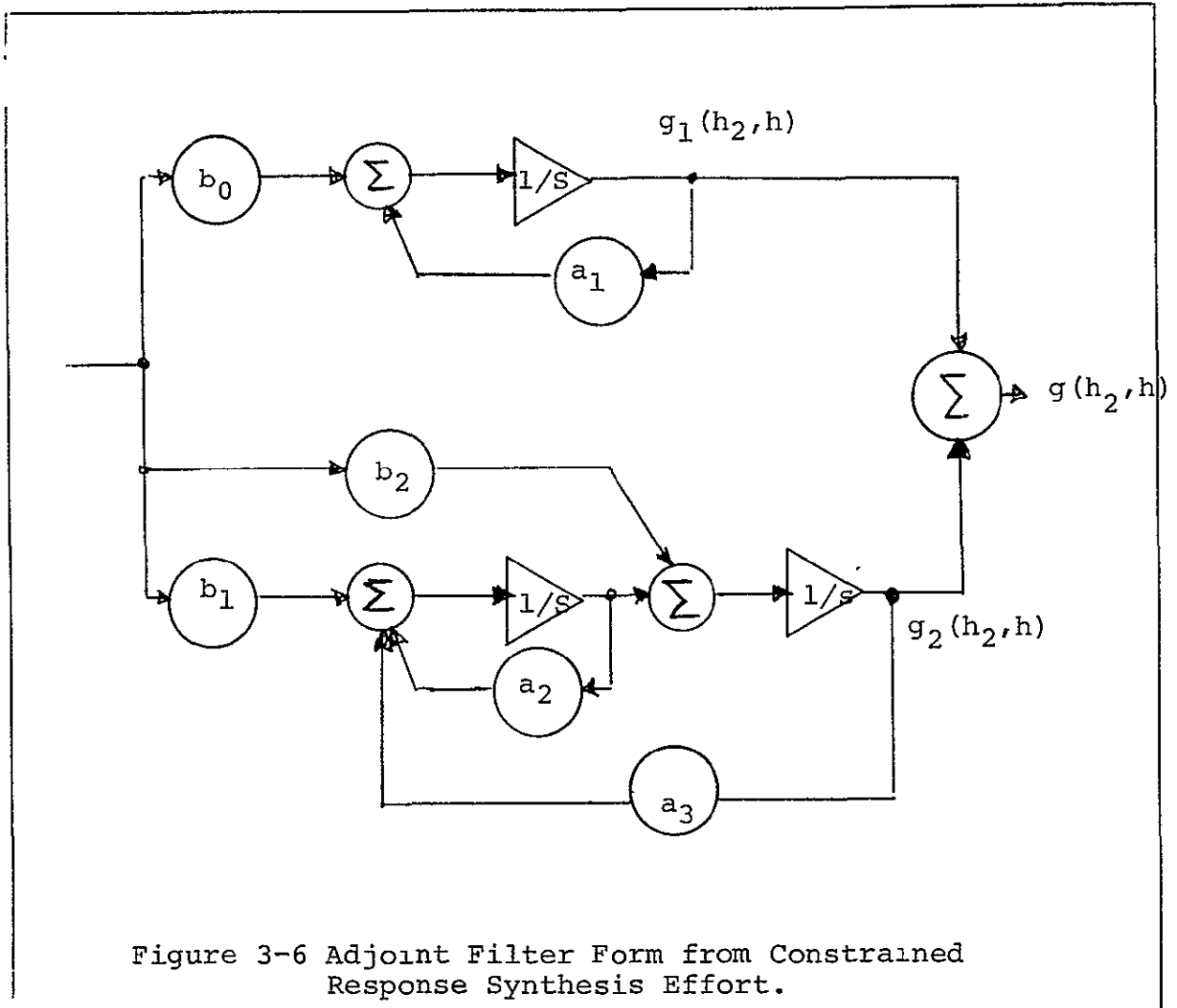
The method gets its name, "constrained response method" from the fact that the response is constrained to the form of equation (3-10). In terms of a "frozen" filter function, this constrained response limits the filter to having exactly one real root and one complex pair at a given altitude. In the parameter optimization method there is no such limitation.

The optimization logic used in determining the direction and magnitude to change each of the coefficients at each of the 16 discrete values of altitude, was developed for application to this specific problem. Details of the method are given in Appendix C.

The computer program is documented in volume 2 of this report. The program name is "OPTFIL".

The actual filter coefficients are derived from the constrained response coefficients. Details of this transformation are given in Appendix D. The result of this transformation is definition of a third-order filter of the form shown in Figure 3-6. The computer programs for performing this transformation are documented in Volume 2 of this report

under the name "ICC" and Filter".



Evaluation of Method

The Constrained Response Optimization method yielded a large-scale zonal wind model meeting the specifications of paragraph 3.3. The average error in the covariances was $14 \text{ M}^2/\text{Sec}^2$. The method is reasonably efficient and adaptable to higher order models. It is recommended for use in any immediate wind filter synthesis efforts. A complete summary of results from this filter is presented in paragraph 3.4.7.

3.4.5 Impulse Response Generation/

Curve Fit Method

This method was never fully developed and evaluated. It does, however, deserve mention here because of its potential promise as a synthesis technique. This method is based on developing a set of impulse response curves, $g(h_2, h)$, which, if matched, would yield the desired covariances. The desirability of this technique lies with the fact that it is a curve that is being fit, rather than the integral of the product of the curve with another curve. The problem is infinitely simpler.

The key to application of the method is the ability or the inability to specify a set of $g(h_2, h)$ curves to be fit.

An approximate method for specifying a set of $g(h_2, h)$ curves was developed during the course of this effort. The method is as follows;

given;

$$\text{COV}(1000, 1000) = \int_0^{1000} g^2(1000, h) dh \approx 1000 * \frac{\overline{g^2(1000, h)}}{1000} \Big|_0^{1000}$$

(3-11)

where,

$$\overline{g(1000, h)} \Big|_0^{1000} = \text{average value of the impulse response curve over the range of altitudes from 0 to 1000 meters.}$$

then;

$$\overline{g(1000, h)} \Big|_0^{1000} = \frac{\text{COV}(1000, 1000)}{1000}$$

For compactness, let:

$$g_{11} = \overline{g(1000, h)} \Big|_0^{1000}$$

Now, in a similar manner,

$$\text{COV}(1000, 2000) = \int_0^{2000} g(2000, h)g(1000, h)dh$$

$$\text{or, } \text{COV}(1000, 2000) \approx \begin{bmatrix} 1000 * g(2000, h) & 1000 \\ 0 & 1 \end{bmatrix} * g_{11}$$

$$\approx 1000 g_{21} * g_{11}$$

$$\text{or } g_{21} = \frac{\text{COV}(1000, 2000)}{1000 * g_{11}}$$

This process can be continued and eventually, all the average values of the $g(h_2, h)$ can be calculated over each 1000 meter interval. The only thing left to do at this point is to fit an altitude varying function through these average values of $g(h_2, h)$.

It would have been interesting to explore this technique further, but time did not permit. It is entirely probable that this technique may result in an even more efficient method of synthesizing the filter coefficients, than the constrained response optimization method actually used. This method is actually another approach to the constrained response method, but it is more direct since all the variances and covariances do not have to be calculated repeatedly as they did when the constrained response approach of paragraph 3.4.4.

3.4.6 Transformation from Altitude to Flight-Time

Domain

In order to be combined and used with the vehicle model, the filter must be converted for use in the flight-time domain. This transformation is derived in Appendix E for the third order filter configuration of Figure 3-6. Coefficients defining the filter are shown in Figures 3-7 through 3-12.

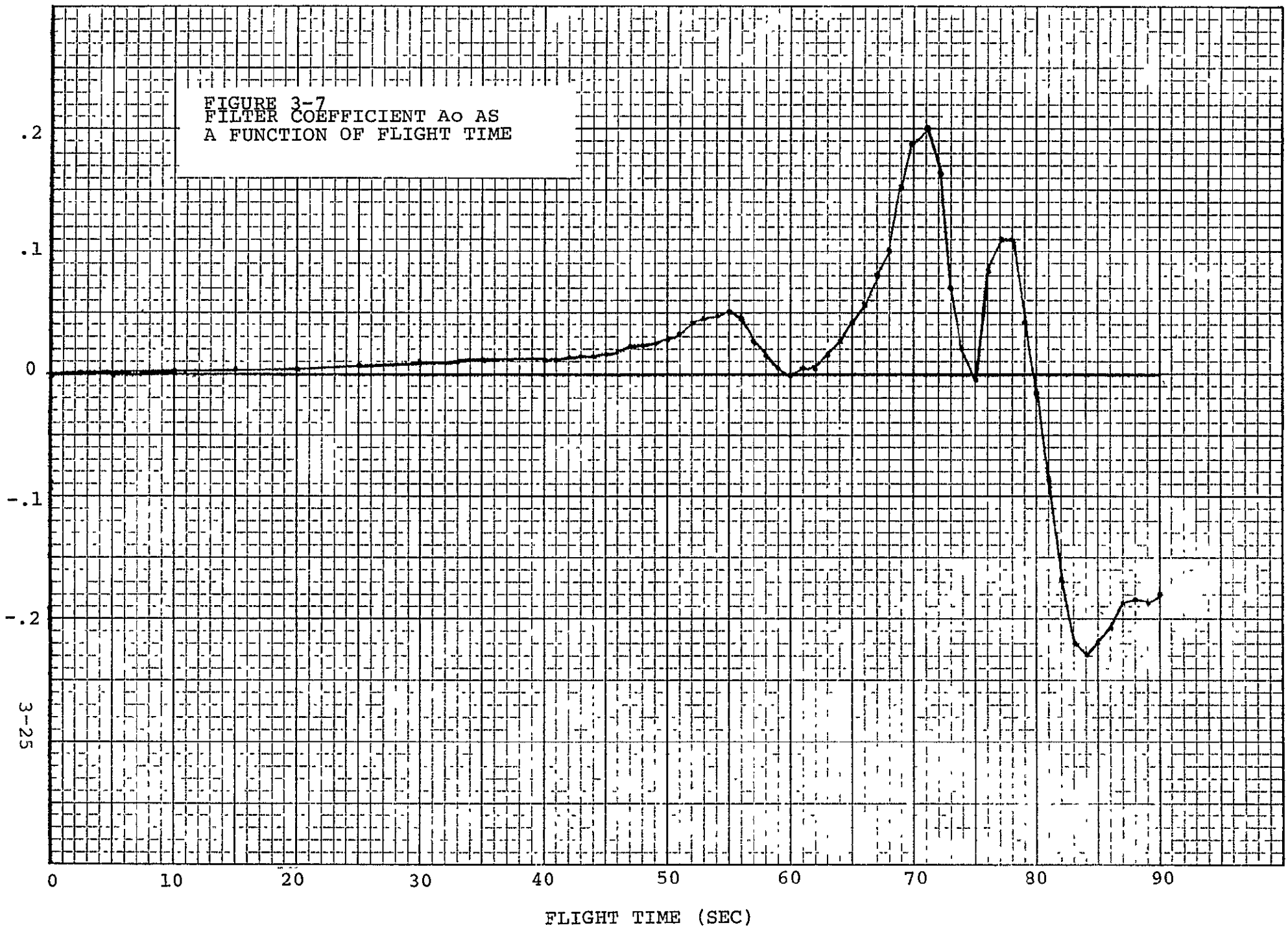
3.4.7 Wind Model Output

The final form of the wind model is that of figure 3-6, resulting from the constrained response optimization method. Filter coefficients are shown in Figures 3-7 through 3-12. The covariances obtained from this model are plotted in Figures 3-13 through 3-15. The method used to obtain the covariance curves from the filter simulation model is described in paragraph 3.4.4. To illustrate the degree to which the filter derived covariances fell within the 90% confidence intervals of the given covariance data, the 9000 meter covariance curve is plotted together with its 90% confidence interval in Figure 3-16. The covariance curve calculated from the filter output is also plotted here.

The 90% confidence band was determined from the Chi-Squared probability tables, (Ref 13), based on an independent sample size of 80.

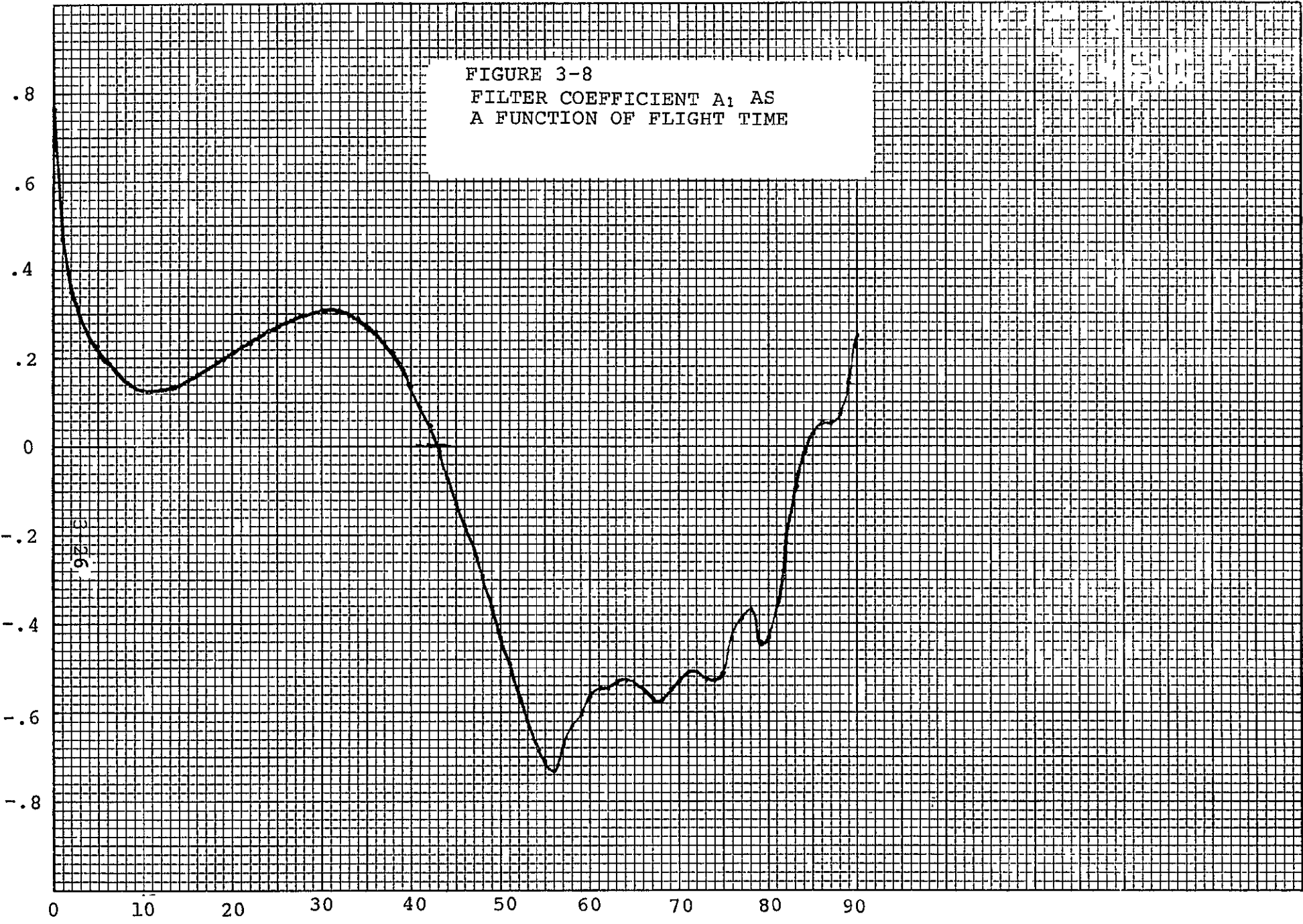
The 90% confidence band is that range of values for which one can be 90% confident that the true variance lies within this interval. Of course, the more samples used in calculating the sample variance, the narrower the confidence band.

FIGURE 3-7
FILTER COEFFICIENT A_0 AS
A FUNCTION OF FLIGHT TIME



3-25

FIGURE 3-8
FILTER COEFFICIENT A_1 AS
A FUNCTION OF FLIGHT TIME



FLIGHT TIME (SEC)

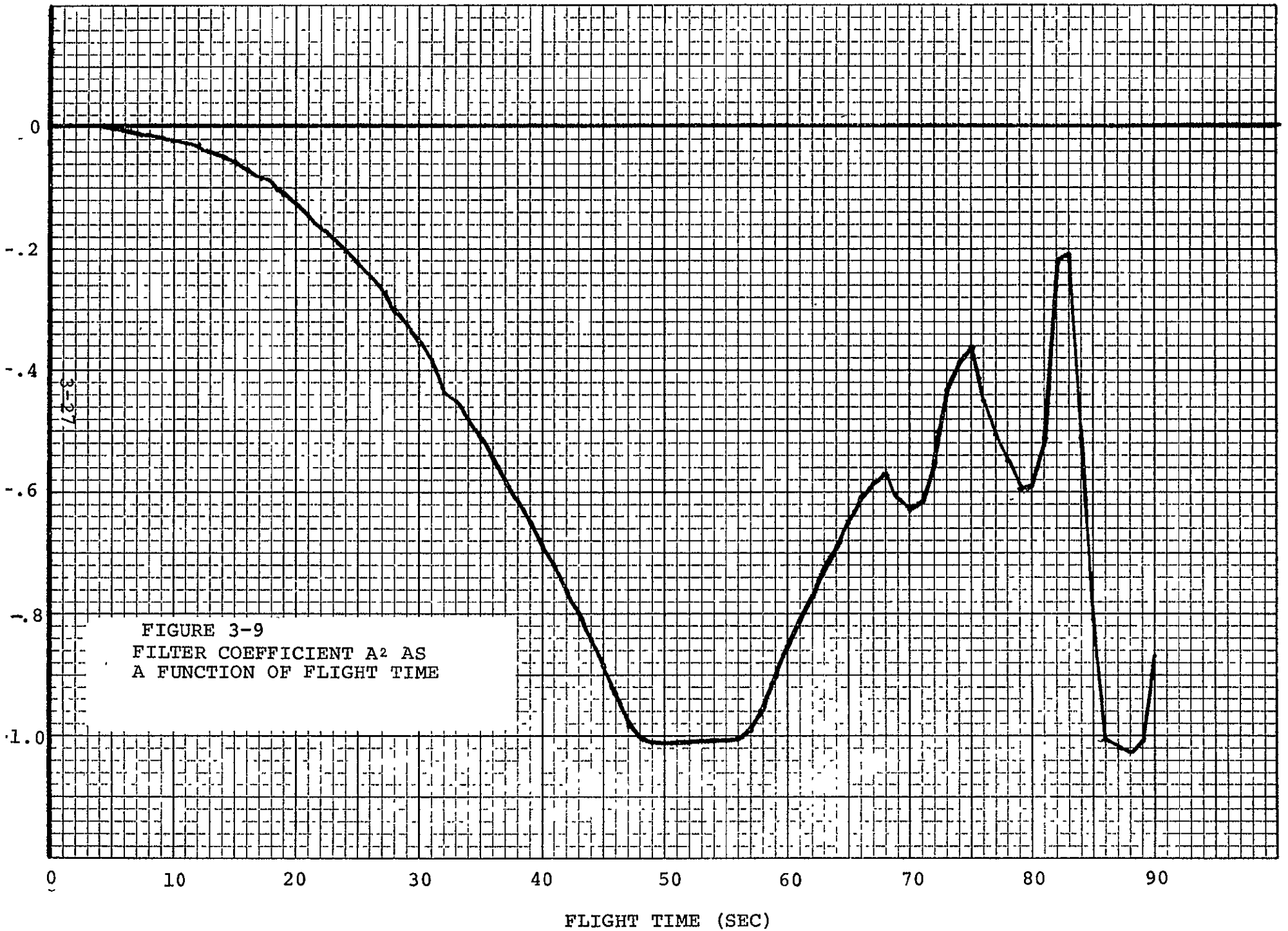
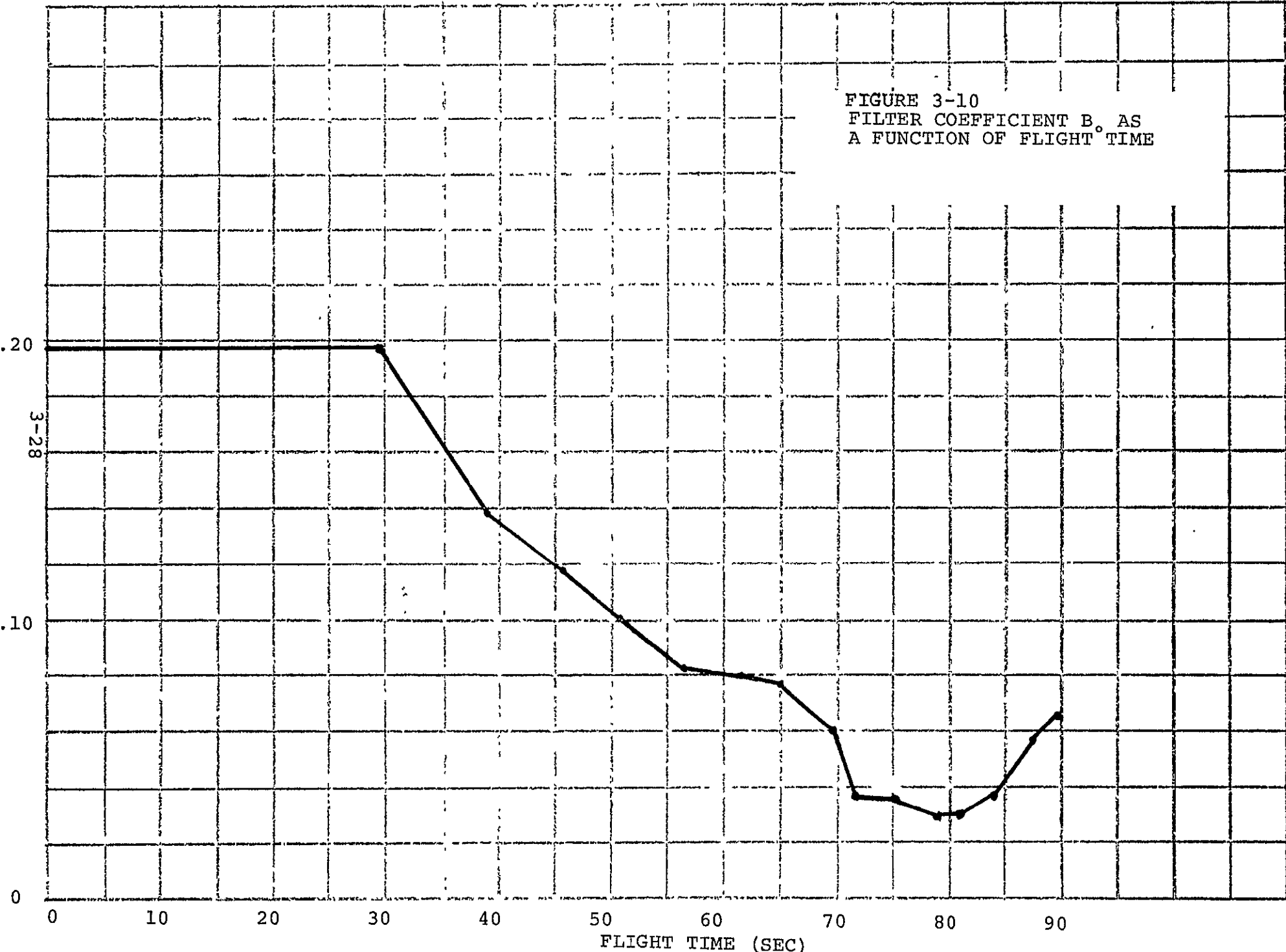


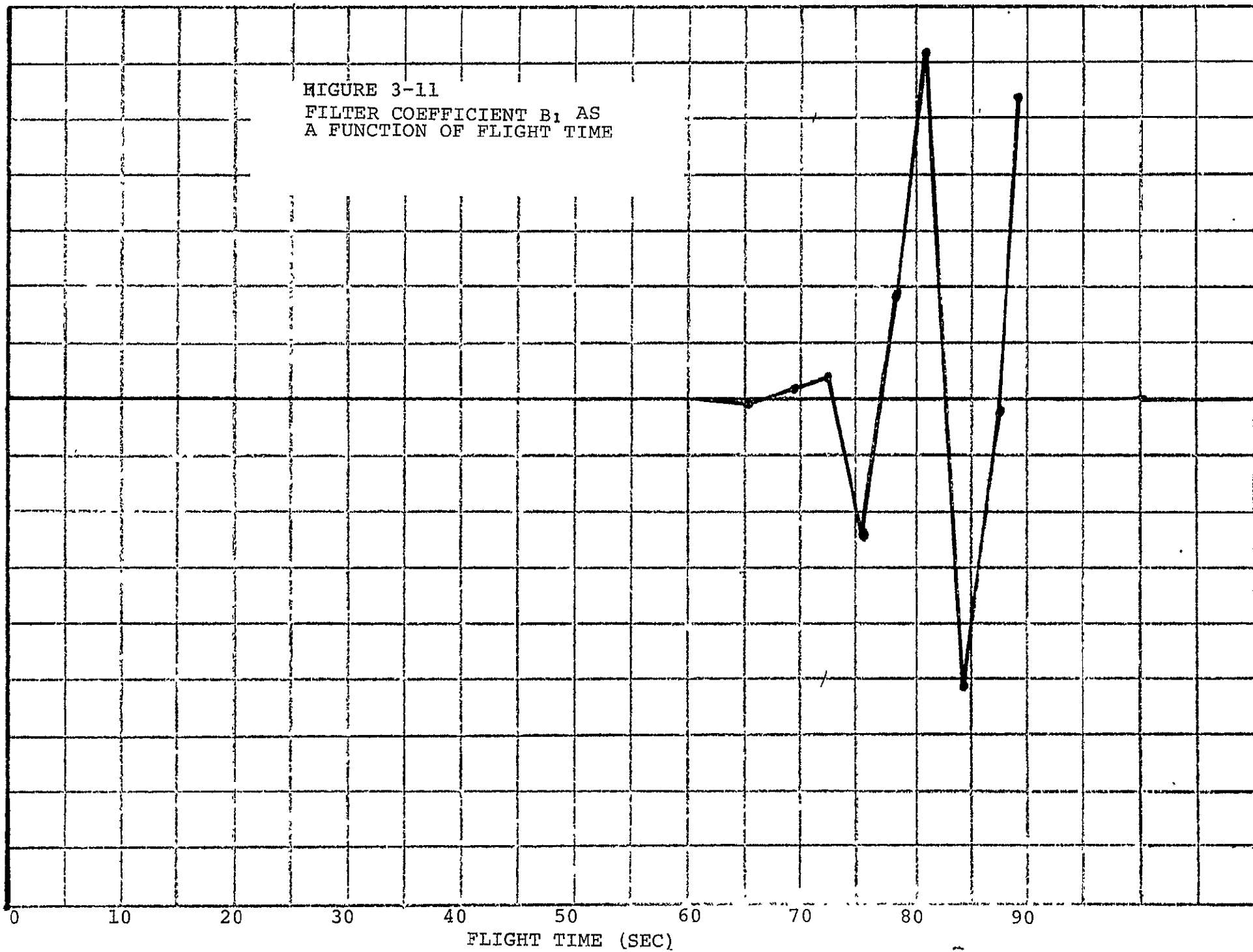
FIGURE 3-10
FILTER COEFFICIENT B_0 AS
A FUNCTION OF FLIGHT TIME



3-28

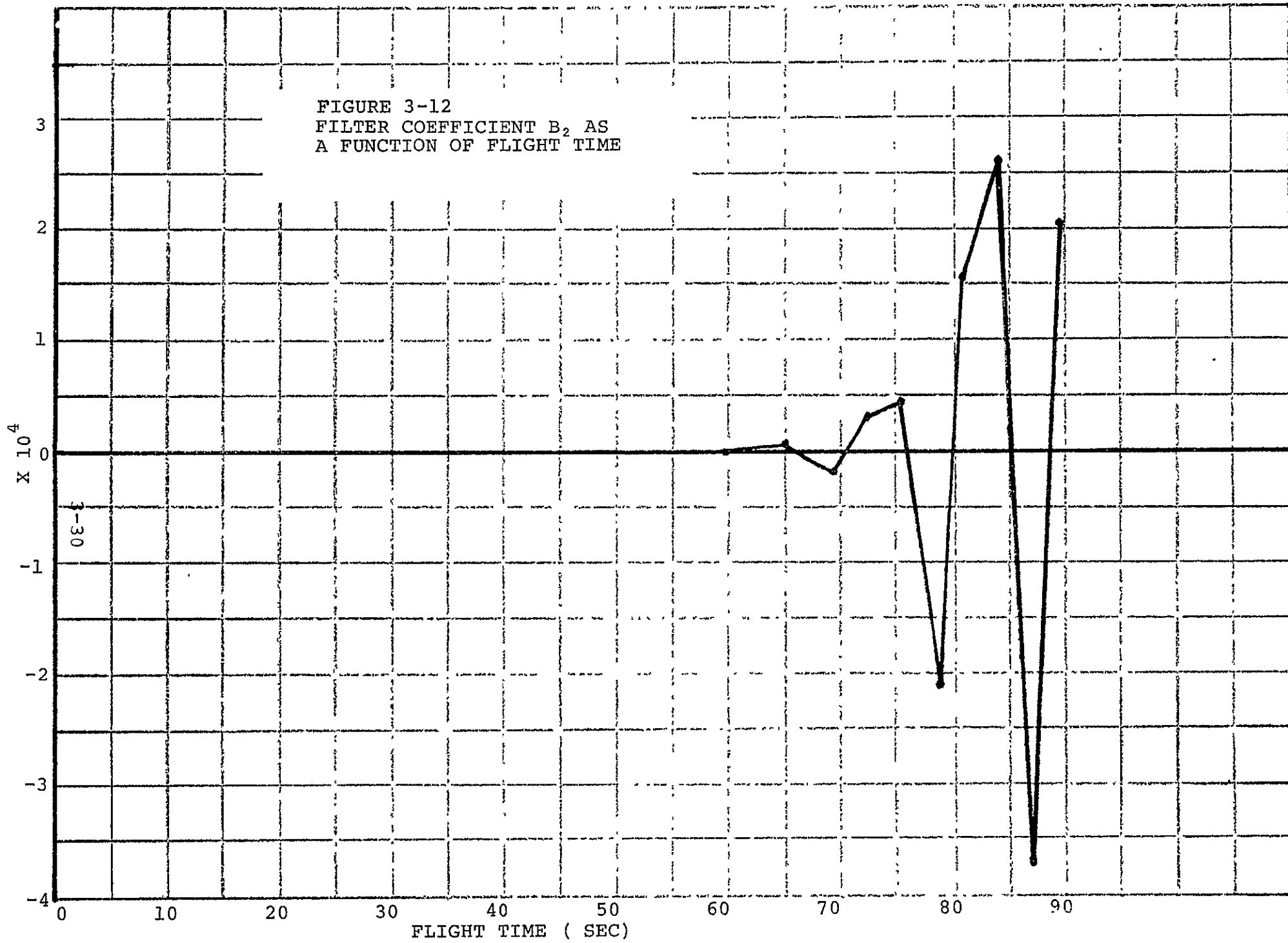
FLIGHT TIME (SEC)

FIGURE 3-11
FILTER COEFFICIENT B_1 AS
A FUNCTION OF FLIGHT TIME



.1
0
3-29
-1

FIGURE 3-12
FILTER COEFFICIENT B_2 AS
A FUNCTION OF FLIGHT TIME



3-30

3-31

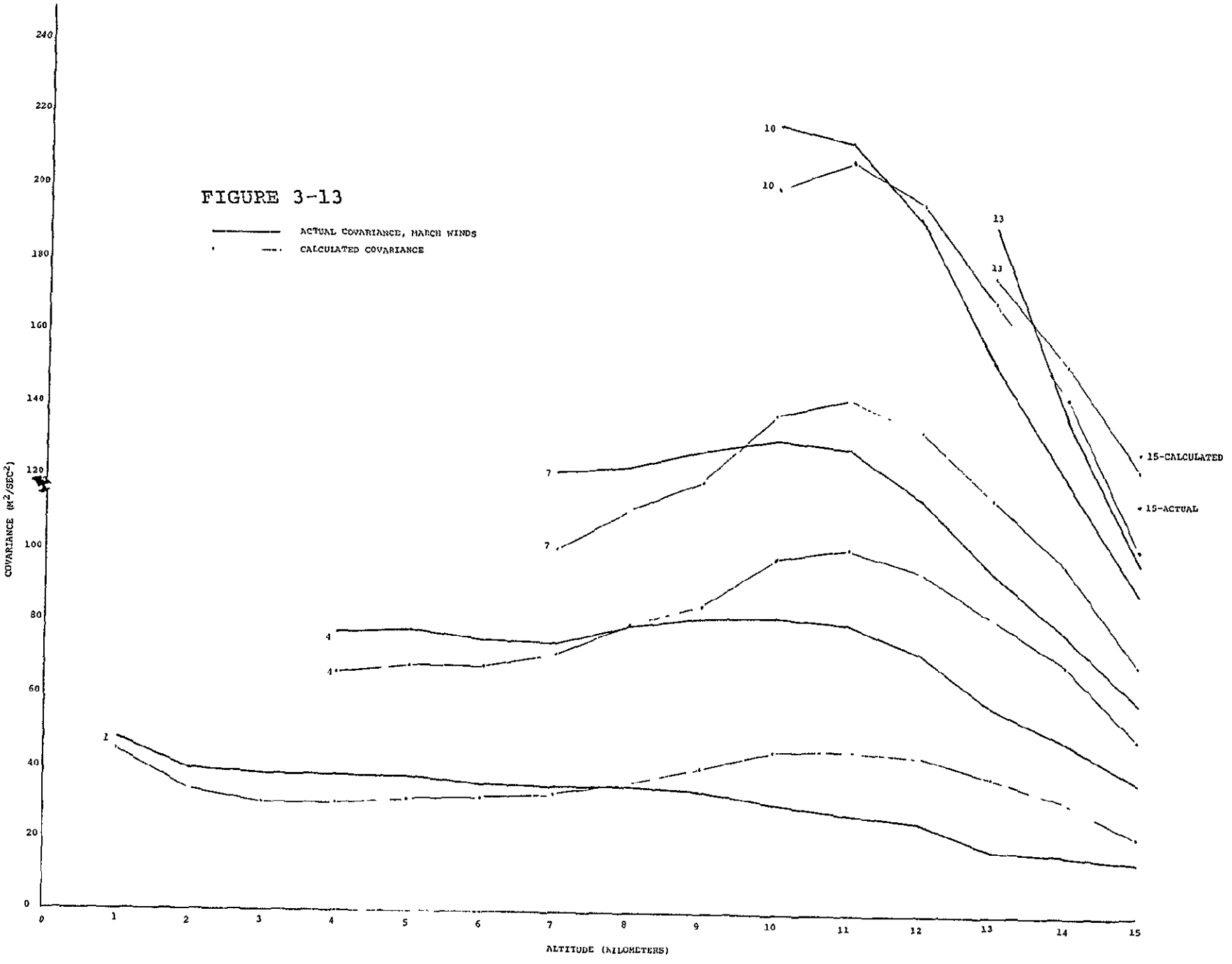
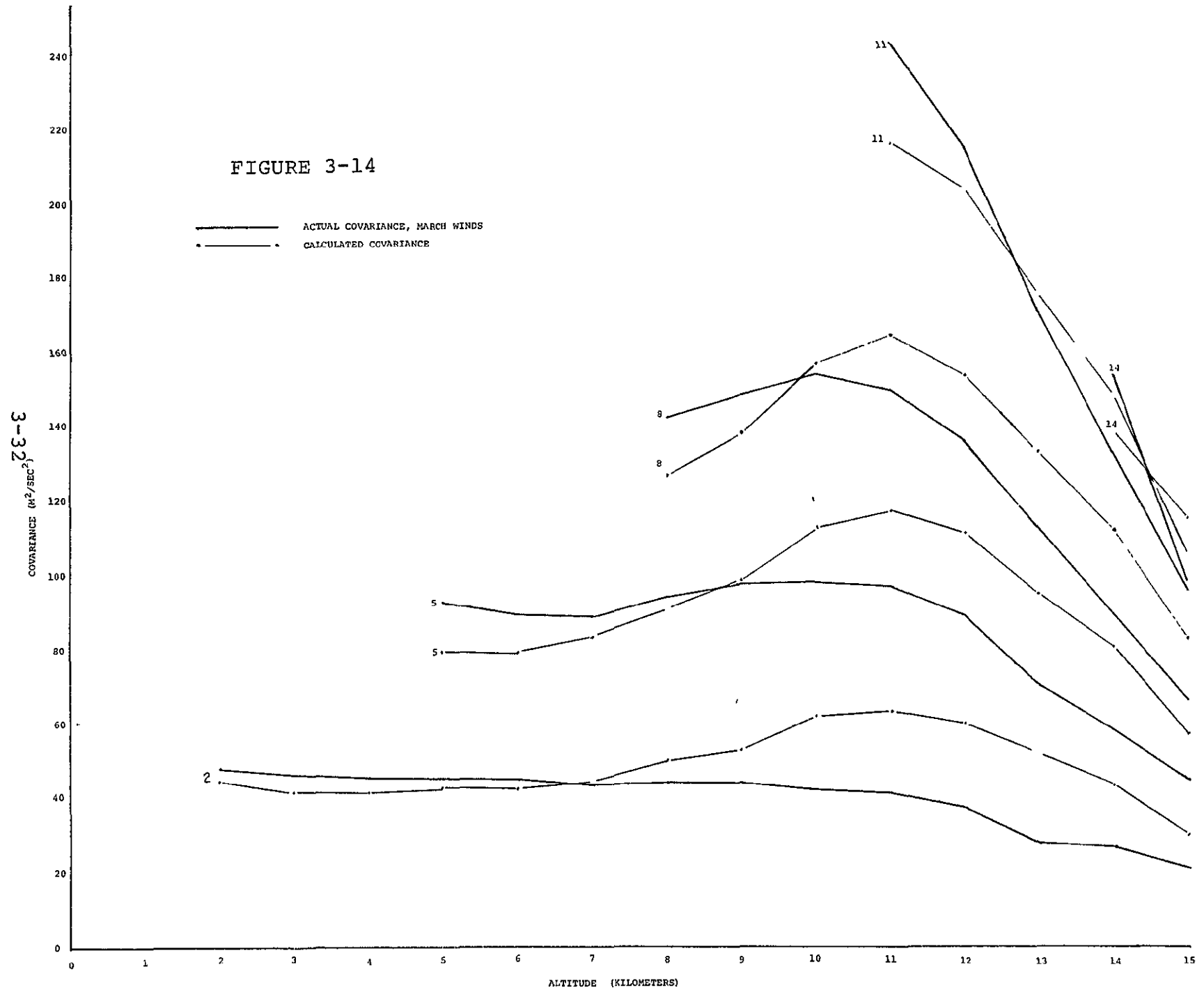


FIGURE 3-13

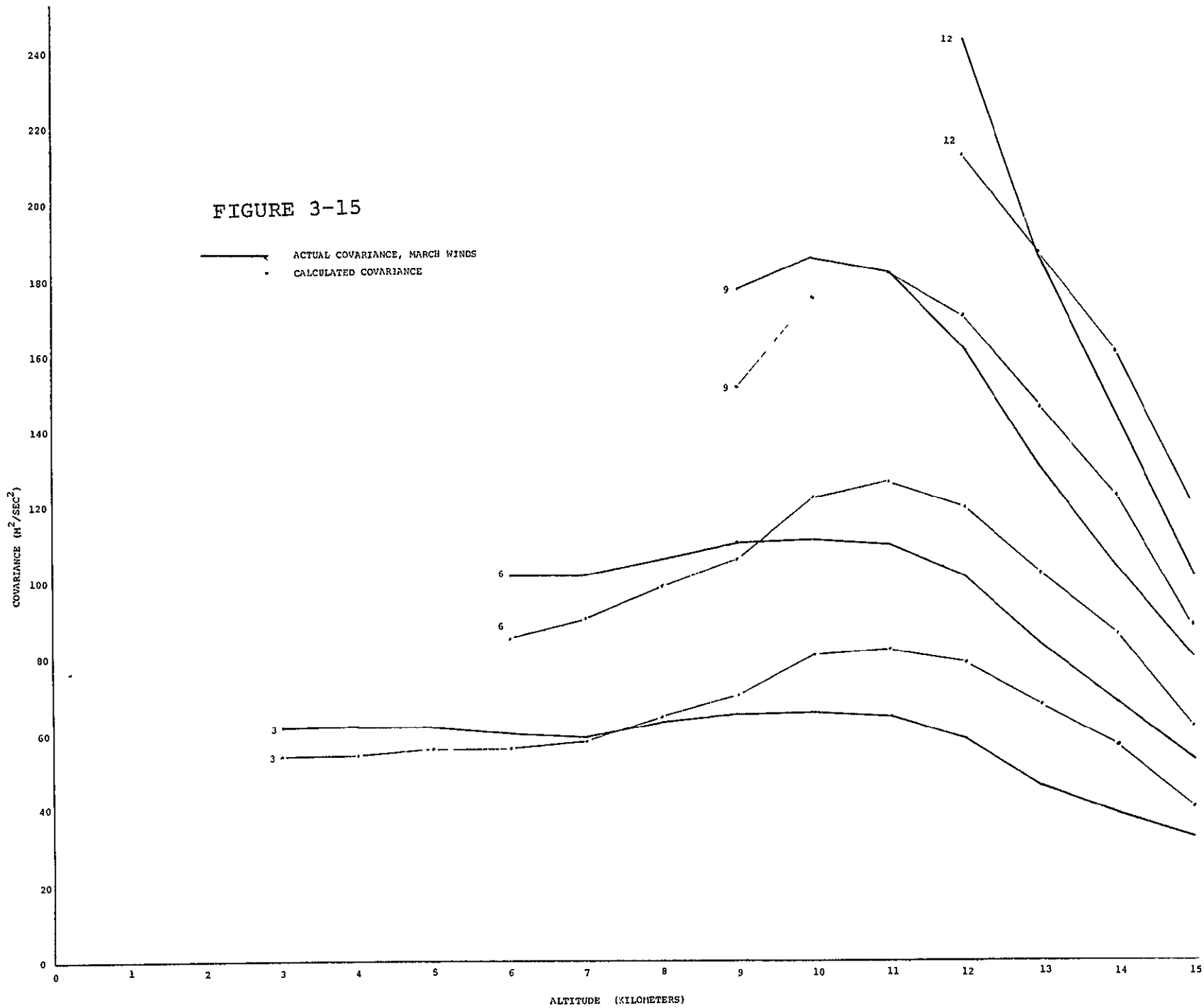
— ACTUAL COVARIANCE, MARCH WINDS
- - - CALCULATED COVARIANCE

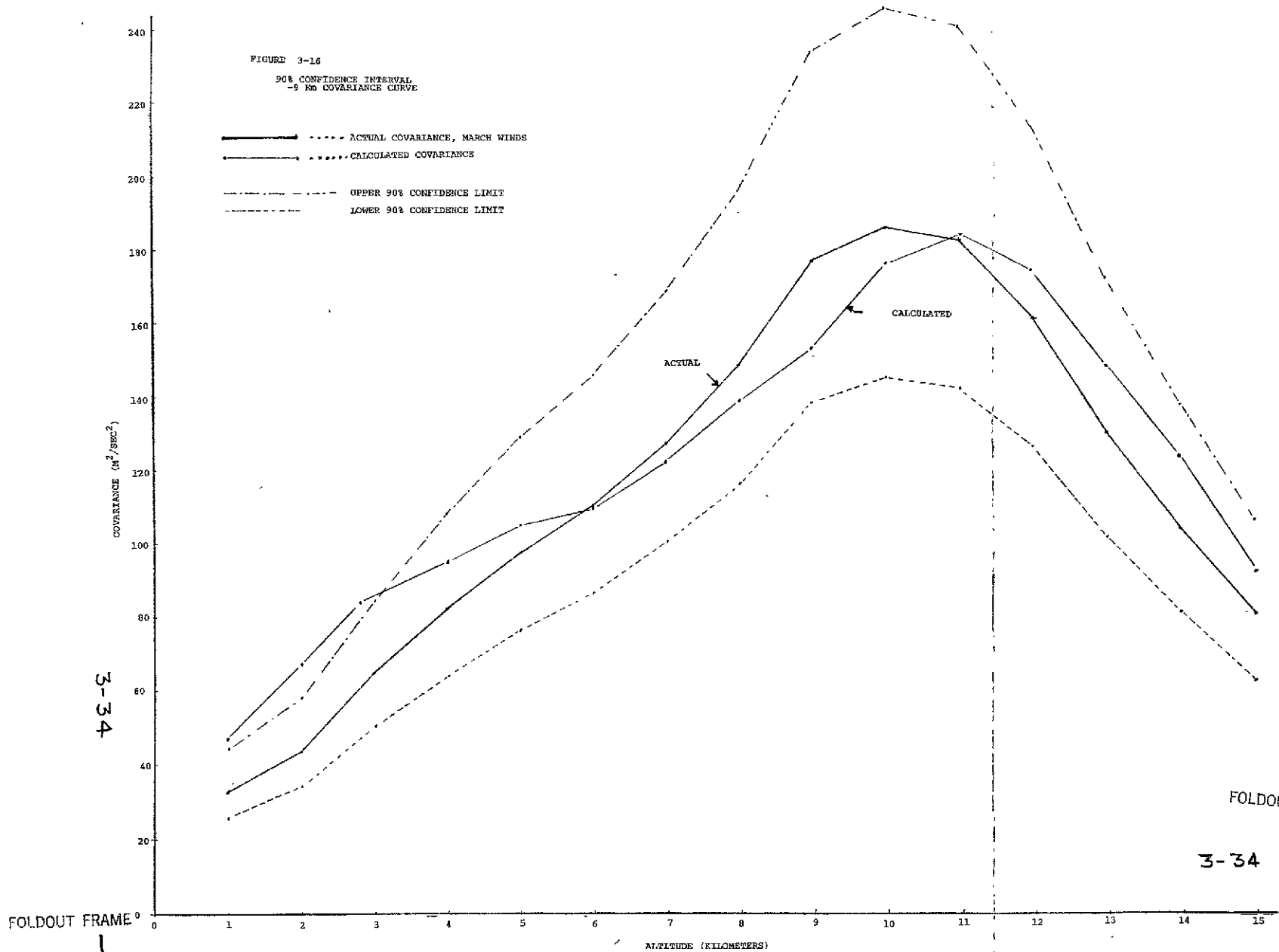
• 15-CALCULATED
• 15-ACTUAL

FIGURE 3-14



3-33





SECTION 4.0
SATURN V VEHICLE MODEL

4. SATURN V VEHICLE MODEL

4.1 FORWARD VEHICLE MODEL

The vehicle model used in this analysis was taken directly from Reference 3. The following changes were made to the model as reported on in Reference 3.

- ° The time varying coefficients were linearized around a new mean value consistent with the new mean wind input.
- ° A thrust stochastic variational model was added to the model.
- ° An XCP stochastic variational model was added to the model.

The AS-504 vehicle model used for determination of Bending Moment Statistics via the adjoint technique includes:

- ° Two Bending Modes
- ° Four Slosh Modes
- ° Control Filters and Actuator Dynamics.

The bending contributions to attitude, attitude rate and engine deflection angle are fed back to the vehicle control system.

The coordinate system is shown in Figure 4-1.

The "forward" linear planar vehicle model from which the adjoint was formed is shown in Figures 4-4, 5, 6 and 7. The DYNASAR computer program for the I.B.M. 7094 was written from these diagrams.

Nomenclature is defined in Appendix F.

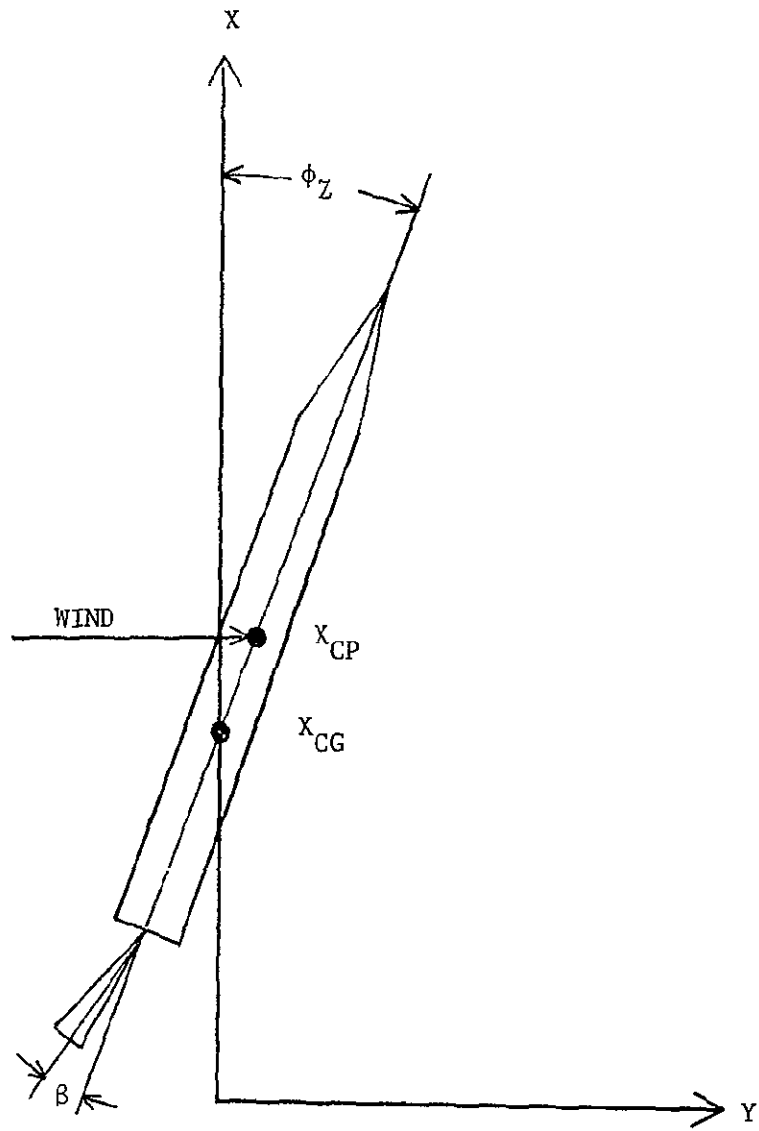


Figure 4-1. Coordinate System

4.1.1 Vehicle Dynamics and Control Equations

This paragraph describes the equations for vehicle dynamics and control shown in Figures 4-4 and 4-7.

The translation equation is,

$$m \ddot{Y} = qAC_N \hat{\alpha} + F_{TCX} \beta + (F_{TX} - F_{AX}) \delta, \quad (4-1)$$

Where: m = Vehicle Mass

\ddot{Y} = Translational Acceleration

$qAC_N \hat{\alpha} = \frac{qAC_N}{\alpha_{mean}} = \text{Normal Force Coefficient Slope}$

F_{TCX} = Axial Force Thrust Control
(4 Engines)

F_{TX} = Axial Force Thrust
(5 Engines)

F_{AX} = Axial Drag Force.

F_{AX} , F_{TX} , F_{TCX} , QAC_N , α_{mean} and m were obtained as functions of time from the 6 D.O.F. non-linear model response to a deterministic mean wind. They were then input as tabular function in the linear model.

The rotation equation is,

$$I_{ZZ} \ddot{\phi}_Z = qAC'_N (X_{CP} - X_{CG}) \alpha - F_{TCX} X_{CG} \beta, \quad (4-2)$$

Where: I_{ZZ} = Vehicle Moment of Inertia about the Center of Gravity

$\ddot{\phi}_Z$ = Yaw Attitude Acceleration

$qAC'_N = \frac{qAC_N}{\alpha \text{ mean}}$ = Normal Force Coefficient Slope

X_{CP} = Vehicle Center of Pressure

X_{CG} = Vehicle Center of Gravity

F_{TCX} = Axial Force Thrust Control.
(4 Engines)

X_{CP} , X_{CG} and I_{ZZ} were obtained as functions of time from the 6 D.O.F.

non-linear model and input as tabular functions in the linear model.

The angle of attack equation is,

$$\alpha = \phi_Z + \frac{W_{\text{wind}} - \dot{Y}}{V_{RS}}, \quad (4-3)$$

Where:

α = Angle of Attack

ϕ_Z = Yaw Attitude Angle

\dot{Y} = Translational Velocity

V_{RS} = Magnitude of the Relative Velocity

A deterministic mean wind profile was input as a tabular function. The mean wind profile was determined from wind readings at Cape Kennedy. V_{RS} was obtained from the 6 D.O.F. non-linear model and input as a tabular function.

The control system used in this study is shown in Figure 4.2.

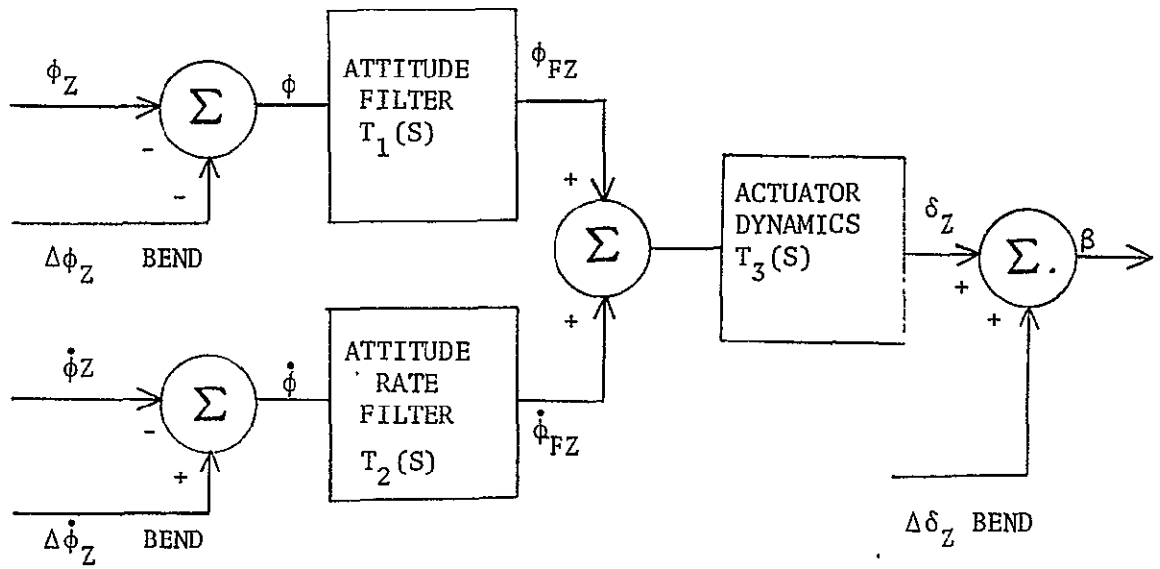


Figure 4-2. Control System Block Diagram

The control law is defined as,

$$\beta = T_3(S) \left\{ T_1(S)\phi + T_2(S)\dot{\phi} \right\} + \Delta\delta_Z \text{Bend.} \quad (4-4)$$

Where: $\phi = -\phi_Z - \Delta\phi_Z$ Bending

$\phi_Z =$ Yaw Attitude Angle

$$\Delta\phi_Z = Y_1'(X_M)\eta_1 + Y_2'(X_M)\eta_2$$

= Attitude Angle Correction Due To Bending

$$\dot{\phi} = -\dot{\phi}_Z + \Delta\dot{\phi}_Z \text{ Bend}$$

$\dot{\phi}_Z =$ Yaw Attitude Rate

$$\Delta\dot{\phi}_Z \text{ Bend} = Y_1'(X_M)\dot{\eta}_1 + Y_2'(X_M)\dot{\eta}_2$$

= Attitude Rate Correction Due To Bending

$$\Delta\delta_Z \text{Bend} = Y_1'(X_E)\eta_1 + Y_2'(X_E)\eta_2$$

= Engine Angle Correction Due To Bending.

The transfer functions $T_1(S)$ and $T_2(S)$ describe the networks designed for control system stability. All break frequencies below 100 radians per second were included. $T_3(S)$ is the transfer function which describes the engine actuator characteristics. Position and rate limits on the actuator are not included.

The transfer functions used are:

$$T_1(S) = \frac{37.63S^3 + 479.54S^2 + 7440.6S + 739.3}{S^4 + 93.25S^3 + 2481.63S^2 + 17528.8S + 821.44}, \quad (4-5)$$

$$T_2(S) = \frac{11.30311S^4 + 48.225S^3 + 6065.15S^2 + 7429.85S + 498784}{S^5 + 147.73S^4 + 6324.4S^3 + 90258S^2 + 462383S + 722876}, \quad (4-6)$$

$$T_3(S) = \frac{1188.87}{S^2 + 29.9286S + 1188.87}. \quad (4-7)$$

Equations 4-1, -2, -3, -4 and -7 are shown in block diagram in Figure 4-4. Equations 4-5 and 4-6 are shown in block diagram form in Figure 4-7.

4.1.2 Bending Dynamics Equations

This paragraph describes the equations for bending dynamics shown in Figure 4-5.

Assumptions

- (1) Engine inertial forces are negligible. There is little tendency for "tail-wag-the-dog" action since gimballed mass is small and motion is small.
- (2) Axial forces, i.e. drag forces, which act normal to the vehicle because of bending along the vehicle, are negligible.
- (3) Aerodynamic damping of the bending motion is negligible.
- (4) Local angle of attack effects are sufficiently small to be negligible. In effect, the rigid body angle of attack is thus used to determine the aerodynamic forcing function on each vehicle segment.
- (5) Bending modes are uncoupled. Structural damping factors are assumed for each mode and are assumed independent.
- (6) Time varying aerodynamic coefficients, thrust forces, and slosh masses are used.
- (7) Engine forces and slosh forces act in wind force plane.

The equation to be solved is,

$$\ddot{\eta}_i + 2\zeta_i \omega_{n_i} \dot{\eta}_i + \omega_{n_i}^2 \eta_i = \frac{\tilde{Q}_{ENG_i} + \tilde{Q}_{AERO_i} + \tilde{Q}_{SLOSH_i}}{T_{\mu_i}}, \quad (4-8)$$

Where: η_i = generalized displacement of i^{th} mode, referenced to vehicle nose.

ζ_i = structural damping of i^{th} bending mode.

ω_{n_i} = i^{th} modal freq

$\tilde{Q}_{\text{ENGINE}_i}$ = Generalized engine force, i^{th} mode.

$\tilde{Q}_{\text{AERO}_i}$ = Generalized aerodynamic force, i^{th} mode.

$\tilde{Q}_{\text{SLOSH}_i}$ = Generalized slosh force, i^{th} mode.

T_{μ_i} = Generalized modal mass.

To obtain each of the generalized forces:

$$\tilde{Q}_{\text{ENG}_1} = F_{\text{TCY}} Y_i(X_E) \beta \quad (4-9)$$

Where: F_{TCY} = Translational force thrust control

$Y_i(X_E)$ = i^{th} mode displacement at the gimbale point.

$$\tilde{Q}_{\text{AERO}_1} = qA \sum_{\substack{\text{All} \\ \text{Segments, } j}} \hat{C}_N Y_{ij} \alpha \quad (4-10)$$

Where: q = dynamic pressure

A = vehicle cross sectional area

$\sum_j \hat{C}_N Y_{ij}$ = i^{th} mode normal force coefficient slope summed
overall vehicle segments j .

$$\tilde{Q}_{\text{SLOSH}_i} = m_{S_K} \ddot{\xi}_K Y_i(X_K) + A_X m_{S_K} \hat{Y}_i(X_{S_K}) \xi_K \quad (4-11)$$

Where: m_{S_K} = K^{th} slosh mass

$\ddot{\xi}_K, \xi_K$ = k^{th} slosh mode acceleration, displacement

$\hat{Y}_i(X_K)$ = i^{th} bending mode slope at X_K

$Y_i(X_K)$ = i^{th} bending mode displacement at X_K

A_X = Axial Acceleration.

Slosh mass, bending mode displacement and slope, bending frequency, bending structural damping, and axial acceleration were obtained from "SA-504 Structural Dynamic Characteristics," D5-15522-4B (ref. 14).

The fourth assumption, which assumes negligible local angle of attack effects was evaluated using the 6 D.O.F. non-linear DYNASAR model. Two runs were made using this model. The first run included local angle of attack effects for each vehicle segment. In the second run, the angle of attack for all vehicle segments was assumed to be identically equal to the rigid-body angle of attack. The second run resulted in consistently lower values of bending moment of between 4 and 5 percent. The peak mean bending moment considering local α effects being 14.81×10^6 N-M and without local α , 14.23×10^6 N-M.

It is felt that at this time 5% is within the error band for our linear model. The additional complexity associated with inclusion of local α effects might be considered later when a better wind model is developed.

Equations 4-8., 9 , 10, and 11 are shown in block diagram form in Figure 4-5 for both bending modes.

4.1.3 Sloshing Dynamics Equation

This paragraph describes the equations for bending dynamics shown in Figure 4-6. The slosh model and equation were obtained from "The Influential Aspects of Atmospheric Disturbances on Space Vehicle Design Using Statistical Approaches for Analysis" by R. Ryan and A. King (ref. 15).

Assumptions

- (1) All sloshing occurs in the wind plane.
- (2) The slosh model for each tank can be represented by a mass, spring and damper as shown in Figure 4.3.

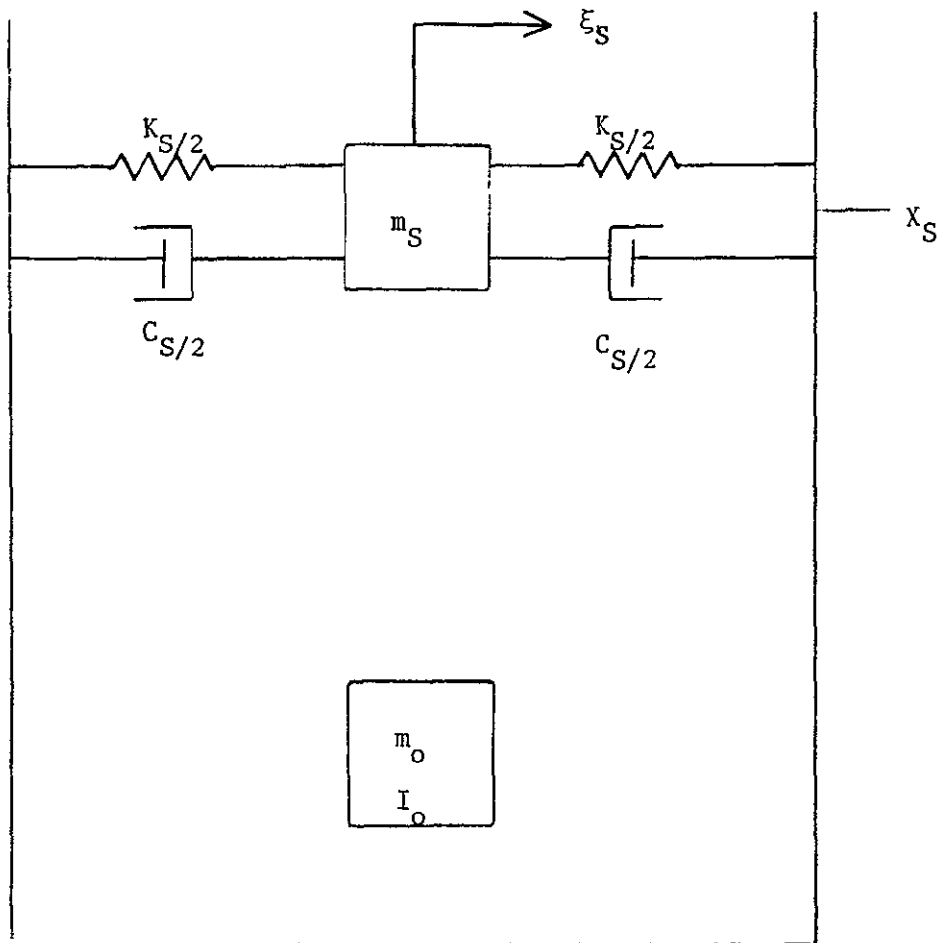


Figure 4-3. Slosh Model

The equation to be solved is,

$$\ddot{Y} + (X_{CG} - X_{Si}) \ddot{\theta}_Z + Y_j(X_{Si}) \ddot{\eta}_j + \ddot{\xi}_{Si} - A_X \ddot{\theta}_Z - A_X [Y_j'(X_{Si}) \dot{\eta}_j] + 2\omega_{Si} \zeta_{Si} \dot{\xi}_{Si} + \omega_{Si}^2 \xi_{Si} = 0. \quad (4-12)$$

Where:

\ddot{Y} = Translational Acceleration of the Vehicle.

X_{Si} = i^{th} Slosh Mode Attach Point.

$Y_j(X_{Si})$ = j^{th} Bending Mode Displacement at the i^{th} Slosh Mass Attach Point.

η_j = Generalized Displacement of the j^{th} Bending Mode.

ξ_{Si} = Displacement of the i^{th} Slosh Mass.

θ_Z = Yaw Attitude Angle.

A_X = Axial Acceleration.

$Y_j'(X_{Si})$ = j^{th} Bending Mode Slope at the i^{th} Slosh Mass Attach Point.

ω_{Si} = i^{th} Slosh Mode Frequency.

ζ_{Si} = i^{th} Slosh Mode Damping.

Slosh mass, slosh frequency, slosh mass location, slosh damping and axial acceleration were obtained from "SA-504 Structural Dynamic Characteristics," D5-15522-4B (ref.5).

The S-II and S-IVB fuel tanks were not modeled because the slosh forces exerted by these tanks were negligible compared to the other four tanks.

Equation 4-12 is shown in block diagram form in Figure 4-6 for the S-IC LOX, S-IC fuel, S-II LOX and S-IVB LOX tanks.

4.1.4 Bending Loads Equation

The bending moment calculation used in this study includes engine control forces, aerodynamic forces, bending dynamics forces and sloshing dynamics forces. The bending moment equation for station 25 is,

$$\begin{aligned} \text{B.M. (25)} = & \hat{M}_{\alpha} \dot{\alpha}(t) + \hat{M}_{\beta} \dot{\beta}(t) + \sum_{j=1}^2 \hat{M}_{\eta_j} \ddot{\eta}_j(t) \\ & + \sum_{j=1}^4 \hat{M}_{\xi_j} \ddot{\xi}_j(t) \end{aligned} \quad (4-13)$$

Where:

\hat{M}_{α} = Bending Moment Coefficient, Angle of Attack

\hat{M}_{β} = Bending Moment Coefficient, Engine Deflection

\hat{M}_{η_j} = j^{th} Mode Bending Moment Coefficient, Bending

\hat{M}_{ξ_j} = j^{th} Mode Bending Moment Coefficient, Slosh

Values for \hat{M}_{α} and \hat{M}_{β} were obtained from "Rigid Body Control Data for the SA-504 LOR Vehicle," R-AERO-DD-46-65 (ref. 16) Values for \hat{M}_{η_j} were obtained

from "A Method for the Determination of Control Law Effect on Vehicle Bending Moment," NASA TM X-53077 (ref.17).

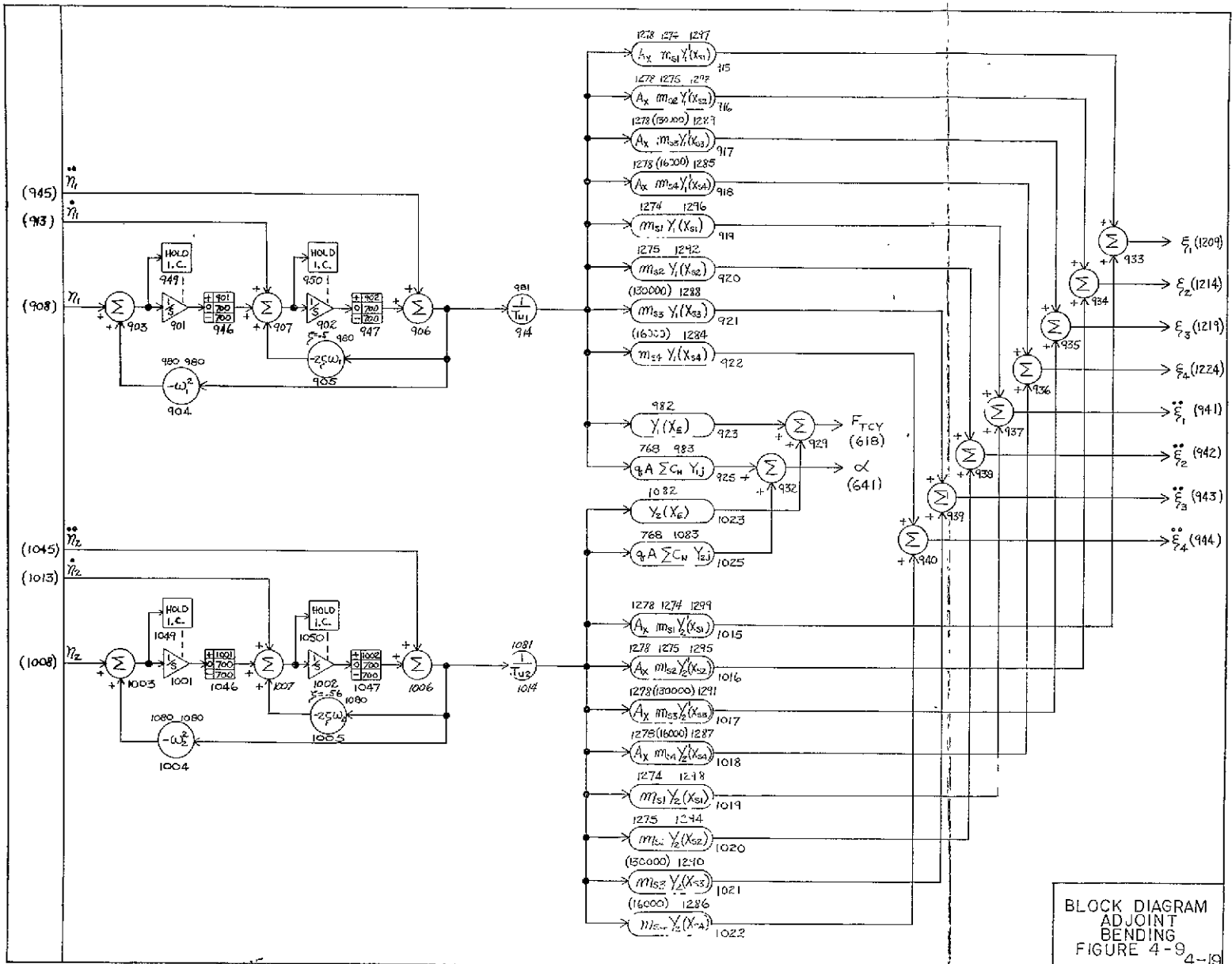
Values for \hat{M}_{ξ_j} were obtained by summing moments due to sloshing aft of station 25.

4.1.5 Stochastic Thrust Model

The stochastic thrust model is very simple. Since covariance data on thrust variations during flight was not available, it was assumed that thrust varied as white noise. The magnitude of the white noise was adjusted using a time varying coefficient. This magnitude was set at a one sigma value of 1% of the total thrust.

4.1.6 Stochastic Center of Pressure Model

This model took the same form as the thrust model. A one sigma value of XCP variation of 5% nominal was selected.

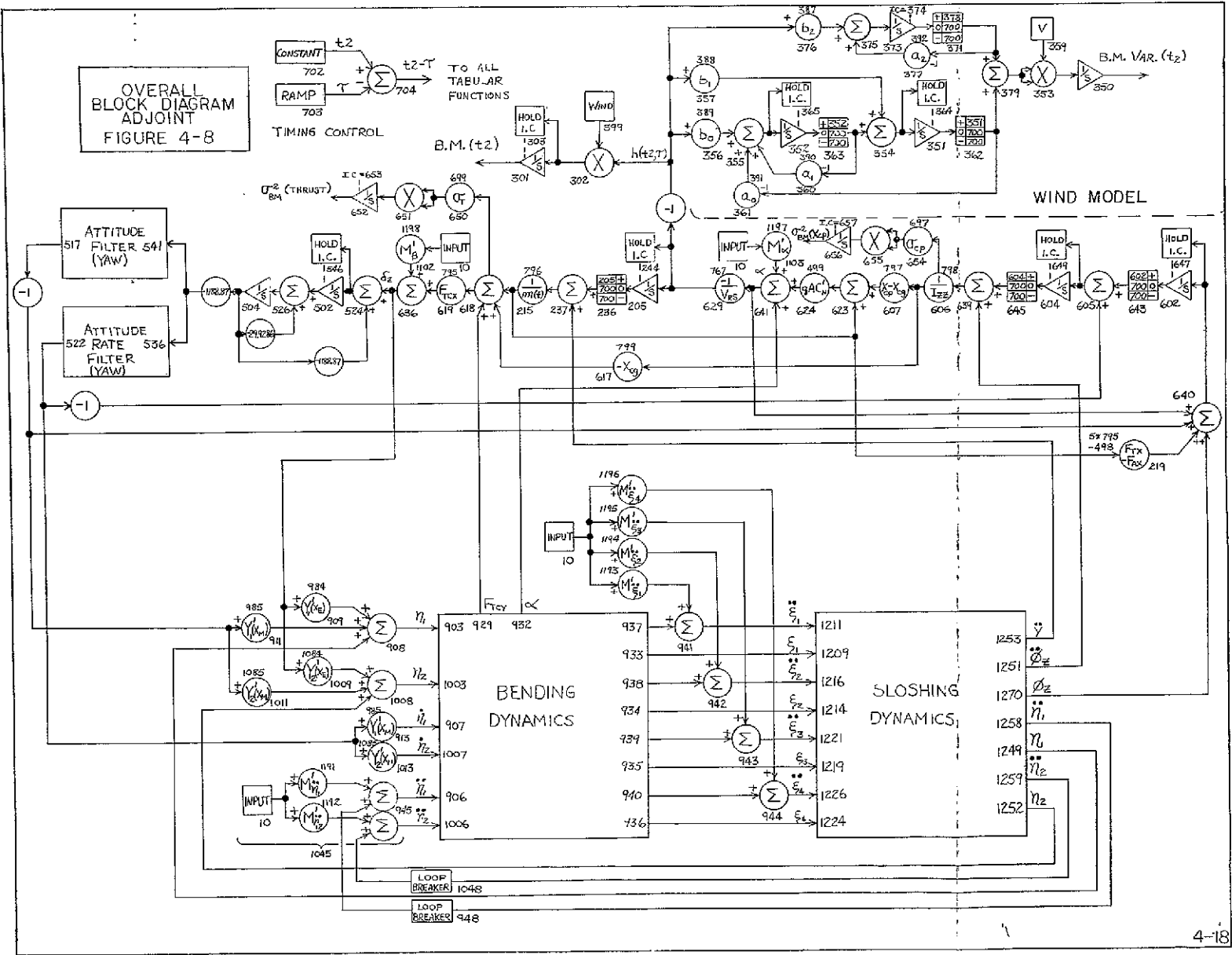


FOLDOUT FRAME
1

BLOCK DIAGRAM
ADJOINT
BENDING
FIGURE 4-9
4-19

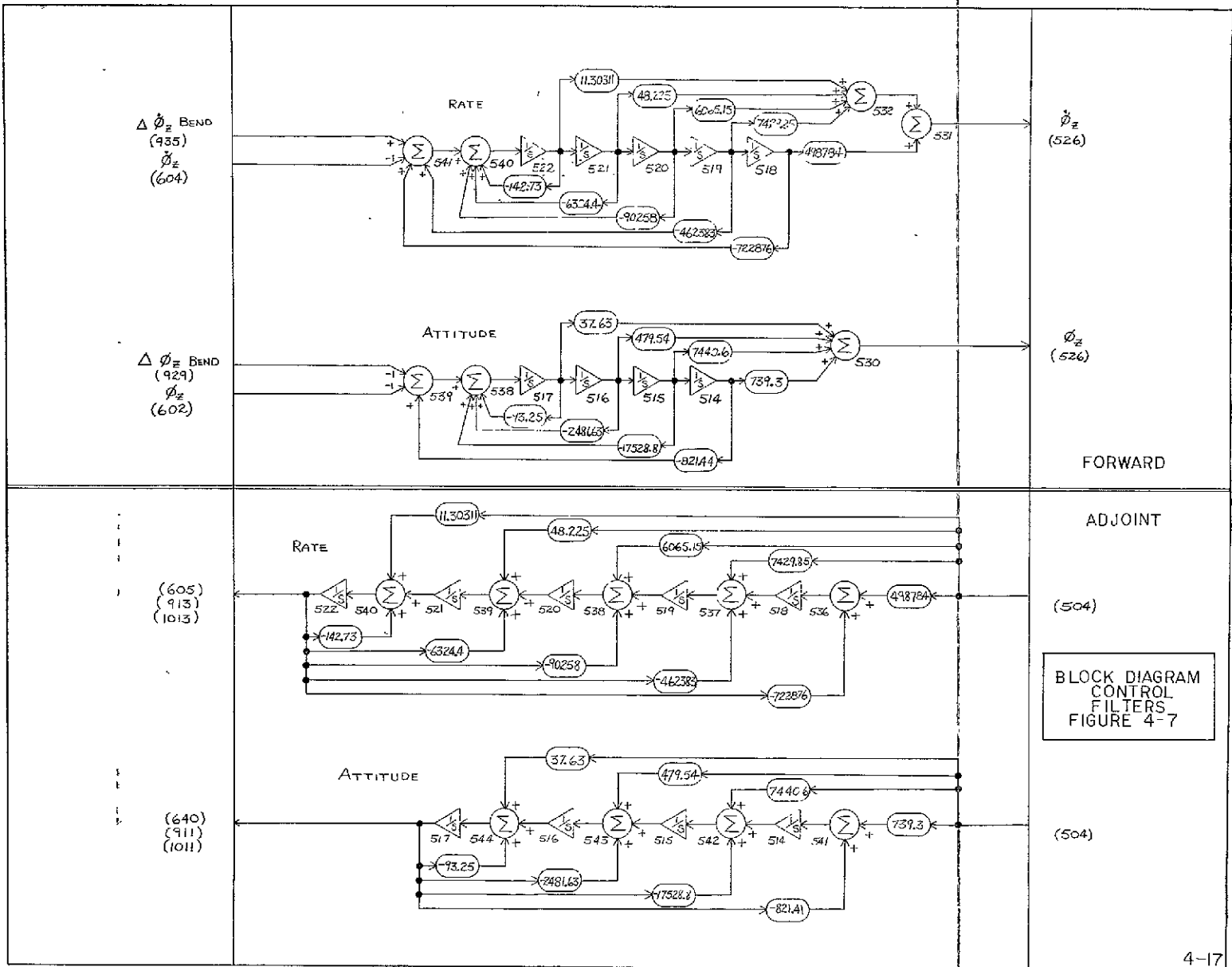
FOLDOUT FRAME
2

OVERALL
BLOCK DIAGRAM
ADJOINT
FIGURE 4-8



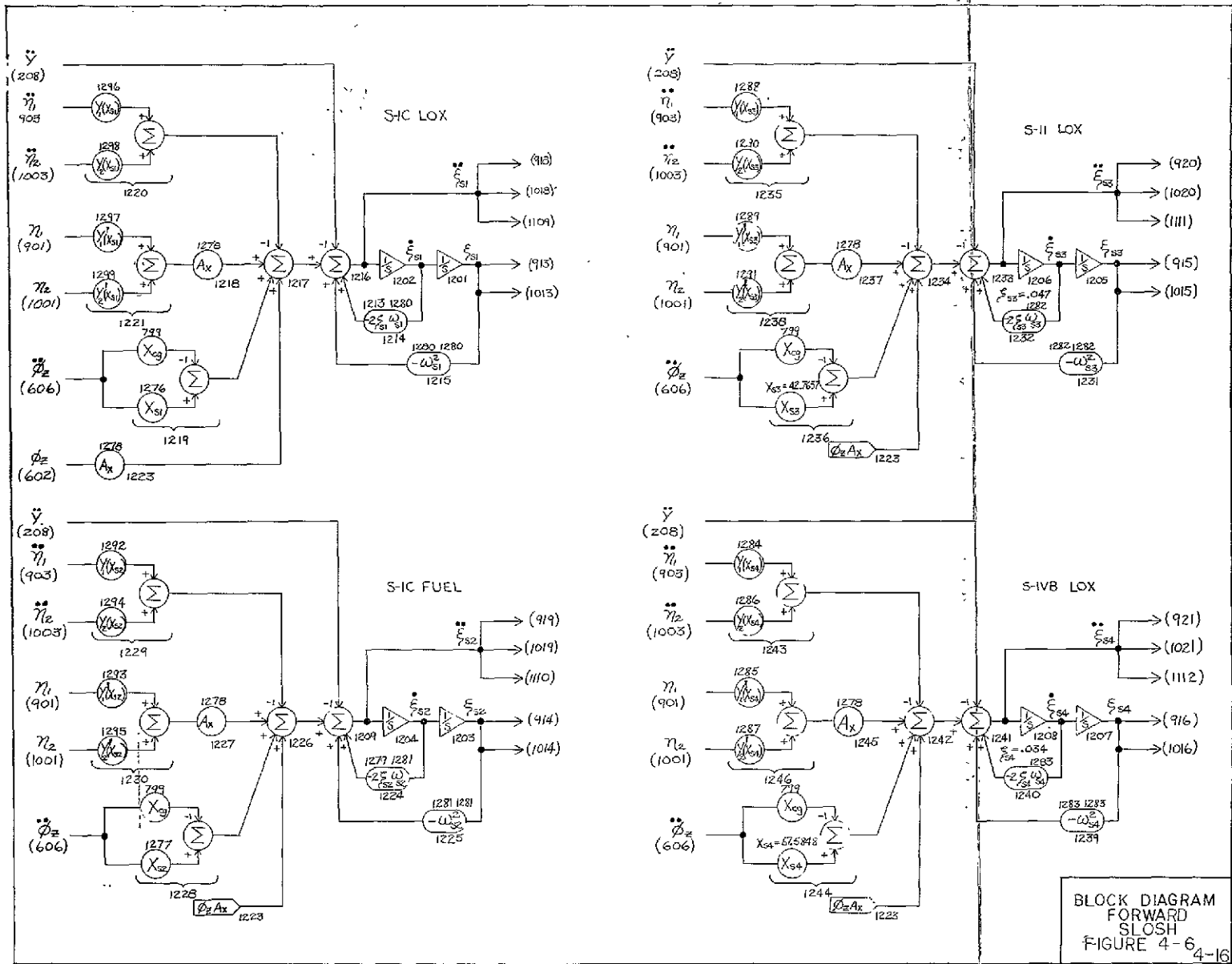
FOLDOUT FRAME 1

FOLDOUT FRAME 2



FOLDOUT FRAME

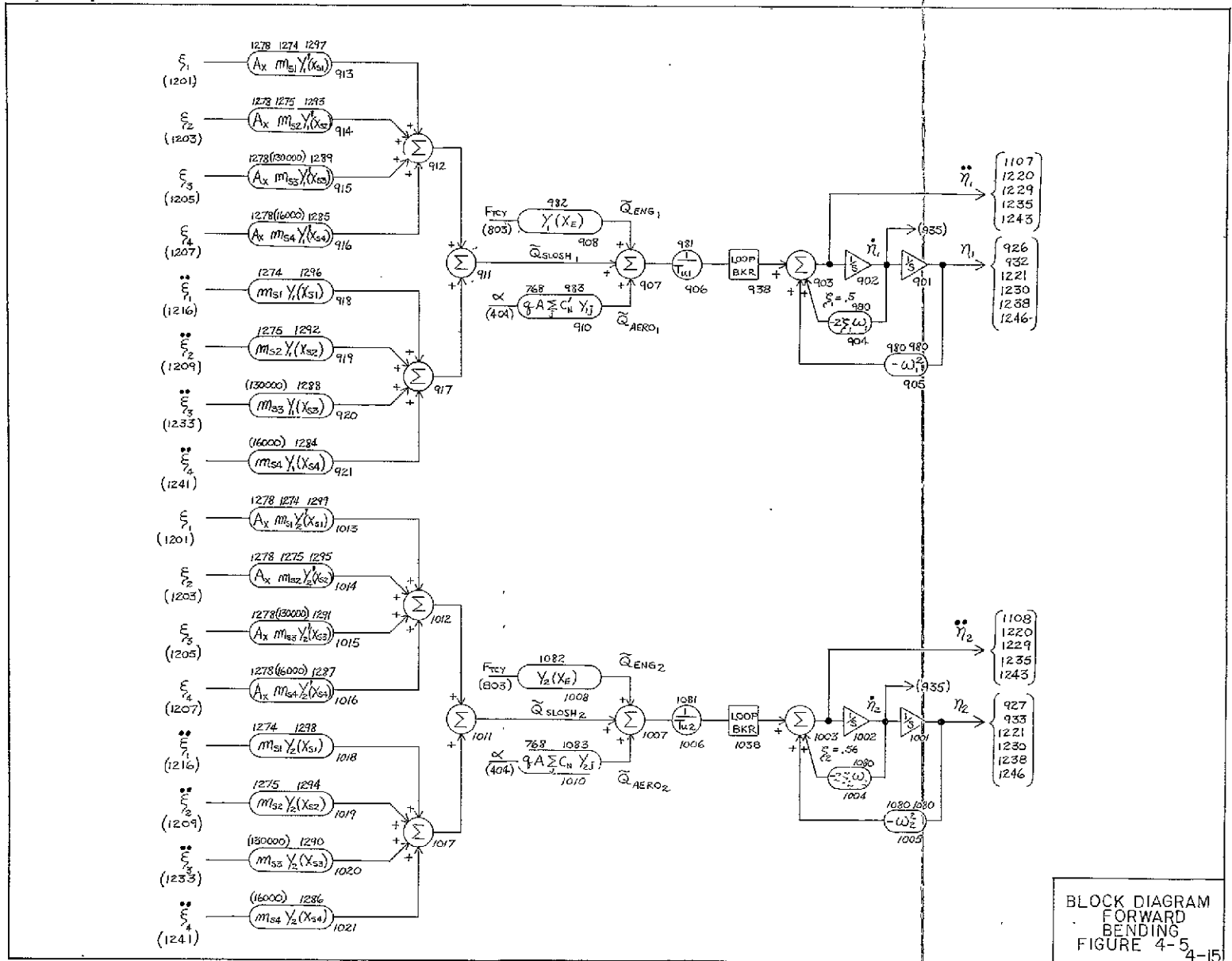
FOLDOUT



BLOCK DIAGRAM
FORWARD
SLOSH
FIGURE 4-6
4-16

FOLDOUT FRAME
1

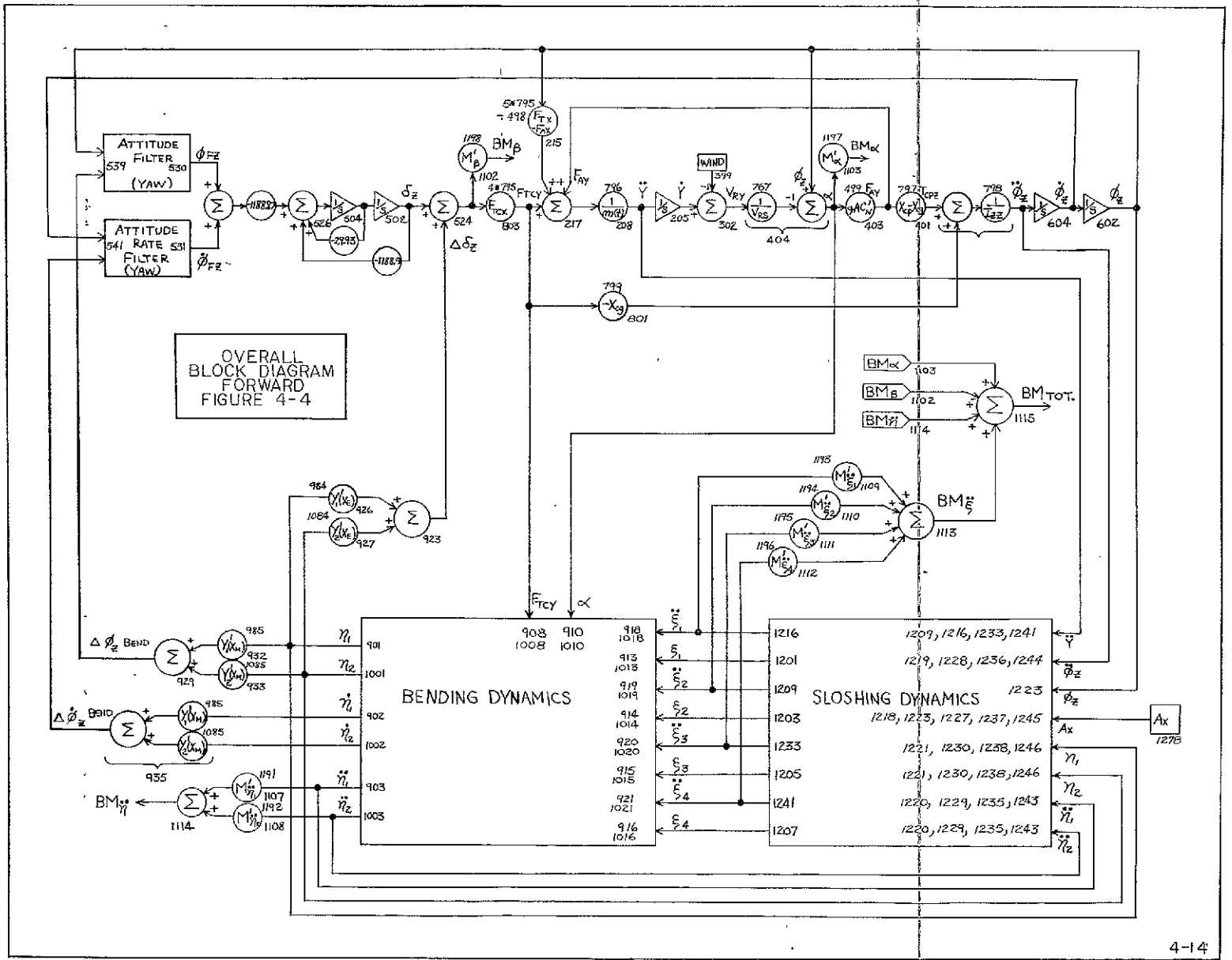
FOLDOUT FRAME
2

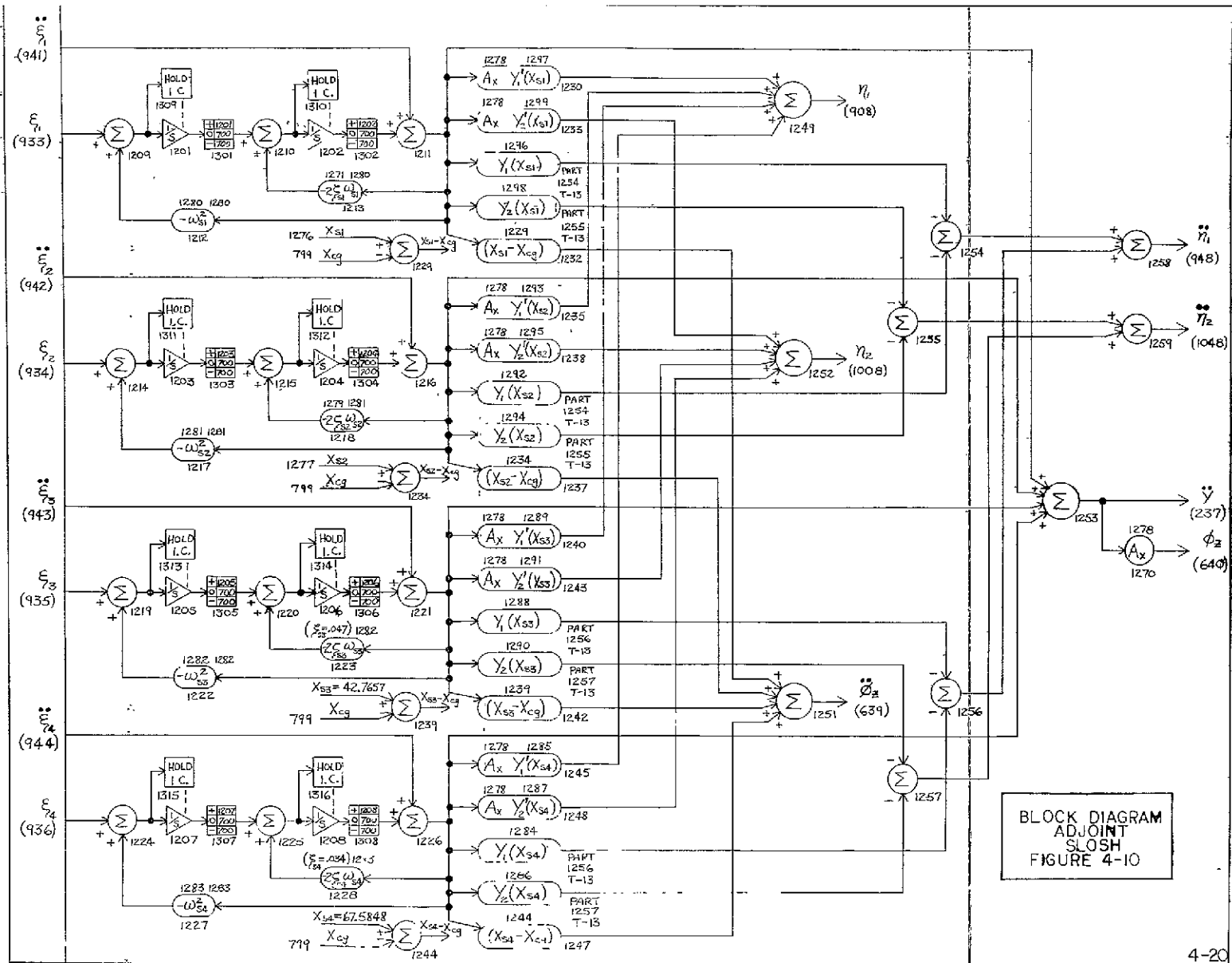


BLOCK DIAGRAM
FORWARD
BENDING
FIGURE 4-5
4-15

FOLDOUT FRAME

FOLDOUT FRAME





BLOCK DIAGRAM
ADJOINT
SLOSH
FIGURE 4-10

FOLDOUT FRAME

FOLDOUT FRAME

4.2 Adjoint Vehicle Model

The adjoint model was formed from the model described in Section 4.1. The nomenclature for the adjoint model is the same as the "forward" model. The interconnections in the adjoint model are designated as in the "forward" model. It should be recognized that the signal present in the adjoint model is not related to the same signal in the forward model. The nomenclature is included to aid in tracing signal flow.

4.2.1 Forming the Adjoint

The adjoint model with filters, bending, and slosh is shown in block diagram form in Figures 4.7, 8, 9, and 10. Each adjoint block diagram was formed from the corresponding "forward" block diagram as indicated below.

| | FORWARD | ADJOINT |
|-----------------------|---------|---------|
| OVERALL BLOCK DIAGRAM | 4-4 | 4-8 |
| BENDING DYNAMICS | 4-5 | 4-9 |
| SLOSHING DYNAMICS | 4-6 | 4-10 |
| CONTROL FILTERS | 4-7 | 4-7 |

The adjoint model was formed using the rules set forth in Rogers and Connolly.

The values for all tabular functions are listed in Appendix G.

Timing control for the adjoint model is shown in Figure 4-8. The final time " t_2 " for which the system weighting function " $g(t_2, \tau)$ " is determined is controlled by changing box 702 in the DYNASAR control deck. The bending moment from a deterministic wind input can be determined by convolving the system weighting function with a deterministic wind profile. The wind profile is input in table 399. The convolution is performed in boxes 301 and 302.

All tabular functions are interpolated based on the output of box 704, " $t_2 - \tau$ ".

4.2.2 Program Initial Value Calculation.

The initial values for all integrators are calculated automatically by the computer program at time $\tau=0$.

The input to the combined adjoint model, $\delta(\tau)$, is simulated by a switch (BOX 10). The output of box 10 equals 1 for $\tau=0$ and equals 0 for $\tau>0$. The input to each integrator that has an initial value is sampled at $\tau=0$ and the initial value is held by a sample and hold circuit. The output of each integrator is held open at $\tau=0$ to prevent the initial value of that integrator from affecting the initial value calculation of the other integrators. For time $\tau>0$ the switches on the output of the integrators are closed and the program runs in its normal operating mode.

4.2.3 Operating the Model

The vehicle adjoint model by itself, when forced by an impulse, yields the vehicle weighting function, $g(t_2, \tau)$. A family of vehicle weighting functions near peak "q α " can be obtained by varying time t_2 , (i.e. Set $t_2 = 65, 70, 75, 80$). The vehicle bending moment at t_2 is calculated by convolving the vehicle weighting function with a deterministic wind profile. Bending moment variance at time t_2 is determined by forcing the combined vehicle-wind adjoint system with an impulse. The bending moment variance is calculated by squaring and integrating the output of the combined model.

The adjoint vehicle model developed during this study uses AS-504 vehicle data and control filters. The time-varying vehicle parameters were obtained using a 6-D.O.F. non-linear model of the AS-504 vehicle developed under contract NAS8-18005 (ref. 6). The 6-D.O.F. model was forced by a mean wind in the YAW plane. Thus, the adjoint model calculations are made about the mean wind operating point.

The combined vehicle-wind model adjoint developed during this study was programmed using DYNASAR on the IBM 7094 computer.

SECTION 5.0

RESULTS

5.0 RESULTS

5.1 Bending Response Statistics

Figure 5-1 shows the mean + 3σ bending moments at Station 25 obtained from application of the adjoint method. This figure shows the mean bending moment, the mean + 3σ bending due to wind variations alone, and the mean + 3σ due to the combined stochastic effects of wind, thrust, and center-of-pressure.

Stochastic variations in thrust and Xcp were considered to be in the form of white noise of magnitude equal to 1% of the thrust level and 5% of the Xcp location. A 5% increase in peak bending moment resulted from adding the stochastic vehicle parameter effects.

Since zonal winds were used as the wind model, rather than scalar winds, the input process can be considered gaussian. Assuming gaussian variations in the vehicle parameters as well, permits the mean + 3σ bending moment to be interpreted as the 99.7 percentile bending moment. Without the assumption of normality this interpretation cannot be made.

Figure 5-2 shows a comparison between the results of Contract NAS8-21134, TMX-53567, and the response obtained from the current model. The differences in the three bending moment curves stems primarily from the differences in the wind model used. The wind model used in NAS8-21134 was an annual wind model the TMX 53565 wind model was an ensemble of wind profiles from annual samples also. In all 3 cases, the peak bending moments are in good agreement.

Sensitivity of the bending response to wind model changes was tested. To check this sensitivity, a "not-so-good" wind model was tried. This wind model had a mean-squared-error double that of the model actually used. Figures 5-3 through 5-5 show the covariance curves from this "not-so-good" wind filter. The maximum effect of this change in wind model occurred at 75 seconds flight time, the point of maximum bending moment variance. The poorer filter yielded a bending moment variance of $17.2 \text{ E}+12 \text{ n}^2\text{-m}^2$. The better filter yielded a variance of $17.7 \text{ E}+12 \text{ n}^2\text{-m}^2$. This is a difference of 5% maximum, for a filter whose mean squared error was double. This supports the conclusion that the filter obtained is an adequate model of the wind.

5.2 Angle of Attack Statistics

Figure 5-6 shows the mean + 3σ angle of attack resulting from wind variations and from the combined effects of stochastic wind, thrust and center of pressure. The effect of the 1% thrust variational model and the 5% Xcp variational model was less than

a 1% increase in angle of attack at 75 seconds.

5.3 Engine Deflection Angle Statistics

Figure 5-7 shows the mean + 3σ engine deflection angle resulting from wind variations alone, and from the combined effects of stochastic wind, thrust, and center of pressure. The effect of 1% thrust and 5% Xcp variational models was to increase the mean plus 3σ engine deflection 5%.

5.4 Run-Time Reduction

An effort was made to reduce the computer run times of the adjoint model. In the previous effort, IBM 7094 run times averaged 40 minutes per run. Adjustment of the predictor-corrector integration technique tolerance controls reduced this average run time to 12 minutes. The possibility of reducing this further through alternate control system filter modeling techniques proved to be impractical. With the 3rd order wind model used in this study, the pacing variable occurred in the wind model and not in the 5th order control filters. The "pacing" variable is that variable which limits the size of the integration interval. It is associated with the loop having the shortest time constant. While the pacing variable was in the control loop filters in the previous effort (Reference 3), it occurred in the wind filter loop in this effort.

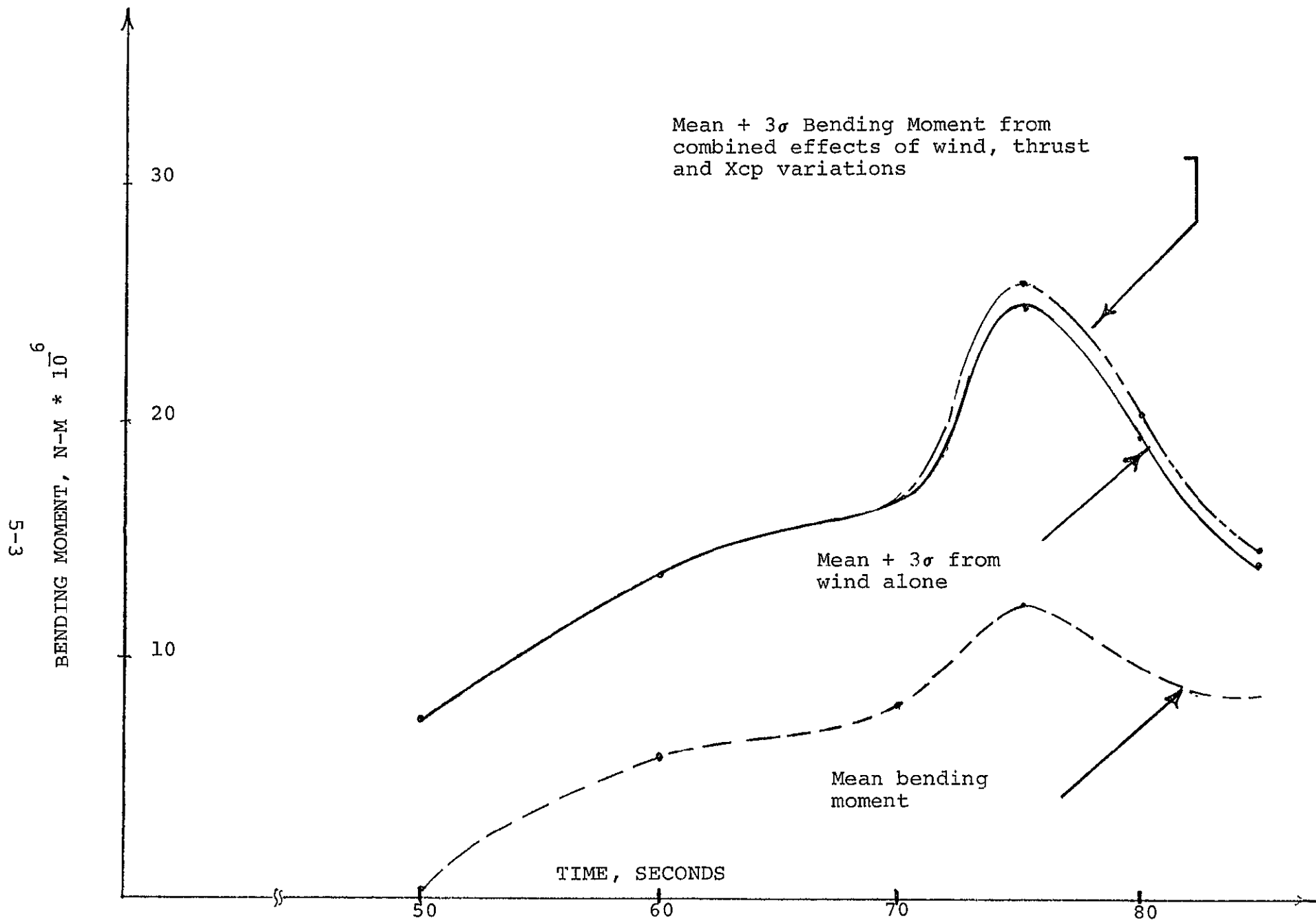


FIGURE 5-1 MEAN-PLUS-THREE SIGMA BENDING MOMENT, STATION 25.

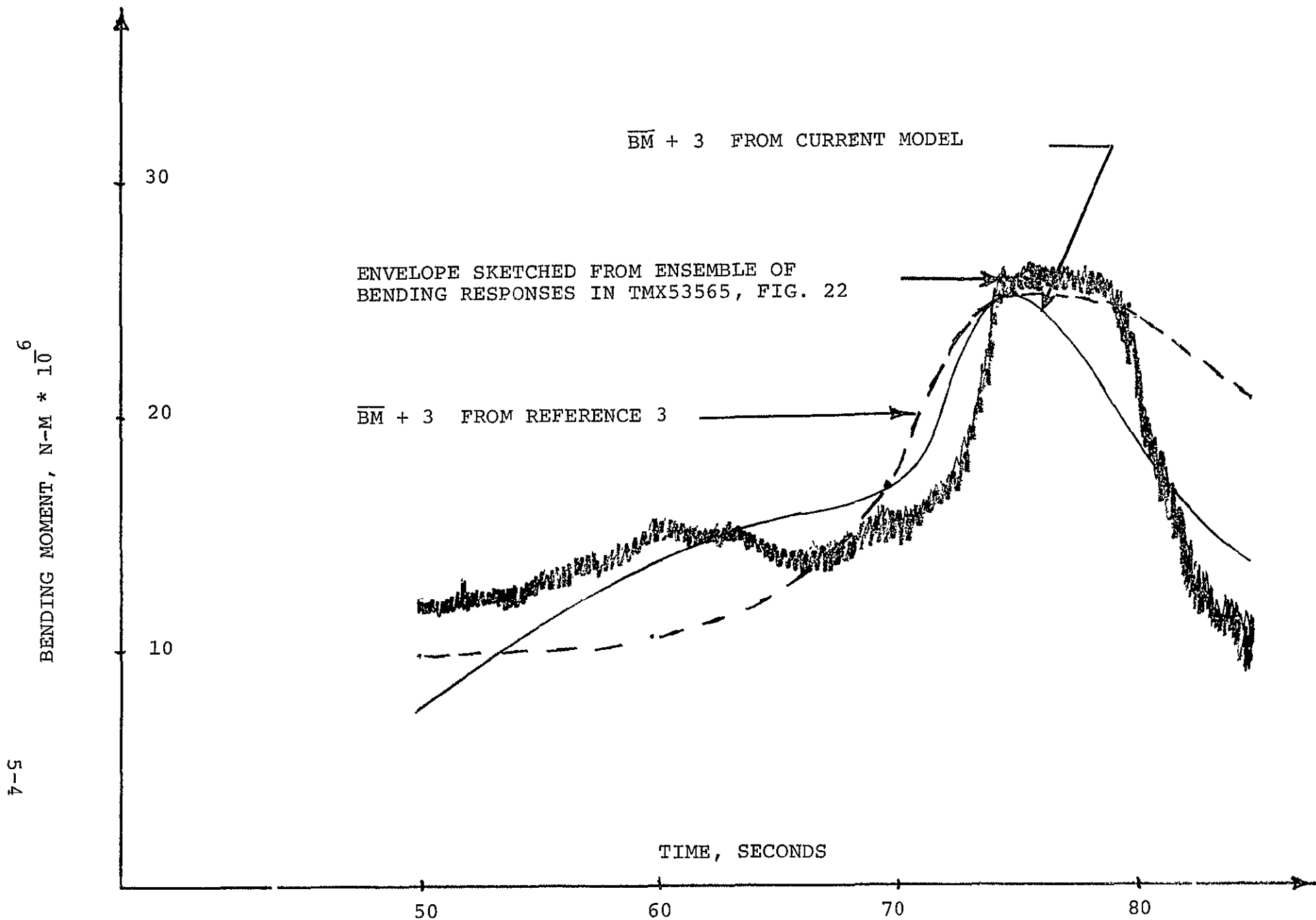


FIGURE 5-2 COMPARISON OF MEAN-PLUS-3 BENDING MOMENTS, STATION 25.

5-5

FIGURE 5-3 COVARIANCES FROM SUBOPTIMAL FILTER

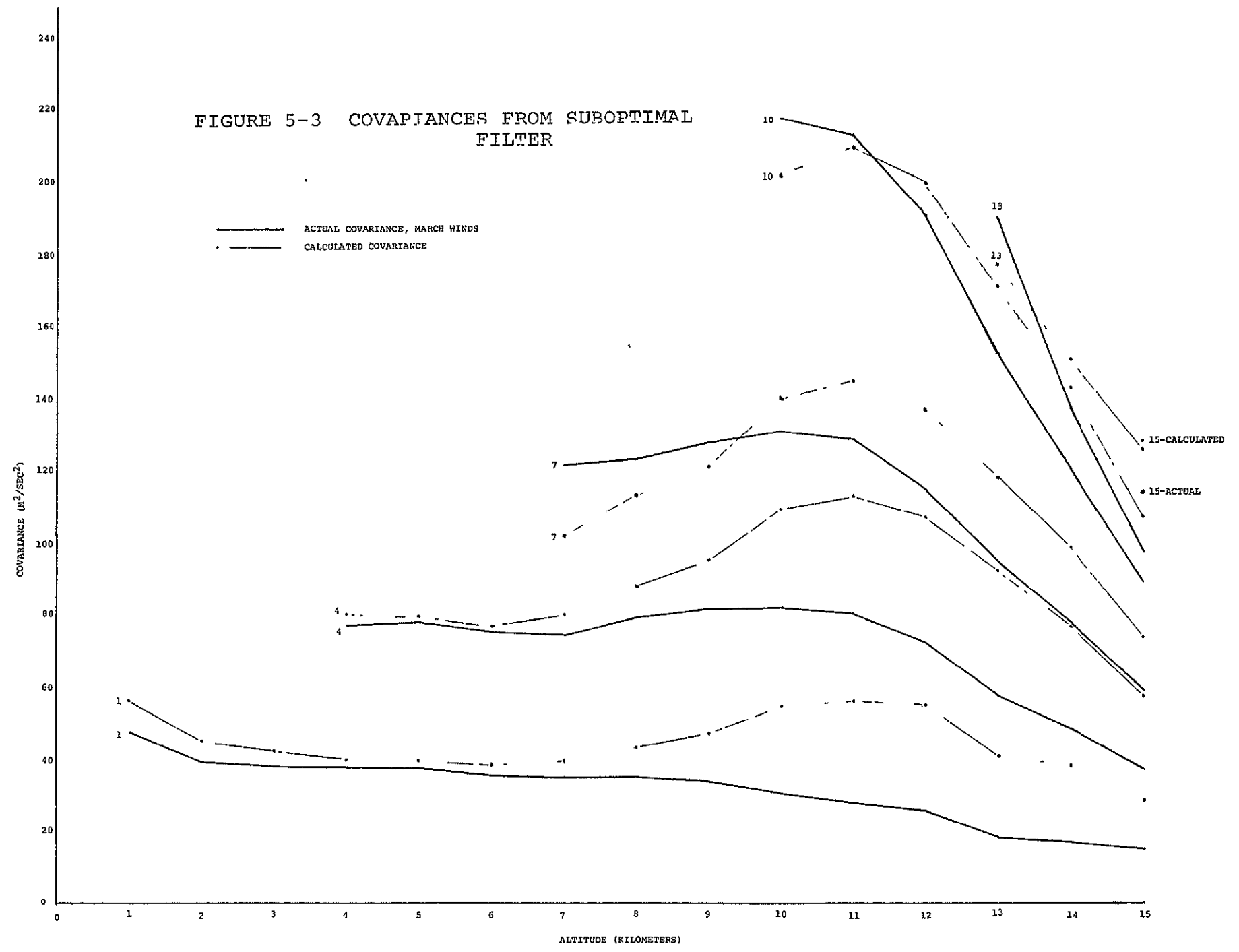
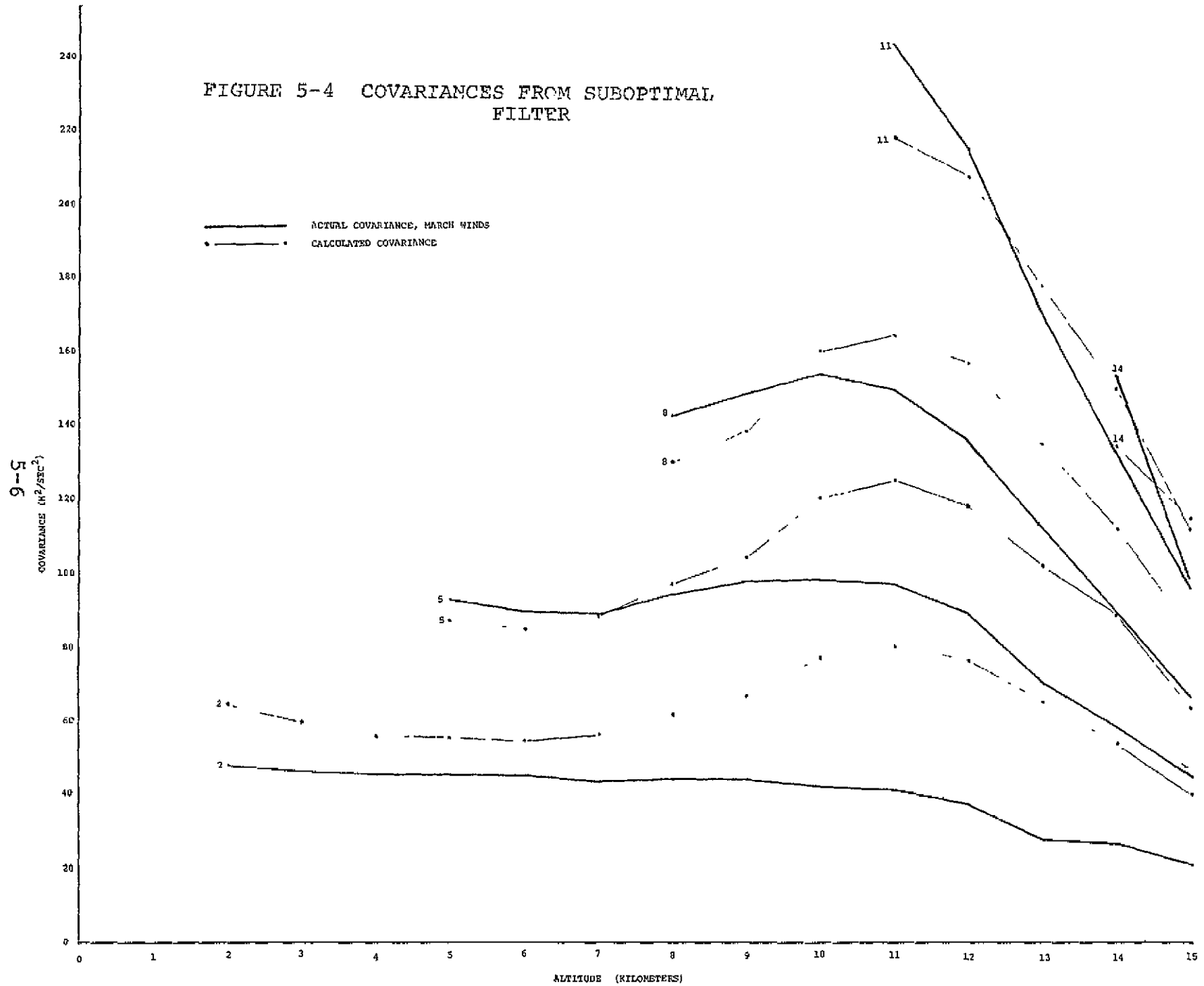
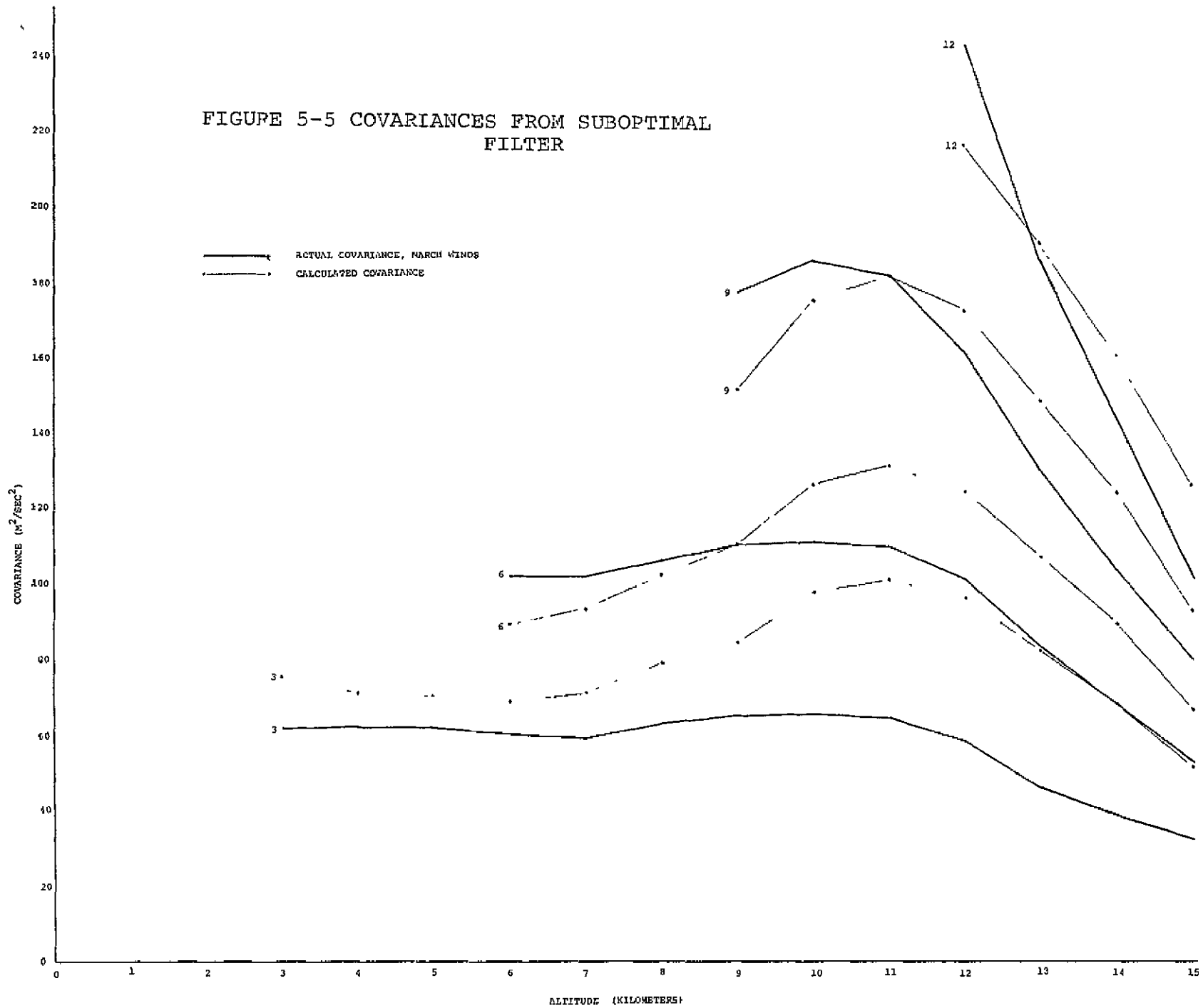
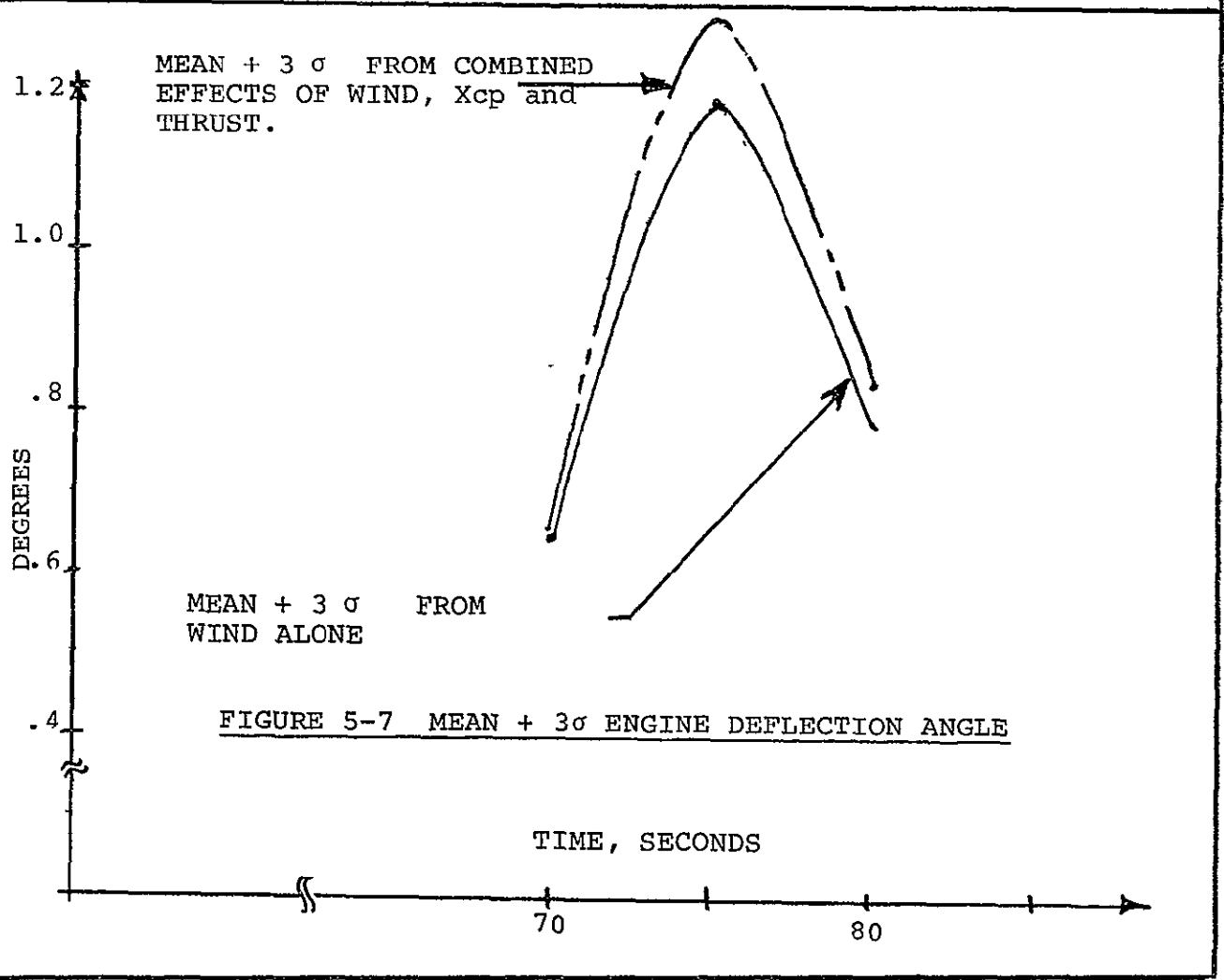
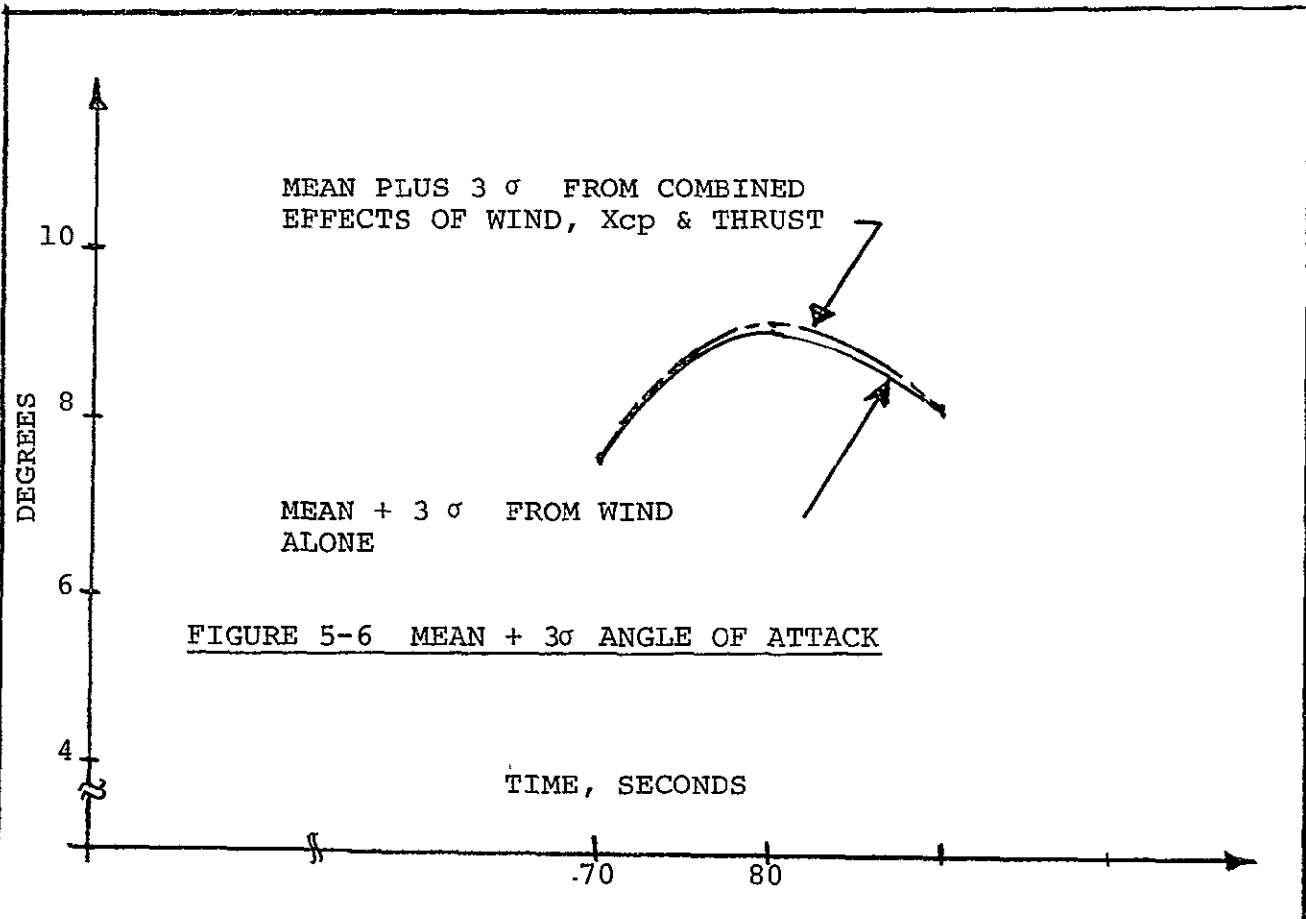


FIGURE 5-4 COVARIANCES FROM SUBOPTIMAL FILTER



5-7





SECTION 6.0

REFERENCES

6.0 REFERENCES

1. Hung, J. C., "Method Of Adjoint Systems And Its Engineering Applications", University of Tennessee, prepared under Contract NASA, MSFC Contract NAS8-11183, October 10, 1964.
2. Skelton, G. B., et.al, "Design Of A Load Relief Control System", Honeywell, Inc., prepared under NASA, MSFC Contract NAS8-20155, May 9, 1966, CR 61169.
3. Rowe, Hurd, Graf, "Determination Of Wind Response Of AS-504 by Statistical Methods", General Electric Company, prepared under NASA, MSFC Contract NAS8-21314, May 22, 1969.
4. Lanning & Battin, "Random Processes In Automatic Control", McGraw Hill, New York, 1956.
5. Rogers And Connolly, "Analog Computation In Engineering Design", McGraw Hill.
6. Hurd, Rowe, Graf, "Development of Adaptive Modular Analysis Techniques", General Electric, prepared under Contract NASA, MSFC, NAS8-18005, July 28, 1967.
7. DeRusso, Roy & Close, "State Variables For Engineers", Wiley, New York, 1967.
8. Palmer, J. L., "Study Of A Nonstationary Adjoint Statistical Wind Model For Flight Control System Analysis", Hayes International Corporation, Birmingham, Alabama.
9. Daniels, G. E. & Smith, O. E., "Scalar And Component Wind Correlations Between Altitude Levels For Cape Kennedy, Florida and Santa Monica, California", NASA TN D-3815, NASA, MSFC, April, 1968.
10. Socggins, J. R. and Vaughan, W. W., "Some Properties Of Atmospheric Turbulence For Space Vehicles", AIAA Paper No. 65-509 presented at AIAA Second Annual Meeting, San Francisco, California, July 26-29, 1965.
11. Socggins, J. R. & Susko, M., "FPS-16 Radar/Jimsphere Wind Data Measured At The Eastern Test Range", NASA TM X-53290, NASA, MSFC, July 9, 1965.

REFERENCES (Continued)

12. Bailey, Palmer & Wheeler, "Launch Vehicle Wind And Turbulence Response By Nonstationary Statistical Methods", Hayes International Corporation, Huntsville, Alabama, NASA Contractor Report, NASA CR-846, August, 1967.
13. Mendenhall, W., "Introduction To Statistics", Wadsworth Publishing Company, Belmont, California, 1965.
14. "SA-504 Structural Dynamic Characteristics", D5-15522-4B, The Boeing Company, March 1, 1968.
15. Ryan, R. and King, A., "The Influential Aspects Of Atmospheric Disturbances On Space Vehicle Design Using Statistical Approaches For Analysis", NASA TMX-53565.
16. "Rigid Body Control Data For The SA-504 LOR Vehicle", R-AERO-DD-46-65, Dynamic Stability Section, R-AERO-DDD.
17. Townsend, D., "A Method For The Determination Of Control Law Effect On Vehicle Bending Moment", NASA TM X-53077.

SECTION 7.0

APPENDICIES

APPENDIX "A"

CALCULATING COVARIANCE DERIVATIVES

The process of calculating derivatives of functions defined by discrete data points is somewhat of an art. There is always a trade off between placing too much faith in the numbers, and introducing smoothing functions which destroy pertinent information contained in the data. By placing too much faith in the sampled data containing uncertainties, tremendous errors in actual derivatives are introduced.

Because of the problems inherent in numerical differentiation, an analytic function description of the covariance data was chosen. Examination of the covariance curves, however, did not suggest any analytical function which would be particularly good to fit to the covariance data. This dilemma was alleviated by separating covariance into a product of its component parts.

$$\text{Cov } (h_1, h) = \rho_{h_1}(h) \sigma(h_1) \sigma(h)$$

The component parts consisted of:

1. Correlation coefficient = $\rho_{h_1}(h)$
2. Stand. deviation = $\sigma(h)$ _____

These two functions of altitude, were plotted and appeared more adaptable to analytical curve fitting. The standard deviation points were fit to a curve of the form;

$$\sigma(h) = B_1 + B_2 e^{B_3 (h-B_4)^2} + B_5 (h/22) B_6 (1-h/22)^{B_7}$$

The standard deviation data was least squared fit to this function. The resulting fit is shown in Figure A1.

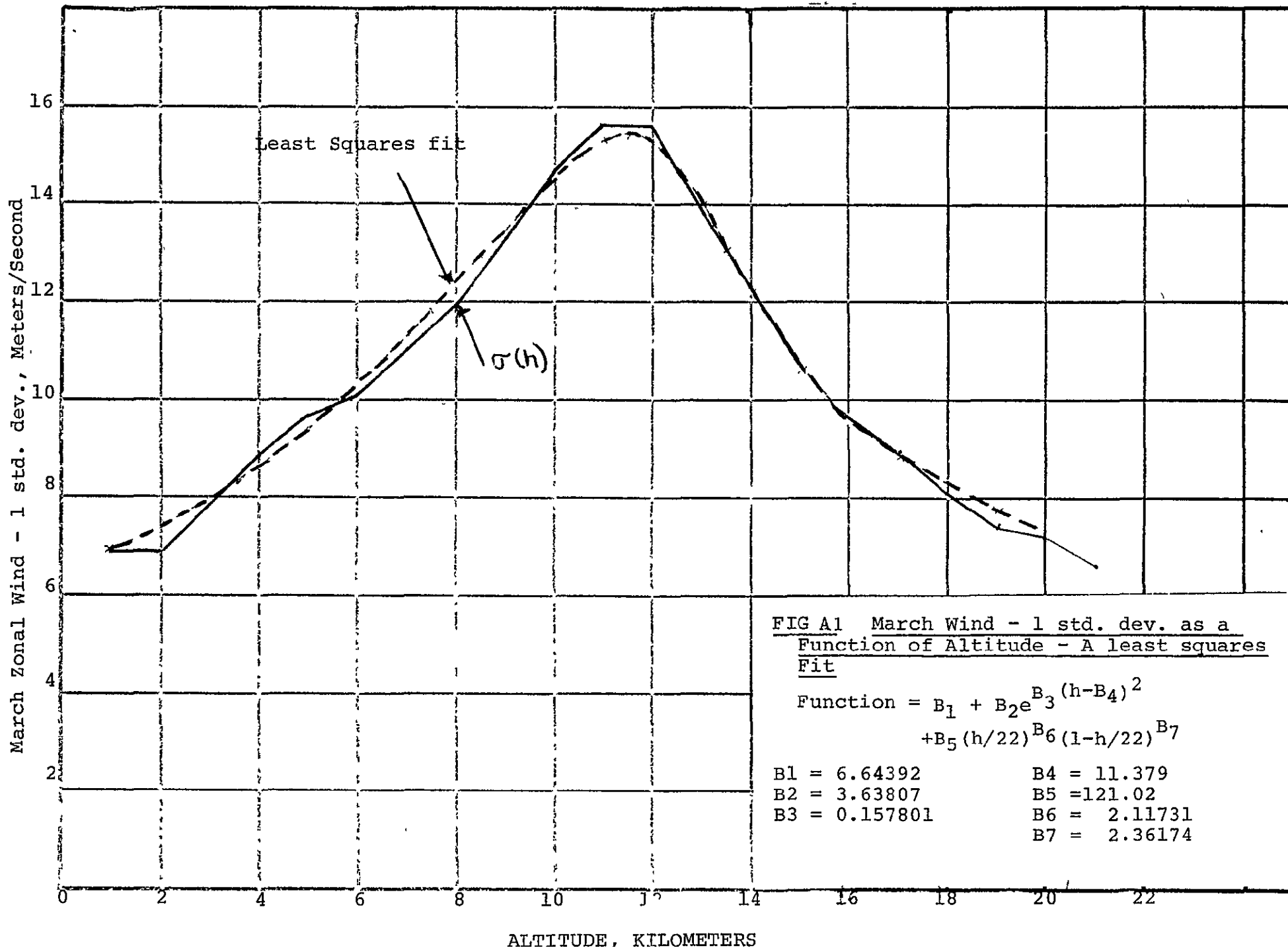


FIG A1 March Wind - 1 std. dev. as a Function of Altitude - A least squares Fit

$$\text{Function} = B_1 + B_2 e^{B_3 (h-B_4)^2} + B_5 (h/22)^{B_6} (1-h/22)^{B_7}$$

- | | |
|---------------|--------------|
| B1 = 6.64392 | B4 = 11.379 |
| B2 = 3.63807 | B5 = 121.02 |
| B3 = 0.157801 | B6 = 2.11731 |
| | B7 = 2.36174 |

The correlation coefficient, $\rho_{h_1}(h)$ for all h , and h were fit in a similar manner. The analytic function selected to describe the correlation coefficient was;

$$\rho_{h_1}(h) = B_1 + B_2 h^{B_3} + B_4 h + B_5 h^2 + B_6 h^3,$$

for $h \leq 10,000$ meters,

and,

$$\rho_{h_1}(h) = B_1 + B_2 h + B_3 e^{B_4 h} * \text{SIN}(K_i(h-h_1))$$

for $h > 10,000$ meters.

The method used to perform these non-linear curve fits is applicable to any defined function. The procedure used is described in "A Method For Solution Of Certain Non-Linear Problems In Least Squares", by K. Levenberg, Quarterly Applied Mathematics, 1944, pp 164-168. The technique has been programmed in Time-Share Fortran for the GE 605/635 and is a standard packaged routine.

APPENDIX "B"

CALCULATING NUMERATOR COEFFICIENTS

For white noise input, the output covariance is found from:

$$C(h_2, h) = \int_0^{h_2} g(h_2, \lambda) g(h, \lambda) d\lambda \quad ; \quad h > h_2 \quad (B-1)$$

$$C(h_2, h) = \int_0^h g(h_2, \lambda) g(h, \lambda) d\lambda \quad ; \quad h_2 < h \quad (B-2)$$

Where;

$g(h_2, \lambda)$ = Weighting function of 2nd order system, weighting an input at λ to an output at h_2 .

From I.C.'s (See Figure B1) we have

$$g(h, h_2) \Big|_{h=h_2^+} = \text{Impulse response at } h_2^+ \text{ due to an input at } h_2 = b_1(h_2) \quad (B-3)$$

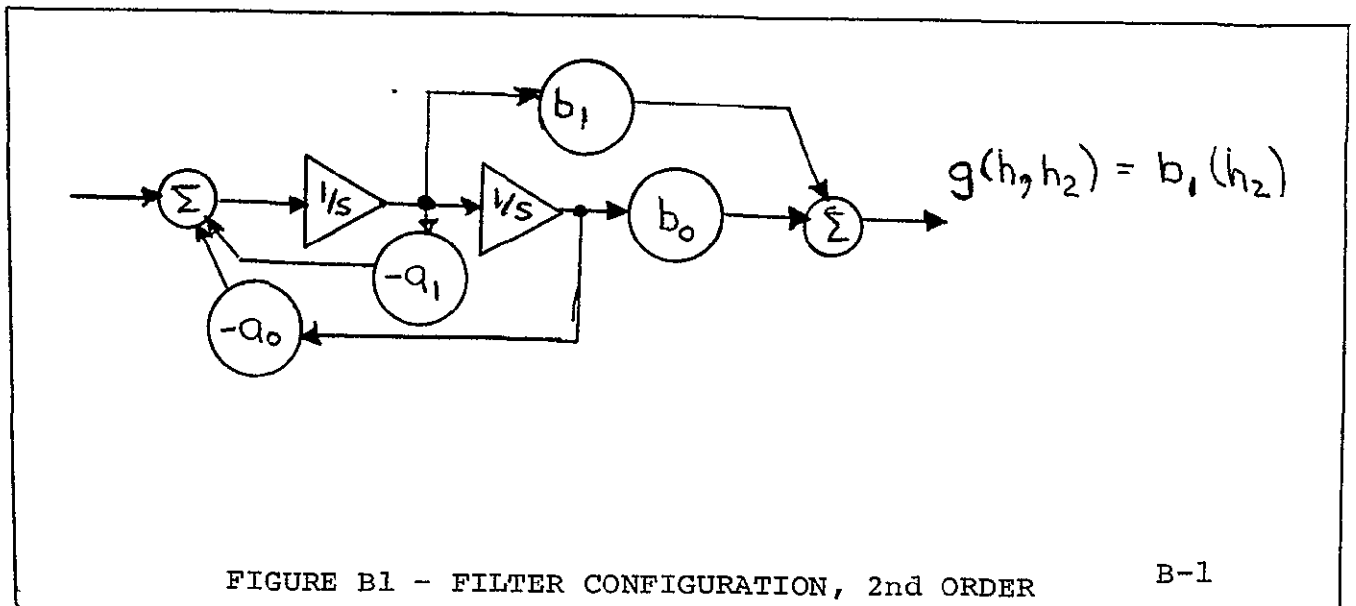


FIGURE B1 - FILTER CONFIGURATION, 2nd ORDER

Taking Derivatives Of (B-1) & (B-2) W/Respect To "h" Yields:

$$\left. \frac{dC(h_2, h)}{dh} \right|_{h=h_2^+} = \int_0^{h_2} g(h_2, \lambda) \frac{dg(h, \lambda)}{dh} d\lambda \Big|_{h=h_2^+} \quad (B-4)$$

$$\left. \frac{dC(h_2, h)}{dh} \right|_{h=h_2^-} = \int_0^h g(h_2, \lambda) \frac{dg(h, \lambda)}{dh} d\lambda \Big|_{h=h_2^-} + g(h_2, h) g(h, h) \Big|_{h=h_2^-} \quad (B-5)$$

Subtracting (B-4) from (B-5) †

$$\left. \frac{dC(h_2, h)}{dh} \right|_{h=h_2^-} - \left. \frac{dC(h_2, h)}{dh} \right|_{h=h_2^+} = g^2(h_2, h_2^-) = \overbrace{b_1^2(h_2)}^{\text{from (B-3)}} \quad (B-6)$$

SO:

$$b_1(h_2) = \sqrt{\left. \frac{dC(h_2, h)}{dh} \right|_{h=h_2^-} - \left. \frac{dC(h_2, h)}{dh} \right|_{h=h_2^+}} \quad (B-7)$$

The following numerical procedure was used to obtain the $b_0(h_2)$ coefficient.

Figure B-2 shows a typical filter impulse response resulting from an impulse input at h_2 . The response is shown for 3 points near h_2 , i.e. h_{10} , h_{11} , h_{12}

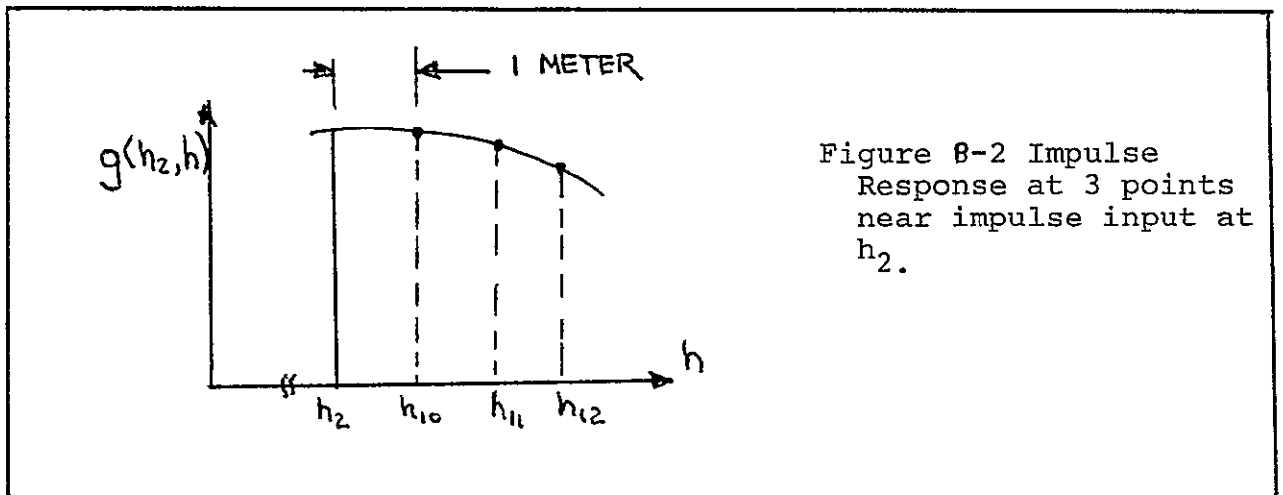


Figure B-2 Impulse Response at 3 points near impulse input at h_2 .

Since $g(h_1, h_2)$ is the impulse response to an impulse in at h_2 , it satisfies the homogeneous D.E.

$$a_0(h_1)g(h_1, h_2) + a_1(h) \frac{dg(h_1, h_2)}{dh_1} + \frac{d^2g(h_1, h_2)}{dh_1^2} = 0 \quad h_1 > h_2 \quad (\text{B-7A})$$

Approximating the derivatives in terms of $g(h_1, h_2)$ at three points near $h_1 = h_2$ (see figure B2) we have:

$$\left. \frac{dg(h_1, h_2)}{dh_1} \right|_{h_1 = h_{10}} = \frac{1}{2} \left[-3g(h_{10}, h_2) + 4g(h_{11}, h_2) - g(h_{12}, h_2) \right] \quad (\text{B-8})$$

$$\left. \frac{dg(h_1, h_2)}{dh_1} \right|_{h_1 = h_{11}} = \frac{1}{2} \left[-g(h_{10}, h_2) + g(h_{12}, h_2) \right] \quad (\text{B-9})$$

$$\left. \frac{dg(h_1, h_2)}{dh_1} \right|_{h_1 = h_{12}} = \frac{1}{2} \left[g(h_{10}, h_2) - 4g(h_{11}, h_2) + 3g(h_{12}, h_2) \right] \quad (\text{B-10})$$

$$\left. \frac{d^2g(h_1, h_2)}{dh_1^2} \right|_{h_1 = h_{10}} = \left[g(h_{10}, h_2) - 2g(h_{11}, h_2) + g(h_{12}, h_2) \right] \quad (\text{B-11})$$

By substituting the equations for the derivatives, (B-8), (B-9), (B-10), and (B-11) into (B-7A) and assuming the 2nd derivative constant over the interval $h_{10} \quad h_{12}$, 3 equations in $g(h_{10}, h_2)$, $g(h_{11}, h_2)$ and $g(h_{12}, h_2)$ result. These 3 homogeneous equations can be equated since they are all = 0. The resulting pair of equations can be solved for $g(h_{11}, h_2)$ and $g(h_{12}, h_2)$, knowing $g(h_{10}, h_2)$ from (B-6).

The equations to solve are:

$$[a_0(h_{11}) - 2a_1(h_{10})] g(h_{11}, h_2) + \left[\frac{a_1(h_{10})}{2} + \frac{a_1(h_{11})}{2} \right] g(h_{12}, h_2) =$$

$$\left[a_0(h_{10}) - \frac{3}{2} a_1(h_{10}) + \frac{a_1(h_{11})}{2} \right] g(h_{10}, h_2)$$

$$[a_0(h_{11}) + 2a_1(h_{12})] g(h_{11}, h_2) + \left[\frac{a_1(h_{11})}{2} - a_0(h_{12}) - \frac{3a_1(h_{12})}{2} \right] g(h_{12}, h_2) =$$

$$\left[\frac{a_1(h_{12})}{2} + \frac{a_1(h_{11})}{2} \right] g(h_{10}, h_2)$$

From (B-6);

$$g(h_{10}, h_2) = \sqrt{\left. \frac{dC(h_{10}, h_2)}{dh_{10}} \right|_{h_{10}=h_2} - \left. \frac{dC(h_{10}, h_2)}{dh_{10}} \right|_{h_{10}=h_2^+}}$$

Therefore by solving the above 2 equations we obtain;

$$g(h_{11}, h_2) \\ \& g(h_{12}, h_2)$$

From knowing these values of g , at 3 consecutive points, the derivatives of g at h_2^+ can be calculated, using equations (B-8) & (B-11).

Referring now, to Figure B1, it is seen that:

$$\left. \frac{dg(h_1, h_2)}{dh} \right|_{h=h_2^+} = \left. \frac{d[b_0(h_2) X + b_1(h_2)] \dot{X}}{dh} \right|_{h=h_2^+} = b_0(h_2) X + b_1(h_2) X$$

$$\& \ddot{X} = -a_1(h_2) \dot{X} - a_0(h_2) X$$

$$\& \begin{matrix} \dot{X} = 1 \\ X = 0 \end{matrix} \Big|_{h=h_2^+}$$

$$\left. \frac{dg(h_2^+, h_2)}{dh_1} \right|_{h_1=h_2^+} = b_0(h_2) - a_1(h_2) * b_1(h_2) \quad (B-12)$$

In (B-12) the only unknown is $b_0(h_2)$ which can now be determined by solving (B-12).

3rd Order Numerator Equations

Since $g(h_1, h_2)$ is the impulse response function;

$$a_0(h_1)g(h_1, h_2) + a_1(h_1) \frac{dg(h_1, h_2)}{dh_1} + a_2(h_1) \frac{d^2g(h_1, h_2)}{dh_1^2} + \frac{d^3g(h_1, h_2)}{d^3h_1} = 0; h_1 > h_2 \quad (B-13)$$

By approximating:

$$\frac{dg}{dh_1}, \frac{d^2g}{dh_1^2}, \frac{d^3g}{d^3h_1} \quad \text{in terms of } g_{10}, g_{11}, g_{12}, g_{13}$$

In a manner similar to the 2nd order system development we can obtain the numerator coefficients;

$$\left. \frac{dg(h_1, h_2)}{dh_1} \right|_{h_1=h_{10}} = \frac{1}{6} [-11g_{10} + 18g_{11} - 9g_{12} + 2g_{13}] = g_0' \quad (B-14)$$

$$\left. \frac{dg(h_1, h_2)}{dh_1} \right|_{h_1=h_{11}} = \frac{1}{2} [-3g_{11} + 4g_{12} - g_{13}] = g_1' \quad (B-15)$$

$$\left. \frac{dg(h_1, h_2)}{dh_1} \right|_{h_1=h_{12}} = \frac{1}{2} [g_{10} - 4g_{11} + 3g_{12}] = g_2' \quad (B-16)$$

$$\left. \frac{dg(h_1, h_2)}{dh_1} \right|_{h_1=h_{13}} = \frac{1}{6} [-2g_{10} + 9g_{11} - 18g_{12} + 11g_{13}] = g_3 \quad (\text{B-17})$$

$$\left. \frac{d^2g(h_1, h_2)}{dh_1^2} \right|_{h_1=h_{10}} = 2g_{10} - 5g_{11} + 4g_{12} - g_{13} = g_0'' \quad (\text{B-18})$$

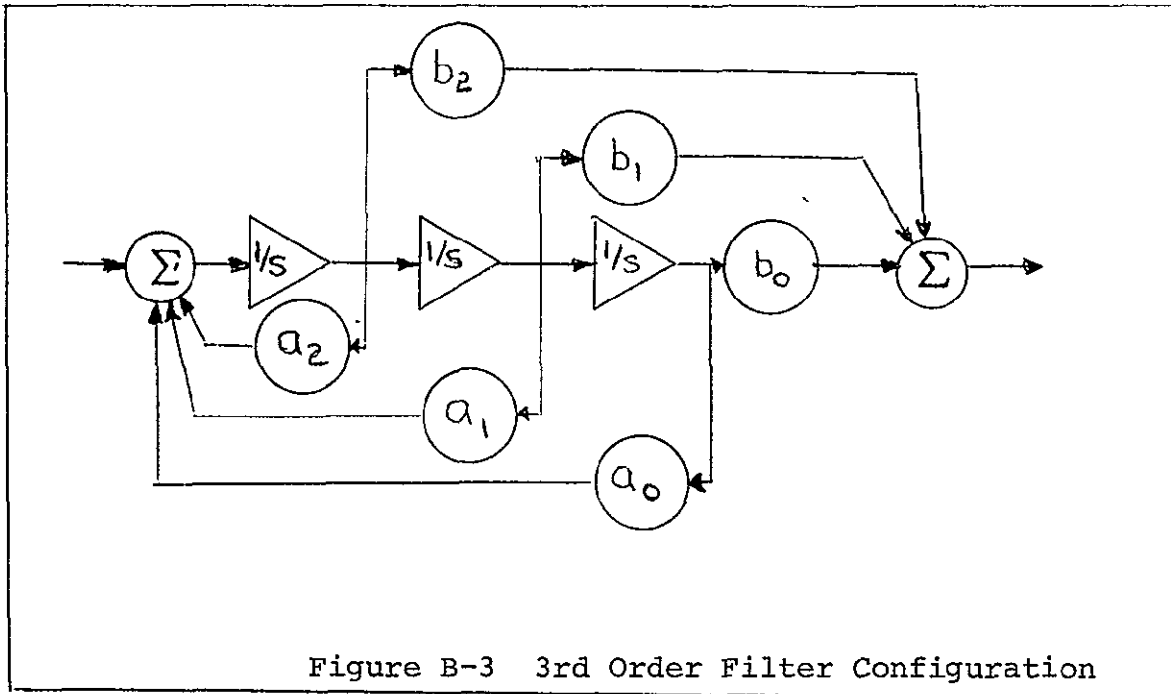
$$\left. \frac{d^2g(h_1, h_2)}{dh_1^2} \right|_{h_1=h_{11}} = g_{10} - 2g_{11} + g_{12} = g_1'' \quad (\text{B-19})$$

$$\left. \frac{d^2g(h_1, h_2)}{dh_1^2} \right|_{h_1=h_{12}} = g_{11} - 2g_{12} + g_{13} = g_2'' \quad (\text{B-20})$$

$$\left. \frac{d^2g(h_1, h_2)}{dh_1^2} \right|_{h_1=h_{13}} = -g_{10} + 4g_{11} - 5g_{12} + 2g_{13} = g_3'' \quad (\text{B-21})$$

$$\left. \frac{d^3g(h_1, h_2)}{dh_1^3} \right|_{h_1=h_{10}} = -g_{10} + 3g_{11} - 3g_{12} + g_{13} = g_0''' \quad (\text{B-22})$$

With these equations in (B-13) and assuming the third derivative constant over the interval we obtain a set of simultaneous homogeneous equations in g_{10} , g_{11} , g_{12} , and g_{13} . As with the second order development, these values can be used to obtain the numerator coefficients. Knowing the values of g_{11} above, the derivatives can be estimated. The following procedure is then used to obtain the "b" coefficients:



Using the nomenclature of Figure B-3 and the same development as for the second order system we see:

$$g(h_1, h_2) \Big|_{h=h_2^+} = b_2(h_2) = \sqrt{\frac{dC(h, h_2)}{dh} \Big|_{h=h_2^-} - \frac{dC(h, h_2)}{dh} \Big|_{h=h_2^+}} \quad (B-23)$$

$$\left. \frac{dg(h, h_2)}{dh} \right|_{h=h_2^+} = \frac{d}{dh} [b_2 X + b_1 X + b_0] X \Big|_{h=h_2^+}$$

$$= b_2[-a_2 X - a_1 X - a_0 X] + b_1 X + b_0 X \Big|_{h=h_2^+}$$

& at $h=h_2^+, X=1; \dot{X}=0, X=0$ so,

$$\left. \frac{dg(h, h_2)}{dh} \right|_{h=h_2^+} = b_1(h_2) - a_2(h_2)b_2(h_2) \quad (B-24)$$

Since $\frac{dg(h_1, h_2)}{dh}$, $b_2(h_2)$ & $a_2(h_2)$ are all known, (B-24) can be solved for $b_1(h_2)$.

In a similar manner:

$$\frac{d^2g(h, h_2)}{dh^2} = b_0(h_2) - a_2(h_2)b_1(h_2) - a_1(h_2)b_2(h_2) + a_2^2(h_2)b_2(h_2) \quad (B-25)$$

The equation is then solved for $b_0(h_2)$; now all numerator coefficients are known.

APPENDIX C - Optimization Algorithm

Although basically a "method of steepest decent" several features were added to make the method as efficient as possible for this specific application. The optimization procedure is as follows:

Let:

$$J = \sum_{i=1}^{16} \sum_{j=i}^{16} \left[\int_{h_1}^{h_2} g(i,h) * g(j,h) dh - \text{COV}(i,j) \right]^2 \quad (C-1)$$

where:

$$\begin{aligned} h_2 &= 16000 \text{ meters} \\ h_1 &= 16000 - 1000 i \text{ meters} \\ g(i, h) &= \text{constrained response function} \\ &= A(i)e^{\alpha_1(h)*h} + B(i)e^{\alpha_2(h)*h} \text{COS}(\omega(h)h + \psi(i)), \end{aligned}$$

COV(i,j) = covariance between altitudes
i, j Kilometers from March
zonal wind table.

J is evaluated for the set of initial values of the coefficients defining g (i,h) above. The initial values are best guesses at what they should be.

The partial derivatives are then calculated for each of the coefficients, A(i), B(i), $\psi(i)$, $\alpha_1(h)$, $\alpha_2(h)$, & $\omega(h)$ for all i and h. This is done by adjusting the value of each coefficient for each i and each h above by 10% and determining the effect on the objective function, J.

The sign and magnitude of the new estimates of the constrained response coefficients are determined from these partial derivatives. The corrections to the original estimates are loaded into a correction- vector, "Q".

If the objective function is made smaller by these new estimates, Q is set equal to and held at .1*Q. A new set of coefficient estimates is now calculated. This process is repeated until no further reduction in the objective function can be made. Q is not changed after it is set at .1*Q. This completes the optimization for this path.

If the objective function is made larger by the new estimates. Q is set equal to $-0.5|Q|$. New estimates are calculated. If the objective function is still not reduced below the value for the first guess estimates, Q is again set equal to $-0.5|Q|$ and new estimates are calculated. This is repeated until success is achieved. When this has been completed, Q is set and held at $Q = 0.1Q$. New parameter estimates are now calculated and the objective function evaluated for these values. This is repeated until no further success is possible.

Since the majority of computation time is spent in determining the partial derivatives, the most effective use of these values should be made. This can be done by determining which set of variables has the largest partials and setting the entire set's partials equal to zero. This may be done only after new estimates for this set have been determined. Setting the partials of this set equal to zero is equivalent to optimizing relative to one less set of variables. New estimates are now calculated and the optimization process is reinitiated. When this is completed the set with the next largest partials is determined. This set's partials are now set equal to zero and the optimization process is again reinitiated. This is done until only one set of variables is left to be adjusted. This represents the maximum usage of the partial derivatives. New partials are now calculated and the complete optimization process is started again. The procedure is stopped when "J" (objective function) is sufficiently small.

APPENDIX "D"

Calculating Filter Coefficients From Constrained Response Coefficients

The problem here is to convert the constrained response coefficients;

$A(h_2)$, $B(h_2)$, $\psi(h_2)$ and $\alpha_1(h)$, $\alpha_2(h)$ & $\omega(h)$ in the response function:

$$A(h_2)e^{\alpha_1(h)*h} + B(h_2)e^{\alpha_2(h)*h}(\cos(\omega(h)*h) + \psi(h_2))$$

to filter coefficients. A filter of the form shown in Figure D-1 was selected because of the ease with which the conversion can be accomplished using this filter form.

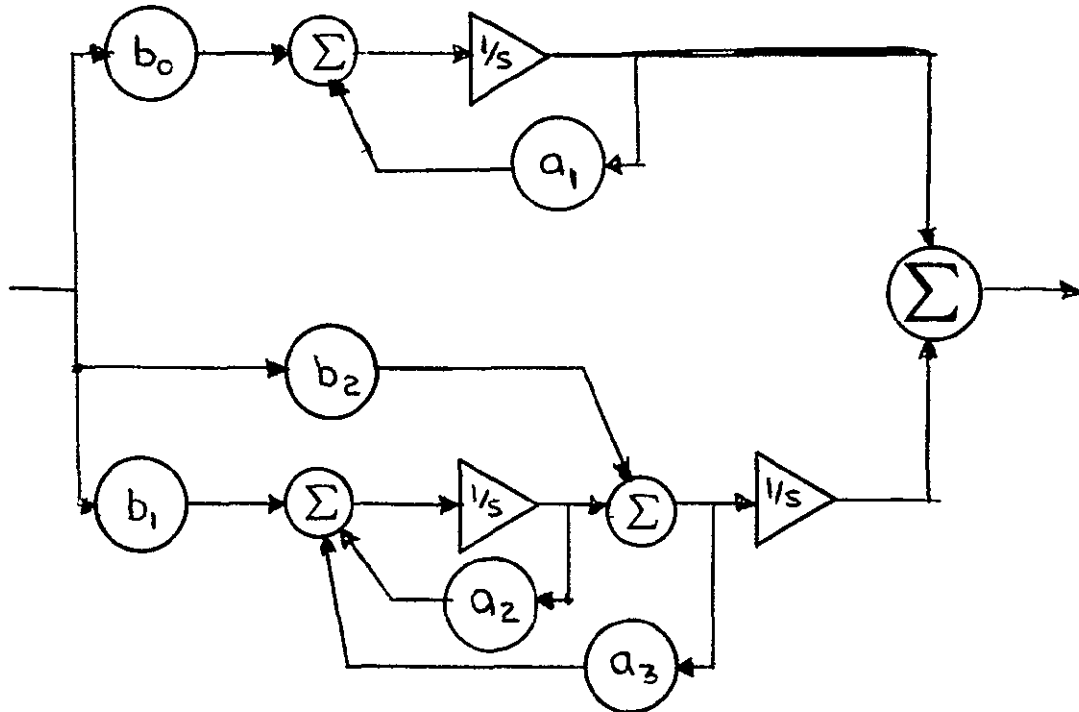


Figure D-1 Third Order Filter Form

As shown in Figure (D-1), the third order filter form is presented as the sum of a first order filter and a second order filter. The first order filter is associated with the first term of the constrained response equation,

$$A(h_2) e^{-\alpha_1(h) * h} ;$$

and the second order filter is associated with the second term,

$$B(h_2) e^{-\alpha_2(h) * h} (\cos(\omega(h) * h + \psi(h_2))) ;$$

Derivation of the coefficients, $a_1(h)$, $a_2(h)$, $a_3(h)$, $b_0(h)$, $b_1(h)$ and $b_2(h)$ is as follows:

$$g_1(h_2, h) = A(h_2) e^{\alpha_1(h) * h}, \quad (D-1)$$

$$\dot{g}_1(h_2, h) = A(h_2) * \left[\alpha_1(h) + \dot{\alpha}_1(h) * h \right] e^{\alpha_1(h) * h}, \quad (D-2) ;$$

where the dot represents the derivative with respect to h.

With (D-1) \rightarrow (D-2), we have

$$\dot{g}_1(h_2, h) = \left[\alpha_1(h) + \dot{\alpha}_1(h) * h \right] g_1(h_2, h) \quad (D-3)$$

or,

$$a_1(h) = \alpha_1(h) + \dot{\alpha}_1(h) * h \quad (D-4)$$

$$b_0(h_2) = A(h_2) \quad (D-5)$$

In a similar, but slightly more complex manner, the second order coefficients are derived.

$$g_2(h_2, h) = B(h_2) e^{\alpha_2(h) * h} \cos(\omega(h) * h + \psi(h_2)) \quad (D-6)$$

Simplifying the notation, for compactness, the derivation continues;

$$\begin{aligned} \dot{g}_2 &= B e^{\alpha_2 h} (\alpha_2 + \dot{\alpha}_2 h) \cos(\omega * h + \psi) \\ &- B e^{\alpha_2 h} [\sin(\omega h + \psi)] \{ \omega + \dot{\omega} h \} \end{aligned} \quad (D-7)$$

$$\begin{aligned}
\ddot{g}_2 &= B e^{\alpha_2 h} (\alpha_2 + \dot{\alpha}_2 h)^2 \text{COS} (\omega h + \psi) + B e^{\alpha_2 h} (2\dot{\alpha}_2 + \ddot{\alpha}_2 h) \\
&\quad * \text{COS} (\omega h + \psi) - B e^{\alpha_2 h} (\alpha_2 + \dot{\alpha}_2 h) \text{SIN} (\omega h + \psi) (\omega + \dot{\omega} h) \\
&\quad - B e^{\alpha_2 h} (\alpha_2 + \dot{\alpha}_2 h) (\omega + \dot{\omega}) \text{SIN} (\omega h + \psi) \\
&\quad - B e^{\alpha_2 h} (\omega + \dot{\omega} h)^2 \text{COS} (\omega h + \psi) \\
&\quad - B e^{\alpha_2 h} (2\dot{\omega} + \ddot{\omega} h) \text{SIN} (\omega h + \psi) \tag{D-8}
\end{aligned}$$

From (D-7);

$$B e^{\alpha_2 h} (\omega + \dot{\omega} h) \text{SIN} (\omega h + \psi) = -\dot{g}_2 + (\alpha_2 + \dot{\alpha}_2 h) g_2$$

and,

$$B e^{\alpha_2 h} \text{COS} (\omega h + \psi) = g_2 \tag{D-9}$$

Now, substituting the relations D9 into D8;

yields:

$$\begin{aligned}
g_2 &= \left[(2\dot{\alpha}_2 + \ddot{\alpha}_2 h) - (\omega + \dot{\omega} h)^2 - (\alpha_2 + \dot{\alpha}_2 h)^2 - \frac{2\dot{\omega} + \ddot{\omega} h}{\omega + \dot{\omega} h} (\alpha_2 + \dot{\alpha}_2 h) \right] g_2 \\
&\quad + \left[2(\alpha_2 + \dot{\alpha}_2 h) + \frac{2\dot{\omega} + \ddot{\omega} h}{\omega + \dot{\omega} h} \right] \dot{g}_2 \tag{D-10}
\end{aligned}$$

where, in equation D-10,

$a_3(h)$ = coefficient of g_2

$a_2(h)$ = coefficient of \dot{g}_2

The $b_1(h)$ coefficients become $b_2(h) = B(h_2) \text{COS} (\psi(h_2))$

$b_1(h) = B(h_2) \alpha_2 \text{COS} (\psi) - B(h_2) \omega \text{SIN} (\psi)$

APPENDIX "E"

Conversion of Filter From Altitude to
Flight-Time Domain

Referring to Figures E-1 & E-2 we can write:

$$z_1(te) = g_1(h) \quad v = \text{velocity, } \frac{dh}{dt} \quad (E-1)$$

$$z_2(te) = g_2(h) \quad (E-2)$$

$$\frac{dz_1(te)}{dt} = \frac{dg_1(h)}{dh} \frac{dh}{dt} ; \quad \dot{z}_1(t) = \dot{g}_1(h) v(t) \quad (E-3)$$

$$\frac{dz_2(te)}{dt} = \frac{dg_2(h)}{dh} \frac{dh}{dt} ; \quad \dot{z}_2(t) = \dot{g}_2(h) v(t) \quad (E-4)$$

Also from figure E1 & E2

$$\dot{z}_1(t) = z_1(t) R_0(t) \quad (E-5)$$

$$\dot{g}_1(h) = g_1(h) C_0(h) \quad (E-6)$$

With (6) → (3)

$$\dot{z}_1(t) = g_1(h) C_0(h) v(t) \quad (E-7)$$

Equating (7) & (5):

$$z_1(t) R_0(t) = g_1(h) C_0(h) v(t) \quad (E-8)$$

Using (1) → (8) yields

$$R_0(t) = C_0(h) v(t) \quad (E-9)$$

In a similiar manner

$$\dot{z}_2(t) = \dot{g}_2(h) v(t) \quad (E-10)$$

$$\ddot{z}_2(t) = R_2(t) \dot{z}_2(t) + R_3(t) z_2(t) \quad (E-11)$$

$$\ddot{g}_2(h) = C_2(h) \dot{g}_2(h) + C_3(h) g_2(h) \quad (E-12)$$

With (2) & (10) → (11)

$$\hat{z}_2(t) = R_2(t)\dot{g}(h)v(t) + R_3(t)g(h) \quad (\text{E-13})$$

Also, differentiating (10) yields:

$$\dot{z}_2(t) = \dot{g}_2(h)\dot{v}(t) + \hat{g}(h)v^2(t) \quad (\text{E-14})$$

With (12) → (14)

$$\dot{z}_2(t) = \dot{g}_2(h)\dot{v}(t) + [C_2(h)\dot{g}_2(h) + C_3(h)g_2(h)]v^2(t) \quad (\text{E-15})$$

Equating (13) & (15) yields

$$R_2(t)v(t)\dot{g}(h) + R_3(t)g(h) = \dot{g}_2(h)\dot{v}(t) + [C_2(h)\dot{g}_2(h)g_2(h)]v^2(t) \quad (\text{E-16})$$

Equating coefficients of $g(h)$ yields:

$$R_3(t) = v^2(t)C(h) \quad (\text{E-17})$$

Equating coefficients of $\dot{g}(h)$ yields

$$R_2(t) = \frac{\dot{v}(t)}{v(t)} + v(t)C_2(h) \quad (\text{E-18})$$

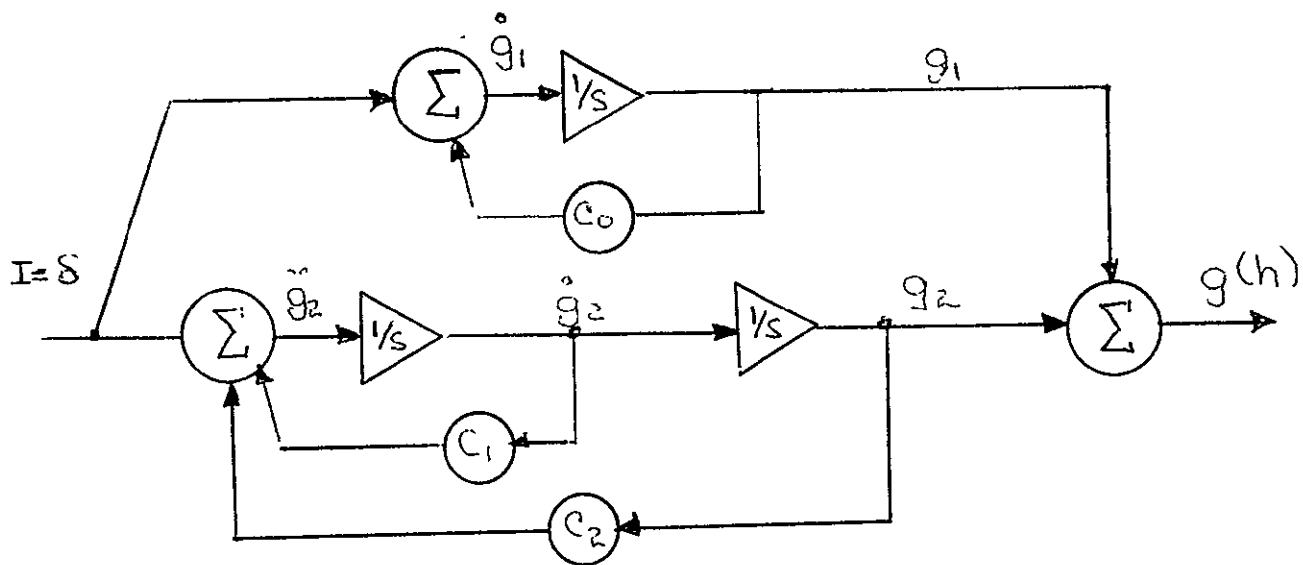


Figure E-1 FILTER ADJOINT IN ALTITUDE DOMAIN

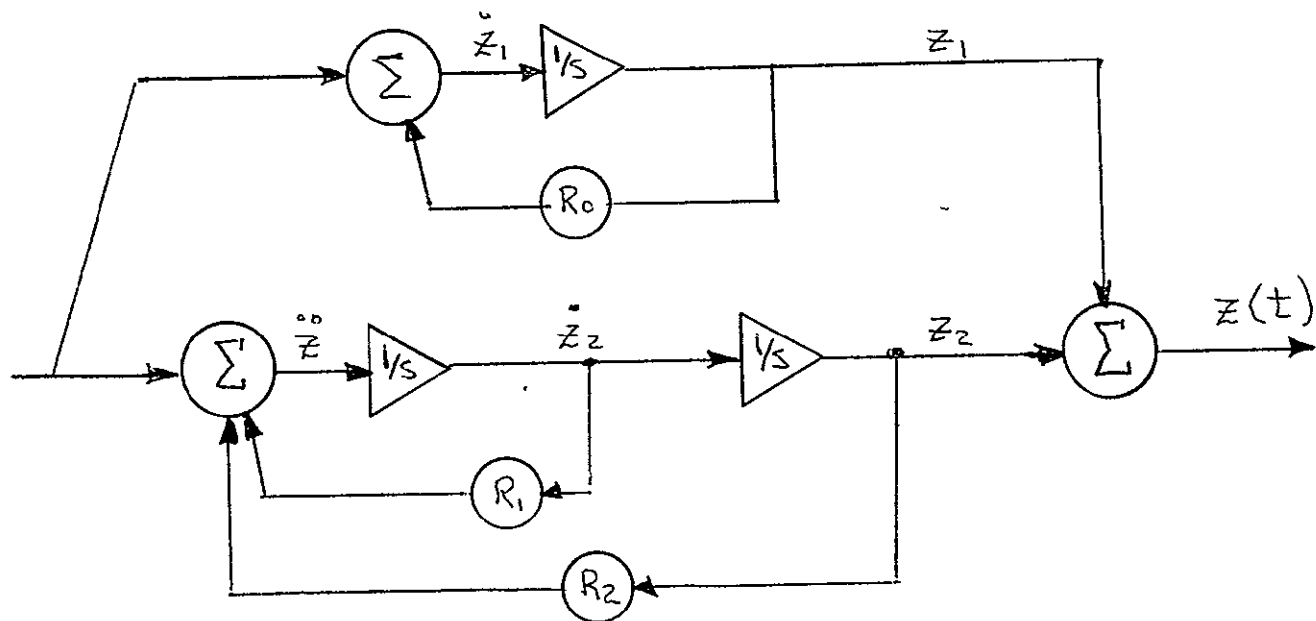


Figure E-2 FILTER ADJOINT IN FLIGHT-TIME DOMAIN

APPENDIX F
VEHICLE NOMENCLATURE

NOMENCLATURE

| <u>SYMBOL</u> | <u>PARAMETER</u> | <u>UNITS</u> |
|--|---|--|
| A | Reference Cross Sectional Area of Vehicle | M ² |
| A _x | Axial (X) Acceleration | M/Sec. ² |
| a ₀ , a ₁ | Wind Filter Coefficients | |
| b ₀ , b ₁ | | |
| B.M. | Bending Moment | Newton-Meters |
| C _N | Normal Force Coefficient | |
| ξ _i , ξ̇ _i , ξ̈ _i | i th Slosh Mode Displacement, Velocity, Acceleration | Meters, Meters/Sec., Meters/Sec. ² |
| φ _Z , φ̇ _Z , φ̈ _Z | Yaw Attitude Angle, Rate, Acceleration | Radians, Radians/Sec., Radians/Sec. ² |
| ω _{η1} , ω _{Si} | i th Mode Bending, Slosh Frequency | Radians/Sec. |

NOMENCLATURE
(Continued)

| <u>SYMBOL</u> | <u>PARAMETER</u> | <u>UNITS</u> |
|-------------------------------------|---|-----------------------------------|
| $C'_N = C_N / \alpha_{\text{mean}}$ | Normal Force Coefficient Slope | |
| $\sum_j C'_N Y_{ij}$ | i^{th} Mode Normal Force Coefficient Slope Summed Over All Vehicle Segments j . | |
| F_{TX} | Axial (X) Force Thrust (5 Engines) | Newtons |
| F_{TCX} | Axial (X) Force Thrust Control (4 Engines) | Newtons |
| F_{TCY} | Translational (Y) Force Thrust Control | Newtons |
| F_{AY} | Translational Aerodynamic Force | Newtons |
| F_{AX} | Axial Aerodynamic Force-Drag | Newtons |
| $h(t_2, \tau)$ | System Weighting Function for Time t_2 | |
| I_{ZZ} | Vehicle Moment of Inertia about the Center of Gravity | Newton-Meter- Sec ² |
| m | Vehicle Mass | Kilograms |
| m_{Si} | i^{th} Slosh Mass | Kilograms |
| M'_α | Bending Moment Coefficient, Angle of Attack | N-M/Rad. |
| M'_β | Bending Moment Coefficient, Engine Deflection | N-M/Rad. |
| M'_{η_i} | i^{th} Mode Bending Moment Coefficient, Bending | N-Sec ² |
| M'_{ξ_i} | i^{th} Mode Bending Moment Coefficient, Slosh | N-Sec ² |
| q | Dynamic Pressure | Newtons/Meter ² |
| \tilde{Q}_i | i^{th} Mode Generalized Force | Newtons |

NOMENCLATURE
(Continued)

| <u>SYMBOL</u> | <u>PARAMETER</u> | <u>UNITS</u> |
|---------------------------------------|---|---|
| T_{CPZ} | Aerodynamic Moment | Newton-Meters |
| T_{ui} | i^{th} Bending Mode | Kilograms |
| V_{RY} | Translational Relative Velocity | Meters/Sec. |
| V_{RS} | Magnitude of Relative Velocity, Space | Meters/Sec. |
| X_{CP} | Vehicle Center of Pressure | Meters |
| X_{CG} | Vehicle Center of Gravity | Meters |
| X_{Si} | i^{th} Slosh Mode Attach Point | Meters |
| $Y_1(X_j)$ | i^{th} Bending Mode Displacement at X_j . | |
| $Y_1'(X_j)$ | i^{th} Bending Mode Slope at X_j . | Rad/M |
| \ddot{Y} | Translational Acceleration | Meters/Sec. ² |
| \dot{Y} | Translational Velocity | Meters/Sec. |
| α | Angle of Attack | Radians |
| β | Total Engine Angle | Radians |
| δ_Z | Engine Angle (Without Bending Correction) | Radians |
| $\Delta\delta_Z$ Bend | Engine Angle Correction Due to Bending | Radians |
| $\Delta\theta_Z$ Bend | Attitude Angle Correction Due to Bending | Radians |
| $\Delta\dot{\theta}_Z$ Bend | Attitude Rate Correction Due to Bending | Radians/Sec. |
| ζ_i, ζ_{Si} | i^{th} Mode Bending, Slosh Damping Ratio | |
| $\eta_1, \dot{\eta}_1, \ddot{\eta}_1$ | i^{th} Bending Mode Generalized Displacement, Velocity, Acceleration, Referenced to Vehicle Nose. | Meters, Meters/Sec., Meters/Sec. ² |